Profilin-1 as a Regulator of Vascular Endothelial-Immune Cell Crosstalk

by

Abigail Gondringer

B.S. Chemical Engineering, Ohio University, 2017

M.S. Biomedical Engineering, Ohio University, 2018

Submitted to the Graduate Faculty of the

Swanson School of Engineering in partial fulfillment

of the requirements for the degree of

Doctor of Philosophy

University of Pittsburgh

2023

UNIVERSITY OF PITTSBURGH

SWANSON SCHOOL OF ENGINEERING

This dissertation was presented

by

Abigail Gondringer

It was defended on

November 9, 2023

and approved by

Dr. Partha Dutta, DVM, Ph.D., Associate Professor, Department of Medicine

Dr. Sanjeev Shroff, Ph.D., Professor, Department of Bioengineering

Dr. Sunder Sims-Lucas, Ph.D., Associate Professor, Department of Pediatrics

Dr. Walter Storkus, Ph.D., Professor, Department of Immunology

Dissertation Director: Dr. Partha Roy, Ph.D., Professor, Department of Bioengineering

Profilin-1 as a Regulator of Vascular Endothelial-Immune Cell Crosstalk

Abigail Gondringer, PhD

University of Pittsburgh, 2023

Actin cytoskeleton plays a key role in vascular endothelial cell (EC) integrity. Cytoskeletal changes promote EC dysfunction and vascular infiltration of immune cells during inflammation. The overall goal of this dissertation is to study the role of Profilin1 (Pfn1), an actin monomer binding-protein and an important regulator of actin cytoskeletal dynamics, in vascular EC-immune cell crosstalk. To this end, we generated an inducible vascular-EC-specific Pfn1 knockout mouse model. We demonstrated that triggering widespread deletion of vascular EC Pfn1 in adult mice leads to severe health complications presenting overt pathologies (EC death, infarct, and fibrosis) in major organ systems and evidence for inflammatory infiltrates, ultimately compromising the survival of animals within 3 weeks of gene ablation. Mice deficient in EC Pfn1 exhibit selective bias towards the pro-inflammatory myeloid-derived population of immune cells, a finding further supported by systemic elevation of pro-inflammatory cytokines. Triggering Pfn1 depletion not only upregulates pro-inflammatory cytokine/chemokine gene expression in EC (a finding consistent with elevated STAT1/interferon signaling) but also potentiates the paracrine effect of EC on pro-inflammatory gene expression in macrophages. Collectively, these findings for the first time demonstrate a prominent immunological consequence of loss of EC Pfn1, and an indispensable role of EC Pfn1 in mammalian survival unlike tolerable phenotypes of Pfn1 loss in other differentiated cell types. Finally, we examine the impact of haplo-insufficiency of EC Pfn1 in a vascular disease context utilizing a mouse model of atherosclerosis, where reduced cytotoxic T cells and elevated B cell populations, paired with reduced pro-atherogenic cytokines CXCL10 and IL7, offer some support for partial EC Pfn1 deletion in modulating chronic inflammation.

Table of Contents

List of Tables

List of Figures

Preface

Completing my graduate work required the advice, dedication, and support of so many people in my life, near and far. A big thank you to my parents and sister for supporting me from day 1 in my academic aspirations, it would not have been possible if not from there! Thank you to my husband Jake, your calm demeanor and consistent support and validation helped pull me through the bad days toward the good. Thank you to all my friends past and present, you are all a piece of this story. To my fellow Pitt BioE friends, there were a heck of a lot of tribulations, but we are all making it through just all right! Big thanks always to Mahboubeh Noori, for believing in me at Ohio University! I would not have had the confidence to pursue my doctoral degree without your support and belief in what I was capable of.

For my scientific support and development, thank you to my advisor Dr. Partha Roy, for his guidance, direction, and mentorship. Having the flexibility to move through a new project concept and build it towards my interests offered a great learning experience. Thank you to my committee members Drs. Partha Dutta, Walter Storkus, Sanjeev Shroff, and Sunder Sims-Lucas for their help and advice in making this work a possibility. Thank you as well to Dr. Alan Wells and the Wells lab and collaborators for offering great advice on my research and presentations over the years.

A final thank you to the Roy lab members and collaborators! Thanks to Dr. David Gau for training and advice, and to fellow grad students Ian Eder, Andrew Orenberg, Pooja Chawla and Jacob Antonello for support and sympathy on the day to day. Thank you as well to all the collaborators who made this possible.

ABBREVIATIONS AND ACRONYMS

ABP	Actin binding proteins
ACE	Angiotensin converting enzyme
Ad-	Adenovirus
ADP	Adenosine diphosphate
AGEs	Advanced glycation end product
ALS	Amyotrophic lateral sclerosis
AMP	Adenosine monophosphate
ATP	Adenosine triphosphate
ApoE	Apolipoprotein E
BMDM	Bone marrow-derived macrophage
CM	Conditioned media
CrPRF	*Chlamydomonas reinhardtii*
DNA	Deoxyribonucleic acid
EC	Endothelial cell
F-actin	Filamentous-actin
FBS	Fetal bovine serum
G-actin	Globular-actin
GFP	Green fluorescent protein
H&E	Hematoxylin and eosin staining
Het	Heterozygous
ICAM	Intercellular adhesion molecule

iNOS	Inducible nitric oxide synthase
IRF	Interferon regulatory factor
KD	Knock-down
KO	Knock-out
LDLR	Low density lipoprotein receptor
LFA	Lymphocyte function-associated antigen
LOF	Loss of function
MAEC	Mouse aortic endothelial cell
MEC	Mouse endothelial cell
OE	Over-expression
oxLDL	Oxidized low density lipoprotein
PIP	Phosphatidylinositol
Pfn	Profilin
PLC	Phospholipase C
PLP	Poly-L-proline
PPI	polyphosphoinositide
Ad(RGD)	Adenoviral(Arg-Gly-Asp)
RNA	Ribonucleic acid
siRNA	Small interfering RNA
STAT	Signal transducer and activator of transcription
TgPRF	*Toxoplasma gondii* Profilin
TLR	Toll Like Receptor
TMX	Tamoxifen

TNFα	Tumor necrosis factor alpha
TRIM	Tripartite motif
VCAM	Vascular cell adhesion molecule
VEGF	Vascular endothelial growth factor
VSMC	Vascular smooth muscle cell
WT	Wild-type

1.0 Introduction

The content of this section is published in part.
Reference: **Abigail Allen**, David Gau, Partha Roy. "The role of Pfn1 in cardiovascular diseases", *Journal of Cell Science*, Volume 134, Issue 9, May 2021, jcs249060.

1.1 Profilin and its Isoforms

Profilins (Pfns) are small (~15kDa) proteins that are expressed in eukaryotes[1]–[5], some parasites[6]–[9], and viruses[10], [11], and are present as a variety of isoforms[12], [13]. Typically, one to two isoforms of Pfn are present in unicellular organisms, though four have been identified in mammals (Pfn1-4), specifically human and mouse. It is expected that Pfns existed prior to viral/eukaryotic divergence, due to structural similarity and similar folding conformation amongst Pfn isoforms and species, even when amino acid sequence similarity is low[14], [15]. For instance, ***Chlamydomonas reinhardtii*** Pfn, or CrPRF, in unicellular alga[8], has high G-actin affinity similar to Pfn1, while showing low affinity for poly-L-proline and phosphoinositides[8]. CrPRF also inhibits nucleotide exchange, underscoring a similar base functionality of Pfns, while still highlighting species-specific Pfn evolution. Thus, the emergent picture is that different Pfns have developed to have functions suited to the need of their specific cell type, species, and localization[8].

Of the mammalian isoforms, Pfn1 is present constitutively, while others (i.e. Pfn2, Pfn3, Pfn4) are tissue specific or constitutively present at reduced levels [14]. Though structurally similar, Pfn isoforms may both diminish and compound similar cellular functions. For instance, Pfn1 has an affinity for actin five times higher than that of Pfn2[13]., while Pfn2, a lower expressed

Pfn in non-neuronal cells, has a demonstrable impact on cell motility at concentrations an order of magnitude less than that of Pfn1[16]. For instance, Pfn2 demonstrated an anti-migratory effect in breast cancer cells (MCF10A and SUM159) by increased actomyosin contractility, while depletion of Pfn1 demonstrated a similar effect[16]. The molecular difference between Pfn1 and Pfn2 is most obvious in the generation of Pfn2 splice variants. Pfn2, a classically neuronal Pfn, undergoes alternative splicing, generating four splice variants. Two of these, Pfn2a and Pfn2b, can be found at reduced concentration in most non-neuronal tissue types [17]. While both isoforms are critical to proper development of the neuronal structure, neurons will still develop with knockout or overexpression of either isoform[18]. Splice variants are also known to interact with other Pfns in development. Specifically, the Pfn2a splice variant cooperates with Pfn1 in the development and fine tuning of the neuronal architecture in murine neurons[18]. Another recently discovered variant, Pfn3, had comparable homology to Pfn1 and Pfn2 and also interacted with actin and poly-L-proline[19]. However, Pfn3 is highly tissue specific, with expression limited to kidney and testis[19]. Similar to Pfn3, Pfn4 has limited role in gamete production as evidenced by mouse spermiogenesis[20]–[22]. Pfn4's sequence domain also has structural similarities to Pfn1, and both are 95% superimposable upon the other, even with low sequence similarity[23]. Due to limited expression of Pfn3 and Pfn4 outside of testes, further literature review and research conducted in this dissertation focused primarily on Pfn1, with some review of Pfn2.

1.2 Biochemical Properties and Cellular Functions of Pfn1

Originally discovered as an actin sequestering protein[2], research has unveiled a diverse functionality of Pfn. Classically, Pfn facilitates actin monomer shuttling to and from actin

filaments. Specifically, Pfn will assemble or disassemble an actin filament depending on the end with which it interacts. Pfn extends actin filaments along the barbed (+) end and dissociates on the pointed (-) end. However, different concentrations and conditions will influence Pfn's interaction with monomeric (G-actin) and filamentous (F-) actin. High concentrations of Pfn1 depolymerize barbed ends of actin filaments at a much faster rate than the spontaneous dissociation of Mg-ATP, Mg-ADP, or Mg-AMP associated actin subunits[24]. However, assembly of actin filaments from ADP-actin:Pfn1 monomers is only 10% faster than that of unaided ADP-actin monomers, and Pfn does not influence rate of elongation of actin filaments compared to unbound AMP-actin[24]. Thus, Pfn displays discrimination between types of actin, potentially due to conformational differences between monomers and the barbed end of filaments [24].

Mutating various Pfn1 residues influences its interaction with actin in actin:Pfn1 monomers, as well as polymerization/depolymerization of actin filaments[25]. In H119E-Pfn1, actin-binding functionality of Pfn1 is blocked, likely due to the amino acid substitution preventing close interaction of actin and Pfn1 and abrogating Pfn1:actin binding [25]. Binding of Pfn1 to the actin filament barbed end is governed in part by sterics, with a crowding actin mutation (A167E) leading to increased actin:Pfn interface packing, and defective cell growth and mitochondrial function[26]. Other mutations influence polymerization functionality of Pfn1, as K125N-Pfn1 directly impacts the actin:Pfn1 interaction by preventing polymer formation [25]. PI(4,5)P2 may also aid in accelerating Pfn1 release from polymerized actin [25]. When a smaller functional Pfn with Y79S mutation is utilized with the mutated actin, Pfn:actin interaction is restored through sterics, and not through increased functionality of the mutated profilin or through improved association with formins[26]. Mutations may also lead to several and stacking defects in Pfn1 function. Specifically, residues like H133S abolish polyproline binding ability of Pfn1, in addition to

reducing actin binding affinity of Pfn1[25]. These point mutations suggest variable functional contributions in the abrogation of Pfn1 function.

Additionally, Pfn is known to bind poly-L-proline (PLP) [27] and phosphatidylinositols (PPI) at the cell membrane. The interface between Pfn and PLP is primarily hydrophobic, with two tryptophan residues critical to the interaction due to their conservation across species[28]. The localization of structural changes indicates a site-specific change in PLP conformation to bind Pfn, specifically in strand F of the beta-sheet of PLP between the NH2 and COOH terminal helices[28]. Select PIPs may also have a direct interaction with actin filments, or Pfn1 itself. Phosphatidylinositol 4,5 bisphosphate (PIP(4,5)P2) has been shown to have an active relationship in actin filament formation at the cell membrane[29]. For instance, residues R88 and R136 of Pfn1 are important to PI(4,5)P2 binding[30]. Indeed, both Pfn1 and Pfn2 bind to PIP(4,5)P2 at comparable concentrations[13]. Pfn has also been shown to compete against phospholipase-C (PLC) for binding to PIP(4,5)P2, thus preventing PIP2 hydrolysis and implying Pfn as a negative regulator of PIP signaling[31]. Collectively, these findings demonstrate that Pfn is a functionally diverse molecule.

1.3 Role of Pfn1 in Physiology

Assembly and disassembly of the actin cytoskeleton is a dynamic, carefully regulated process. Actin filament assembly dynamics take place at physiological concentration of Pfn-actin dimers to limit growth by dissociation of Pfn, even at a saturated concentration of actin-Pfn dimer[32]. Weakly actin-binding Pfns (E82A, R88K) elevated dynamic filament growth and regulation, while tightly actin-binding Pfns (K125E+E129K) reduced filament elongation rate[32],

supporting a role for weakly binding Pfns in dynamic actin filament regulation and growth. In addition to functional Pfn regulation, release is further mediated by the FH2 domain of formin actin polymerases that accelerate actin filament elongation[32]. It is likely that mammalian cells maintain a Pfn-actin concentration near saturated levels so that actin filament dynamics are constrained, not by diffusion or concentration, but rather by kinetics of Pfn release. Ideally, Pfn binds weakly to ATP-F-actin, but strongly to ATP-G-actin, further facilitating dynamic actin assembly[32]. Specifically, elevated levels of Pfn positively correlate with elevated levels of F-actin within cells[33].

Further, Pfn has an emerging role in regulating dendritic spine formation. Pfn has been found in dendritic spines post-synaptic stimulation[34] and actin filament treadmilling in the spine head is critical to synaptic growth[35]. In spine development and maturation, Pfns play differential roles, with Pfn1 important to spinogenesis and expression profile in mature spines, and Pfn2a is central to spine stability and plasticity, as well as synaptic function[36]. Exogeneous delivery of urokinase-type plasminogen activator (uPA, promotes spine recovery) induced Pfn expression in dendritic spines and stabilized dendritic filopodia[37]. Additionally, the pre-synaptic protein Piccolo binds Daam1 (formin) which contacts Pfn2 for interaction and subsequent polymerization[38]. F-actin in particular will localize in the dendritic spine[39] and monomeric G-actin is enriched in the dendritic spine by a PIP3-dependent pathway mediated in part by Pfn(1/2)[40]. Mutations in Pfn have demonstrated defects in growth cone formation, arresting outgrowth[41]. Similar behavior has been observed for Pfn1, as Pfn1 coordinates the actin cytoskeleton and microtubules in the growth cones of axons, promoting axonal growth and regeneration[42]. Indeed, delivery of Pfn1 has been shown to stimulate axonal regeneration, offering Pfn1 as a therapeutic target for treating the injured nervous system[42].

There are a variety of proteins that function similarly to Pfn. One of these proteins, twinfillin, plays an important role in endocytosis, vesicular secretion, ADP-actin monomer complex formation, and PI(4,5)P2 interaction[43]. Like Pfn, twinfillin is present in various species, such as yeast, mouse and drosophila. However, twinfillin does not bind actin filaments or promote depolymerization, and may be designed to recycle ADP-actin monomers to actin filament sites[43]. Another Pfn, Pfn2, associates with dynamin1 via PLP rich dynamin binding sites. Pfn2 binding to dynamin1 may inhibit PIP binding, thus preventing ternary complex formation in membrane trafficking and signal transduction [44]. This binding interferes with SH3 binding of SH3 ligands (i.e. endophilin, amphyphysin, Grb2, other endocytic associated proteins), where Pfn2 overexpression inhibits endocytosis, and lack of Pfn2 increases endocytosis and recycling of membrane components.

Pfn-like proteins also have a demonstrated role in immune response. Indeed, early reports posited that the Pfn1 plays a critical role in lymphocyte function-associated antigen (LFA)-mediated adhesion of T lymphocytes to the endothelium, through PI3 kinase activation leading to actin assembly[45]. This has been demonstrated for other forms of Pfns (*T. gondii*)[6]. Specifically, mice with chronic *T. gondii* infection demonstrated improved ability to survive co-infections, potentially through activation of toll-like receptor-11 (TLR11)[46]. Indeed, parasitic isoforms of Pfns [6], [47]–[49] have demonstrated that Pfn vaccines can be used as immune adjuvant to excite immune cells response and protect host survival. This improved survival is expected through the action of the TLR11/12 ligand *T. gondii* profilin (TgPRF), that helps reduce bacterial infection[47]. TgPRF stimulation of TLR11 promotes production of MCP-1 and migration of $Ly6C^{hi}$ $CCR2^{+}$ monocytes, providing protection against pathogens unrelated to *T. gondii*[47]. Balb/c mice immunized with the parasitic variant of Pfn, then infected with *N.*

caninum, showed moderate protection from infection as well as regulatory T cell and dendritic cell activity through an unknown mechanism[7]. To further support this finding, $Ly6G^{hi}$ neutrophils produce TNFα and iNOS, with migration dependent on MCP-1 and CCR2 presence[47], demonstrating a requirement for proinflammatory cytokines and chemokines to stimulate activation of lymphocytes.

Additionally, Pfn plays an apparent role in wound healing (requires promotion of anti-inflammatory response), underscoring a context-specific role for Pfn1 in inflammation. It has been shown that Pfn deficiency leads to defects in cell migration and adhesion[50] and that *chickadee* (*Drosophila* Pfn) is a critical element in wound closure[51]. Embryos deficient in *chickadee* fail to utilize the Jun N-terminal (JNK)-pathway, leading to incomplete wound closure due to inappropriate cytoskeletal rearrangement[52]. Loss of JNK pathway regulation impairs Pfn function, leading to impaired wound closure and cytoskeletal recruit of differentiated cells via actin cytoskeletal recruit[51]. These findings reveal a role for Pfn1 in inflammation that offers a fascinating opportunity for investigation.

1.4 Role of Pfn1 in Inflammation and Pathology

Pfns have been implied in various pathologies stemming from a critical regulatory role in actin shuttling as well as interaction with PLP and PIPs, with the range of pathologies presented in Figure 1. Interestingly, the association of Pfn1 level with pathology is variable across diseases, even within different forms of cancer. In the context of triple negative breast cancer (TNBC), a normal level of Pfn aids in tumorigenic ability of TNBCs, as either overexpression (OE), or total knockdown (KD), of Pfn limits the stem-like phenotype of cancer cells, and thus the tumor

initiating potential of these cells [53]. To underscore this finding, reduced Pfn1:actin interaction also reduces renal cancer tumor growth[54]. For instance, it has been shown that elevated cytoplasmic Pfn1 expression in metastatic clear cell renal cell carcinoma (ccRCC) is associated with high grade and stage, and reduced progression-free survival[55]. Elevated expression of Pfn1 is especially evident in metastatic versus primary RCC[56], and serves as a candidate late stage marker for ccRCC[57]. Pfn1 is also not overexpressed in normal adjacent kidney tissue, but overexpressed in RCC tissue and RCC-associated stromal tissue[58]. As such, the role of Pfn1 is context specific and regulated by various residues, as seen by variable phosphorylation of Pfn1 residue S137[59]. S137 phosphorylation enhances the oncogenic properties of MCF-7 breast cancer cells[59]. Perturbing different binding functionalities of Pfn1 can also induce contrasting effect. Disturbing actin binding ability by mutating residue R74 (R74E) enhances tumor development, though disturbing PLP binding (H133S mutation) has the opposite effect[59].

A number of neurological deficiencies display dysregulated Pfn expression, such as FMRP[36], [60], Parkinson's Disease, PARK15 (Pfn2 overexpression or nuclear transport)[61], [62], Charcot-Marie-Tooth type 2 (CMT2) (decreased Pfn2 expression in lymphoblasts and neurons from affected individuals) [63] and Miller-Dieker syndrome (lissencephaly) (17p13 deletion affects Pfn function(17p13.3)[4]. Various mutations in Pfn1 have also been discovered in ALS[64]–[67]. Genetic characterization of ALS patient cohorts found Pfn1 mutations at p.A20T, M114T, G118V, and p.Q139L[64], C71G[64], [65], p.T109M[67], p.Q117G[67], pR136W[68], p.L88L[68], p.E117D[69], H120E[70], rs13204[68], and E117G[65], [66], [69], [71]–[73], with some of these mutations (G118V, C17G) being validated in mouse models[74]–[78]. It appears that all pathogenic mutations have some propensity to aggregate, leading to ALS disease features[79]. Pfn1 mutations found in ALS typically lie near conserved actin and/or PLP binding

residues and adversely influence Pfn1 interaction with poly-proline and/or actin[80]–[82]. Indeed, studies conducted in *Drosophila* found that WT Pfn1 delivery improved filopodia formation, F-actin content, and synaptic formation as compared to ALS-causing Pfn1 variants C71G and M114T, suggesting loss of function mutations[83]. Further, Huntington's disease (HD) patients have reduced Pfn expression in cortical tissues, as well as in *in vitro* and *in vivo* models[84]. Specifically, Pfn is degraded around mutant htt leading to an imbalance of F/G-actin, while restoration of Pfn in *Drosophila* repairs toxic effects from htt[84], [85], a finding supported in a HD rodent model[86]. Additionally, protein-protein interaction has been discovered between Pfn2 and htt[87]. Finally, in a yeast model of spinal muscular atrophy (SMA), *tdSMN* (splicing defects in Pfn) *S. pombe* develop overly extensive actin networks that are difficult to depolymerize[88]. Of note, SMN knockdown alters Pfn2 expression, specifically increasing Pfn2a isoform present in neuronal cells[89]. Both Pfns appear to interact with SMN through utilization of Pfn polyproline domains, though Pfn2 binds more strongly than Pfn1[90]. Pfn2a binds to proline motifs in SMN, and S230L SMN variant disrupts Pfn2a:SMN interaction[91]. It appears that Pfn2 and SMN co-localize in neurite outgrowth, while knockdown of Pfn1 and Pfn2 inhibited neurite outgrowth, and disruption of SMN levels led to dysregulation of Pfn1-mediated microfilament growth[92]. SMN-depleted U87MG astroglioma cells also presented abnormal RhoA/ROCK pathway activation and increased Pfn1, demonstrating that both Pfn1 and Pfn2 are regulated in part by SMN[93], though to different degrees.

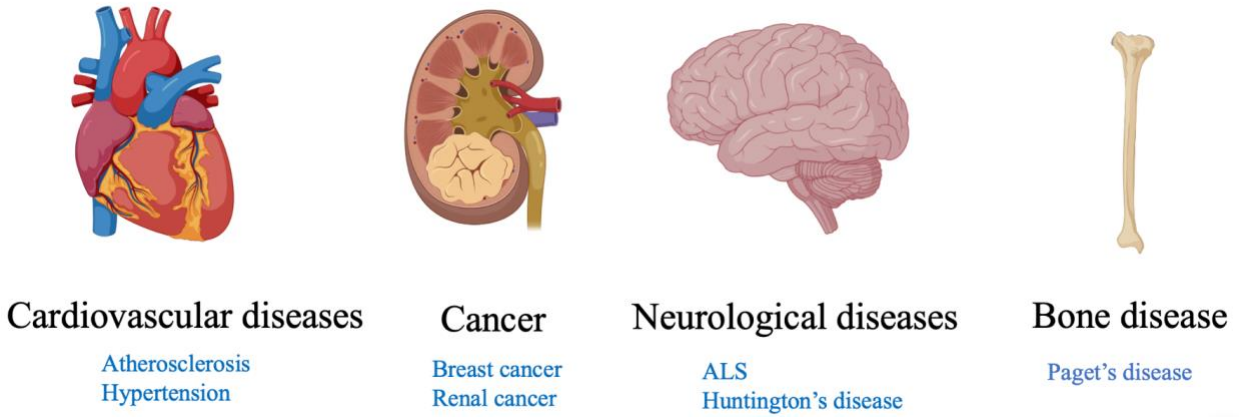

Figure 1. Schematic highlighting the role of Pfn1 in a variety of diseases.

Broadly, Pfn1 dysregulation is present in cardiovascular diseases, cancer, neurological disorders, and bone disease, though the degree to which Pfn1 contributes may need further investigation. Created with biorender.com.

1.5 Involvement of Pfn1 in Cardiovascular Diseases

The role of Pfn1 in biochemical and physiological regulation, and its dysregulation in the context of a variety of inflammatory pathologies, support its utility in further pathological studies. Additionally, the actin cytoskeleton aids in functional endothelial regulation, with an essential role attributed to Pfn1. Paired with past research revealing a role for Pfn1 in immune regulation, the role of Pfn1 in endothelial and immune cell regulation, specifically in the context of cardiovascular disease, was considered in further detail.

1.5.1 Atherosclerosis

Atherosclerosis is a disease of medium and large arteries, where vascular wall alteration characterized by local cholesterol accumulation, endothelial dysfunction, and inflammation lead to formation of atherosclerotic plaques as seen in Figure 2[94], [95]. Typically, fatty streaks develop into fibrotic plaques, as lipid-rich macrophages infiltrate the vascular intima and smooth muscle cells create layers and form occlusive fibrotic lesions[3]. Plaques are capped by connective tissue, which embeds the core of lipids, necrotic debris, and vascular smooth muscle cells (VSMCs), monocyte-derived macrophages, and activated T lymphocytes[96]. In Westernized society, heart disease and stroke are the most common cause of death[97]. For instance, ischemic heart disease, one possible complication of atherosclerosis, has a mortality rate of approximately 100-200 out of 100,000 in the United Kingdom. Though mortality rate has been decreasing in developed countries since the 1950s[98], ischemic heart disease remains the leading cause of death globally[99].

The Rotterdam study provided human data linking arterial stiffness and atherosclerosis[100]. In aged adults, increased aortic stiffness demonstrated increased coronary calcification[100]. Healthy vasculature in *ApoE*$^{-/-}$ mice also had higher stiffness (77kPa) than that present in the soft, foam cell and lipid-loaded lesion (~2-10kPa)[101], [102]. Atherosclerosis is also a flow-based pathology, as lesions lead to perturbed flow at vascular junction points[103]. YAP/TAZ (mechanotransducer) activation aids in atherogenesis in the presence of disturbed flow, while YAP/TAZ knockdown reduces inflammatory characteristics of endothelial cells[104], as knockdown of YAP/TAZ in leukocytes reduced expression of VCAM-1 and limited leukocyte:endothelial cell adhesion[105].

Proteomic study of aortic degeneration found an association with the cytoskeleton (calponin, actin, Pfn)[106], and recent findings support a role for the actin cytoskeleton in atherosclerosis. For instance, deletion of calponin 2, an actin filament-associated protein, in macrophages may lead to an attenuated phenotype of atherosclerosis, as calponin 2 deletion attenuates release of inflammatory cytokines present in atherosclerosis (M-CSF, IL3, ILα and VEGF)[107]. Indeed, BMP-2 overexpression increased VSMC migration and induced myosin expression[108], and enhanced proliferation and migration of hypoxic VSMCs via the actin/CD44/MMP-2 pathway[16]. Additionally, elevated membrane cholesterol content increased VSMC stiffness and adhesion, while cholesterol-depleted VSMCs and those cultured on soft substrate produced reduced stiffness and adhesion, as well as cytoskeletal disorganization[17]. Thus, as the arteries and surrounding matrix stiffen with age, atherosclerosis may develop further[109].

Emerging data has shown a specific role for Pfn in inflammation. For instance, Pfn1 expression increases under chronic inflammatory conditions[110]–[112]. In an *in vitro* assay, flow induces cytoskeletal stress within endothelial cells[113]. Specifically, homocysteine (elevated in atherosclerosis) in HUVEC subjected to flow conditions led to elevated expression of Pfn1, though only in the presence of homocysteine[114]. Interestingly, Pfn1 is highly overexpressed in human atherosclerotic plaques as compared to the normal adjacent vessel wall, with serum levels of Pfn1 correlating with disease severity[111]. This is observed in stromal cells, where presence of extracellular Pfn1 increases DNA synthesis and chemotaxis in VSMCs, supporting a role for extracellular Pfn1 as an atherogenic mediator[111]. This elevated Pfn1 expression also correlated with the F4/80 macrophage marker[112]. Promising data shows that this trend can be reversed by attenuating Pfn expression. PfnHet (single allele expression in all cell types) *Ldlr*$^{-/-}$ mice fed a high

cholesterol diet (HCD) showed reduced atherosclerotic lesion size, macrophage accumulation, and CD36 (fatty acid import) expression and oxLDL uptake macrophages[110]. Additionally, eNOS activation and NO signaling were apparent in PfnHet mice, displaying preserved endothelial function[110].

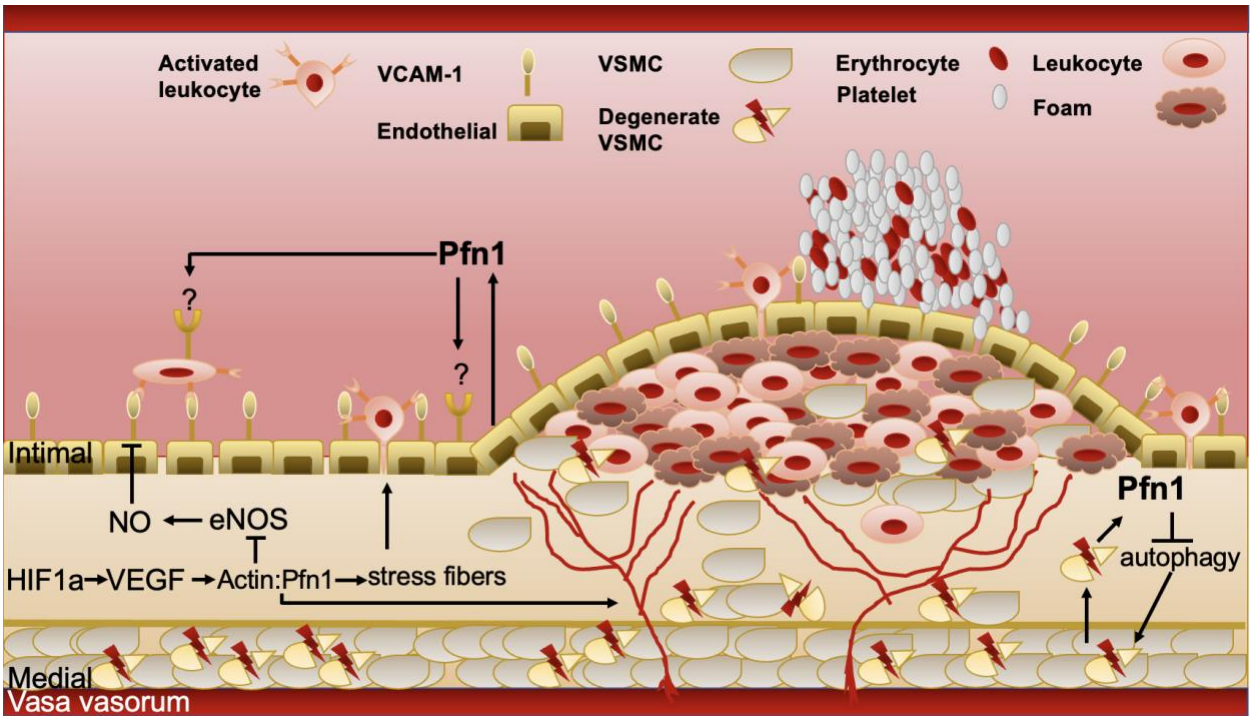

Figure 2. Pfn1's role in atherosclerosis.

Atherosclerosis is typified by vascular wall hardening, plaque formation and vascular occlusion, and endothelial dysfunction. Pfn1 influences the behavior of multiple cell types by mediating vascular permeability, angiogenesis, NO signaling, among others. Briefly, hypoxic conditions promote HIF1a production and thus VEGF stimulation. VEGF facilitates actin:Pfn1 interaction, which can then lead to stress fiber formation, endothelial dysfunction, and vascular permeability. Actin:Pfn1 interaction also promotes angiogenesis, potentially from the vasa vasorum, leading to further nutrient delivery to, and growth of, the plaque. The specific mechanism of action of Pfn1 in atherosclerosis is unclear. Extracellular release of Pfn1 may lead to uptake of Pfn1 by ECs or leukocytes, enabling immune homing and invasion at sites of vascular permeability. This may be mediated by a specific or non-specific cell-surface receptor for Pfn1. Following VSMC death, elevated Pfn1 may contribute to medial degeneration by blocking VSMC autophagy.

1.5.2 Hypertension

Hypertension (high blood pressure) has a mortality rate of 20 in 100,000 in the form of hypertensive heart disease[99]. Primary causes of hypertension are typically age[98], general adiposity[115], and salt intake. In 1959, a large population study in Framingham, MA, US determined some correlation between cardiovascular disease and hypertension[116] and an increase in cardiovascular events are observed in patients with increased blood pressure upon follow-up[117]. Specifically, systolic hypertension correlated with older and elderly patients, while diastolic hypertension predominated in the under 45 age group[118]. Large artery stiffness in the elderly is supported as a risk factor for cardiovascular disease, and further findings showed that antihypertensive therapy reduced cardiovascular morbidity in elderly patients with systolic high blood pressure[119].

Similar behavior of the actin cytoskeleton and Pfn is present in pulmonary hypertension, where upregulation of Pfn1, cofilin, and LIMK2 (regulates actin remodeling) lead to remodeling of actin filaments, and increased vascular resistance, as well as enhanced VSMC invasion[76]. Stress fiber formation has also been observed, suggesting a role for triggering vascular remodeling through some internal mechanical stress[120]. Elevated Pfn1 expression significantly correlates with untreated hypertensive patients[121]. This finding has been supported in spontaneous hypertensive rats (SHR) injected with adenoviral Pfn1 vector, where higher Pfn1 expression in the thoracic artery led to increased systolic blood pressure and vascular wall thickening[122]. Further, endogenous Pfn1 is elevated in the hypertrophic myocardium of SHR rats[123]. Adenoviral overexpression of Pfn1 induces cardiomyocyte hypertrophy[124], while myocardial hypertrophy is limited by Pfn1 silencing[125]. Indeed, ouabain increased Pfn1 expression in Sprague-Dawley rats[126], and in a rat model of ouabain-induced hypertension, blockade of Pfn1 expression

reduced cerebral vascular damage[127]. Pfn1 is primarily present in the cytoplasm, particularly near the nucleus of cardiomyocytes, with moderate expression within VSMCs[123]. This appears to indicate association of Pfn1 with cardiac vasculature, particularly in dysfunction.

A significant increase in arterial remodeling was observed in Pfn1 overexpressing SHR rats[128]. Pfn1 transgenic mice demonstrate contractile dysfunction specific to the left ventricle[129]. Pfn1 overexpressing transgenic mice likewise had increased Rho/ROCK II signaling in mesenteric arteries, inhibited eNOS signaling, vascular hypertrophy and high blood pressure[130]. Elevated Jnk kinase offers further support for upregulation of hypertrophy[30]. It is also important to note that in acute myocardial infarction (potential complication of hypertension), an elevated level of Pfn1 is secreted when platelets aggregate in the coronary thrombus, with the amount of Pfn1 increasing the longer the thrombus is occluded[131]. Given its role in cardiovascular ailments of several varieties, this research suggests a role for Pfn1 throughout disease pathogenesis.

It is postulated that Pfn1 expression is increased in in hypertension through angiotensin II (AngII), potentially via JAK2/STAT3 signaling pathway[132]. AngII-induced aortic inflammation increased Pfn1 expression, which is enhanced following ACE2 deficiency[133]. Interestingly, knockdown of Pfn1 reduces AngII-induced VSMC proliferation, in addition to blocking ERK1/2 phosphorylation and superoxide production[134]. Overexpression of Pfn1 or R88L-Pfn1 in vasculature led to elevated phosphoERK1/2 and increased systolic and mean blood pressure in FVB mice[120]. Increased Pfn1 expression also reduces eNOS Ser1177 phosphorylation and NO release in SHR rats[123], indicating impaired endothelial function[125]. Other research has found that Pfn1 overexpression promotes phosphorylation of p38, oxidative stress and hypertension[128]. This would suggest that Pfn1 is upregulated in hypertension through activation

AngII-mediated inflammatory pathways and can be mediated either by an AngII or some downstream inhibitor, such as one against Pfn1. Potential contributing mechanisms of action of Pfn1 in hypertension are presented in Figure 3.

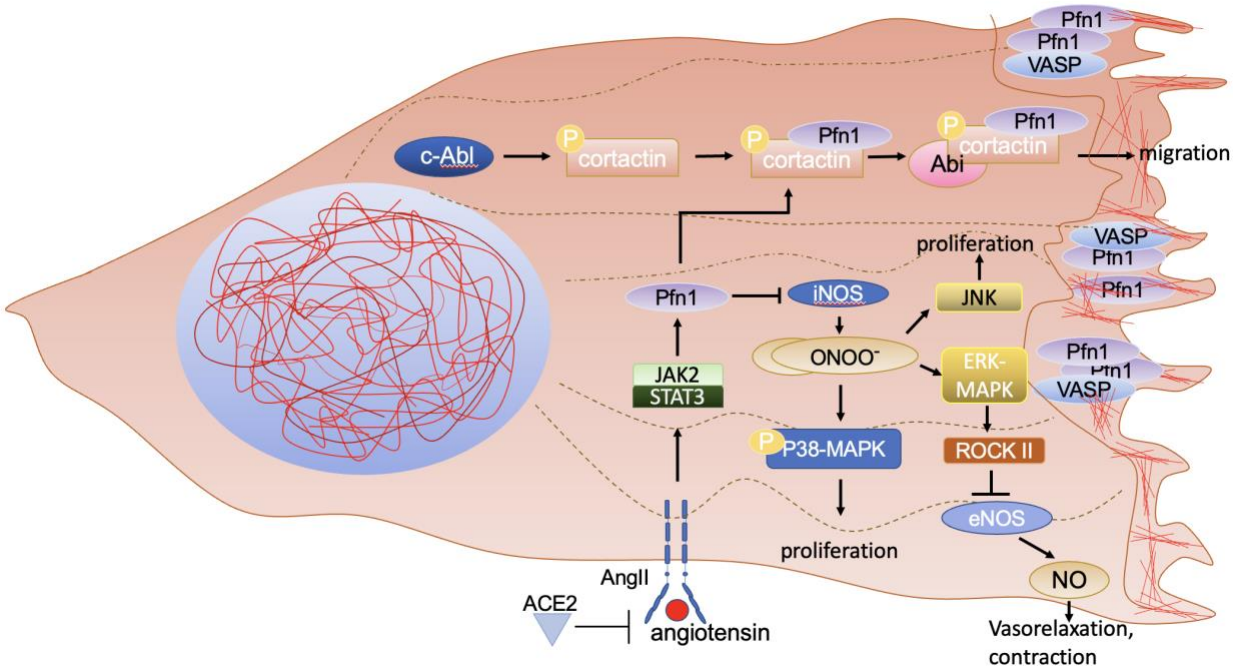

Figure 3. Pfn1's role in hypertension.

Hypertension is characterized by VSMC migration, proliferation, and hypertrophy. Angiotensin II induction may lead to elevated Pfn1 expression and facilitate overactivation of hypertrophic signaling pathways. Increased Pfn1 increases actin polymerization and thus activation of ERK, p38, and ROCKII, that promote VSMC proliferation and contraction. Activation and transport of Pfn1 to the leading edge by Abi/cortactin is mediated through PPI interaction, causing VSMC migration.

1.5.3 Diabetes

Diabetes and dyslipidemia are major risk factors for atherosclerosis. Approximately one third of the adult population (both male and female) in the United States is considered obese

(BMI>30)[135], and 12-14% of the U.S. adult population may be afflicted by diabetes[136]. Diabetes, given its endothelial and vascular abnormalities, predisposes patients towards atherosclerosis-related mortality and morbidity[137]. Alongside atherosclerosis, endothelial dysfunction is a contributing factor to diabetic vascular disease. For instance, type 2 diabetics with no history of heart attack have the same likelihood as a non-diabetic who has suffered a heart attack[138]. Additionally, insulin has an anti-atherogenic effect in *ApoE*$^{-/-}$ mice, as insulin reduces peroxide and cholesterol production by macrophages[138].

Indeed, Pfn may be a factor contributing to development of diabetes[139]. Profilin-like protein may be involved in blood glucose regulation[140]. Further, obese women observed in a proteomic study of protein content of adipose tissue had elevated Pfn1 expression, specifically in elderly patients[141]. In mesangial cells, exposure to high glucose leads to an increase in Pfn1 expression[142]. In an *in vivo* diabetic study, high fat diet (HFD) in C57BL/6J mice led to elevated Pfn1 expression in epididymal and white adipose tissue[112]. PfnHet mice fed HFD had blunted inflammatory cytokines, decreased accumulation of macrophages in adipose tissue, and preserved regulatory T cells[112]. These data provide preliminary evidence for a role mediated by Pfn1 in diabetes, specifically in blunting inflammatory response.

An early indicator of both forms (type I and II) of diabetes is diabetic retinopathy[53]. Pfn1 is elevated in the diabetic retinal or aortic endothelial cells[54]. In this capacity, elevated Pfn1 contributes to proliferation of microvessels in the retina, which may be balanced by preventing onset of elevated Pfn1 expression[143]. In rats with diabetic retinopathy, angiopoietin-like protein-4 (ANGPTL-4; a regulator of inflammation and angiogenesis) is elevated, leading to activation of the Pfn1-signaling pathway and induction of diabetic retinopathy[55]. 7-ketocholesterol (oxysterol) was used to stimulate endothelial cells, eliciting Pfn1 expression as well as recruitment

of STAT3 and other coregulatory factors to the profilin promoter at the oxysterol sensitive site[144], [145].

Additionally, a key cause of mortality and morbidity in diabetes, diabetic cardiomyopathy, may be regulated in part by Pfn1[146]. Pfn1 overexpression triggered elevated ICAM-1 expression and reduced VASP phosphorylation, as well as endothelial cell apoptosis in cultured rat aortic cells[147]. While LDL and oxysterols lead to Pfn1 overexpression, inhibiting Pfn1 synthesis limits LDL-mediated ICAM-1 expression[147]. Exogenous AGEs (influence inflammation and endothelial dysregulation) delivered to Sprague-Dawley rats initiated cardiac dysfunction, which was reduced in Pfn1-knockdown rats[148]. AGEs-treated HUVEC had induction of Pfn1 expression, alongside increased activation of the RhoA/ROCK pathway[149]. RhoA appears to further activate ROCK as well as its targets mDia and Pfn1, leading to endothelial dysfunction observed in diabetic retinopathy[150]. Additionally, when ROCK activation is inhibited, AGE-induced cardiac hypertrophy is mitigated, and Pfn1 overexpression is reduced. These findings suggest that Pfn1 signaling pathways play an essential role in the development and perpetuation of diabetes as per Figure 4.

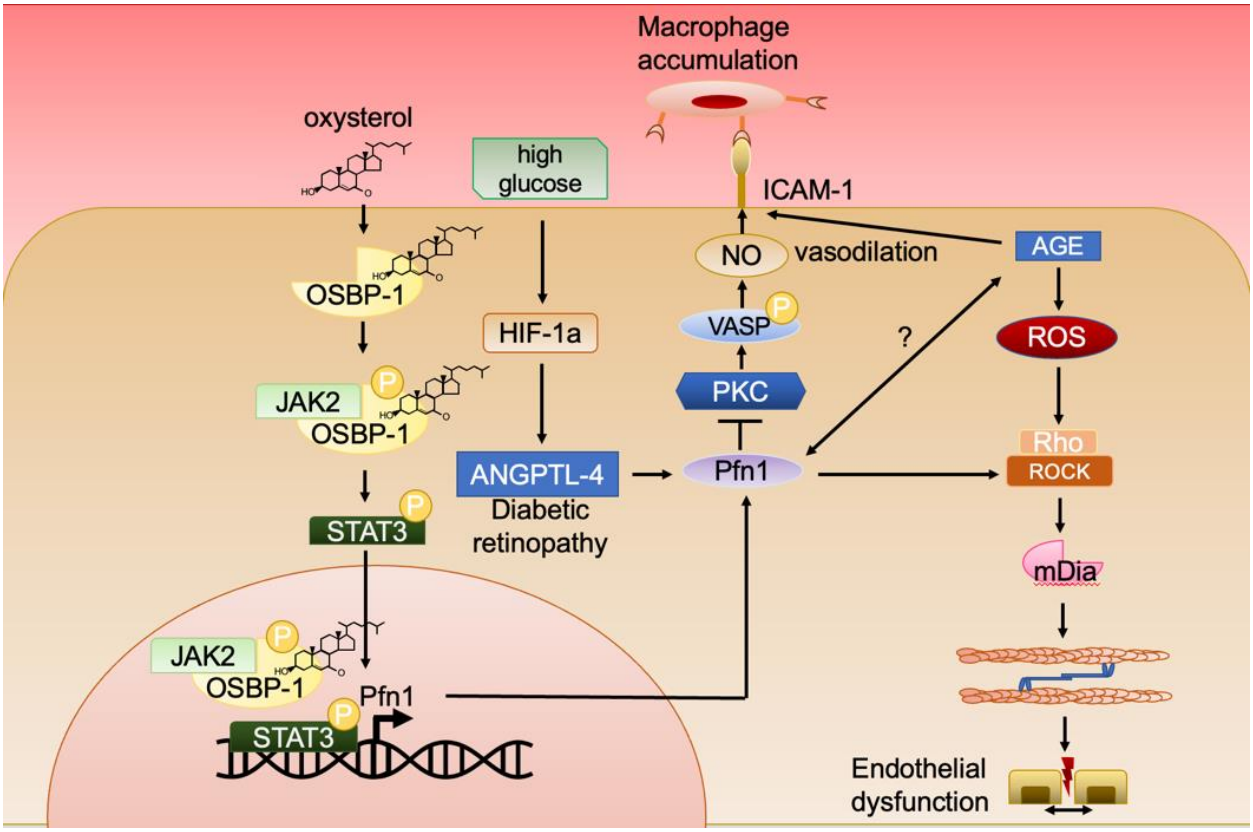

Figure 4. Pfn1's role in diabetes is multilayered.

Elevated oxysterol present in diabetes binds OSBP-1, leading to Jak2 binding and phosphorylation of OSBP-1 at Tyr-394. OSBP-1-Jak2 binding complex then facilitates binding, Jak-mediated phosphorylation and activation of STAT3, and translocation into the nucleus. STAT3 is thus primed to bind the Pfn1 promoter and stimulate gene expression. In diabetic retinopathy, high glucose and HIF-1a activation lead to angiopoietin-like protein-4 (ANGPTL-4) elevation and Pfn1 signaling pathway activation. Pfn1 activation may then reduce PKC activation, blocking VASP phosphorylation and activation. Reduced VASP phosphorylation and reduced NO signaling may facilitate elevated vasodilation, ICAM-1 binding and macrophage accumulation, though the specific mechanism is not yet clarified. Inflammation also plays a key role in diabetes. Production of AGE enables ROS production and Rho/ROCK activation. Aberrant Rho/ROCK/mDia signaling perturbs actin cytoskeleton assembly, causing vascular permeability and endothelial dysfunction. AGE also stimulates ICAM-1 expression, providing a potential mechanism for increased ICAM-1 expression present in diabetes. As AGE both promotes and is promoted by Pfn1 expression, a feedforward signaling loop is likely present, though the specific mechanism is not clear.

1.6 Hypothesis and Specific Aims

Pfn1 has been revealed as a key regulator of pathogenic response in cardiovascular disease, solid tumors, and neurological disorders[53], [54], [65], [88], [110], [111], [151]–[153]. While there is an established correlation between variable Pfn1 expression and disease development, further research is required to investigate the mechanistic role of cell-type specific Pfn1 expression in pro-inflammatory and immunomodulatory regulation. Specifically, preliminary findings in a postnatal endothelial Pfn1 depleted model showed dramatic reduction in vascularization, offering a promising target to limit aberrant vascularization in heavily vascularized disorders (solid tumors, cardiovascular diseases). Previous research from our lab has investigated constitutive single-allelic endothelial cell-specific Pfn1 depletion, and existing research on the role of Pfn1 in the chronic inflammatory condition of atherosclerosis does not clarify a cell-type specific role[110], [154]. An immunomodulatory role for Pfn1 is supported in vascular disorders [47], [110]–[112], [155], though the role of a total KO endothelial-cell *in vivo* model requires further investigation in both an acute (short term Pfn1 depletion) and chronic (long-term Pfn1 depletion paired with inflammatory stimulus) setting. It stands to reason that reduced Pfn1 in vascular cells such as endothelial cells would promote an anti-inflammatory response. However, the role of endothelial Pfn1 depletion in acute and chronic inflammatory settings is not clear. As such, I hypothesize that *endothelial Pfn1 is a regulator of inflammatory response.*

Specific Aim 1: Investigate the immunomodulatory role of vascular endothelial loss of Pfn1 *in adult mammals*.

Specific Aim 2: Determine the consequence of vascular endothelial loss of Pfn1 *on atherosclerosis development.*

The aims specified in this dissertation will illuminate a cell signaling role for endothelial Pfn1 *in vivo* that has not yet been elucidated. By investigating the role of endothelial Pfn1 in acute (10-18 days post-gene deletion) and pathogenic (atherosclerosis progression) settings, we will unveil a key function of endothelial Pfn1 at the molecular level. These studies will provide a molecular understanding of Pfn1's regulatory role in endothelial: immune cell interaction, and further existing knowledge of vascular endothelial Pfn1 as an immunomodulatory protein. Additionally, studies conducted in the atherosclerotic setting provide a preliminary basis for endothelial-specific Pfn1 loss in the pathogenic context *in vivo*. Understanding a cell-type specific function for Pfn1 also underscores its utility as a potential therapeutic modality and will support future investigation into pharmaceutical remediation measures for Pfn1 in cardiovascular diseases. Research that has been published are noted in this dissertation (Chapter 1, 3), with preliminary studies conducted in Chapter 4 under review.

2.0 Materials and Methods

2.1 Cell Culture

Generation and culture conditions of hTERT-immortalized mouse EC bearing floxed-Pfn1 alleles have been described recently (25). For Pfn1 gene deletion, ECs were infected with either Ad-GFP (control) or Ad-Cre (also has a GFP reporter: Vector Biolabs, Malvern PA) at 400 MOI. Media was changed 24hr after infection, and ECs were used for experiments 5-6 days after initial infection. ECs were serum-starved for 24 hours prior to CM collection. Murine VHL-deleted variant of RENCA (referred to as RVN cells) [8] cells were cultured in DMEM with 10% (v/v) FBS and antibiotics. Human VHL-negative 786-0 cells (source: ATCC) were cultured in RPMI-1640 media supplemented with 10% (v/v) FBS and antibiotics. HmVEC-1, a widely used immortalized human dermal microvascular EC line (ATCC; CRL-3243 – referred to as VEC), were cultured in MCDB-131 (Life Technologies; Carlsbad, CA) growth medium supplemented with 10% (v/v) FBS, antibiotics, 10 ng/mL EGF, 1µg/mL Hydrocortisone and 10 mM L-Glutamine. For adenovirus infection, cells were plated, allowed to attach and then infected with adenovirus encoding either GFP (Ad-GFP) or Pfn1 (Ad-Pfn1) at a MOI of 500 for 24h, before further incubation for an additional 48h in fresh culture media prior to use. For knockdown studies, cells were transfected with 50 nM of either smart-pool control or Pfn1 siRNA for 72h as previously reported [9].

Primary bone marrow derived monocytes (BMDM) were centrifuged out of long bone collected from C57BL6/J mice at maximum speed (>8000g) for 3 minutes and collected bone marrow was filtered and plated overnight in MEMα without nucleosides supplemented with 10%

v/v fetal bovine serum (FBS) (Corning, Corning NY), and 100U/mL Penicillin, 100μg/mL Streptomycin (Sigma- Aldrich, Burlington MA). Non-adherent cells were collected the next day and stimulated with 10ng/mL mCSF (R&D Systems, Minneapolis MN) for 7 days to produce M0 macrophages. After 7 days, macrophages were replated and exposed to the CM derived from EC with or without additional stimulation of 100ng/ml IFNγ (Peprotech, Cranbury NJ) for 24 hrs.

2.2 Cell Migration

For transwell migration experiments, 25,000 RVN cells were plated in triplicate in the upper chamber of 8.0 μM transwell plates in the serum-free media, and allowed to migrate either towards a 10% FBS gradient or VEC-conditioned media established in the lower chamber for 20h (control wells contained serum-free media in the lower chamber as well). Non-migrating cells in the upper chamber were removed by swabbing; transmigrated cells were fixed in 3.7% formaldehyde and then stained with DAPI. Images were acquired at 10 random fields at 10X magnification for enumeration of nuclei using ImageJ. For cell proliferation assay, one-thousand RCC cells were plated per well in 96-well plates using quadruplicate determinations, with proliferation assessed by time-course analyses of DAPI-stained nuclei based on images acquired over 3 to 5 random fields per well.

2.3 Animal Studies

$Pfn1^{flox/flox}$ mice (kindly provided by Dr. Reinhard Fassler, Max Planck Institute) were crossed with CDH5-Cre-ERT2 mice (kindly provided by Dr. Ralf Adams, Max Planck Institute) to generate $Pfn1^{flox/flox}$-Cre-ERT2 mice. Cdh5-Cre- ERT2:$Pfn1^{flox/flox}$ mice, as described in our previous study[151], were backcrossed into BALB/C background for 6 generations prior to experimental studies. Pfn1 gene excision was performed by intraperitoneal injection of 100 μl TMX (dissolved in peanut oil at a concentration of 10 mg/ml) daily over a course of five days in 5-6 week-old mice. Details of genotyping primers and PCR-based genotyping details to confirm floxed alleles of Pfn1, Cre, and Cre- mediated excision of Pfn1 were previously described[154]. Animals were euthanized for whole blood isolation by cardiac puncture and harvesting of various organs of interest (lung, liver, kidney, heart, and spleen). All animal experiments were conducted in compliance with an approved IACUC protocol according to University of Pittsburgh Division of Laboratory Animal Resources guidelines. Pups were subjected to daily intragastric injection of 50μl of 2 mg/ml tamoxifen (to excise Pfn1 gene in Cre-positive animals) over a course of 3 days (from either P0-P2 or P2-P4) and kidneys (P8-P10) were collected from age-matched wild-type (WT) and homozygous pfn1 knockout mice for histological staining.

CDH5-Cre-ERT2:$Pfn1^{flox/WT}$ mice, as described in our previous study[54], [156], were backcrossed into C57BL6/J background for experimental studies in a pro-inflammatory background. Partial Pfn1 gene excision and ablation was performed by intraperitoneal injection of 100μl tamoxifen (dissolved in peanut oil at a concentration of 10 mg/ml) daily over a course of five days in 5-6 week old mice. Details of genotyping primers to confirm floxed alleles of Pfn1, Cre, and Cre- mediated excision of Pfn1 are described in [154]. One month after gene excision,

mice were subjected to intraperitoneal injection of $2x10^{11}$ PFU AAV8 encoding constitutively active mutant (D377Y) form of mouse PCSK9 (Proprotein convertase subtilisin/kexin type-9; referred to as AAV8-mPCSK9 from hereon; Vector Biolabs, Malvern PA) and fed a high-cholesterol diet (HCD - D12336i, Research Diets, New Brunswick NJ) for 3 months to develop atherosclerosis[157], [158]. Animals were euthanized for whole blood isolation by cardiac puncture and harvesting of various organs of interest (liver, heart, spleen, and long bone).

2.4 Cytokine and Lipid Analysis

Mouse serum (prepared from whole blood and further diluted with PBS at a 1:1 ratio) and mouse EC CM were probed for cytokine/chemokine expression levels by Luminex analysis by service provided by Eve Technologies (Calgary, AB Canada) using the MD32 (32-analyte murine discovery panel) panel. For mouse serum analyses, analyte values were normalized to the average of wild-type animals across litters. For CM analyses, analyte values were normalized to the corresponding average WT CM values per analyte basis.

Conditioned media were collected from the culture dishes following overnight incubation of cells in serum-free media. The collected media were filtered (0.45 μM size) and concentrated using a 10-kDa cutoff filter. The concentrate was reconstituted with 2× Laemmli sample buffer and boiled before being analyzed by gel electrophoresis.

Mouse serum (prepared from whole blood and further diluted with PBS at a 1:1 ratio) were probed for cytokine/chemokine expression levels by Luminex analysis by service provided by Eve Technologies (Calgary, AB Canada) using MD32 (32-analyte murine discovery panel) panels. For mouse serum analyses, analyte values were normalized to the average of wild-type animals within

litters. Lipid panel analysis was conducted for LDL, HDL, total cholesterol, and triglycerides by University of Pittsburgh Division of Laboratory Animal Resources (DLAR) (Idexx #6290, Westbrook ME) to confirm lipid elevation in atherosclerotic mice.

2.5 Flow Cytometry Analysis

Whole blood or spleen was passed through a 70μm cell strainer, treated with 1X RBC lysis buffer to reduce red blood cell contamination, and incubated with Brilliant Stain Buffer (BD Biosciences, San Jose, CA) to prevent signal overlap between blue and ultraviolet markers. Samples were stained with either a full panel of immune-cell specific antibodies or buffer only for 30 minutes at 4oC, spun, and fixed in fixation/permeabilization buffer overnight, followed by next-day intracellular factor staining for 30 minutes at room temperature (See supplementary table S3A for immune panel antibody and the respective dilution information). Samples were run on a Fortessa FACS Aria II and the data were analyzed by FlowJo (FlowJo Inc., Ashland, OR) software.

Whole blood, spleen, bone marrow, or thoracic aorta was passed through a 70μM cell strainer, treated with 1X RBC lysis buffer to reduce red blood cell contamination, and incubated with Brilliant Stain Buffer (BD Biosciences, San Jose, CA) to prevent signal overlap between blue and ultraviolet markers. Samples were stained with either full panel of immune-cell specific antibodies or buffer only for 30 minutes at 4oC, spun, and fixed in fixation/permeabilization buffer overnight, followed by next-day intracellular factor staining for FOXP3 for 30 minutes at room temperature (Table 1 for immune panel antibody and the respective dilution information). Samples were run on a Fortessa FACS Aria II and the data were analyzed by FlowJo (FlowJo Inc., Ashland, OR) software.

Table 1. Flow cytometric antibodies and dilutions. Source company and catalog number, along with preferred fluorophore, are provided.

Antigen	Fluorophore	Dilution	Catalog	Cat#
CD45.2	R718	1:50	BD Biosciences	567585
MHC Class II (IA/IE)	BV510	1:200	BD Biosciences	743871
CD11b	BV421	1:400	BD Biosciences	562605
F4/80	APC-Cy7	1:25	Biolegend	123118
Ly6G	BV786	1:200	BD Biosciences	740953
CD19	BUV395	1:100	BD Biosciences	563557
CD11c	BV650	1:100	BD Biosciences	564079
Ly6C	PE/Cy7	1:100	BD Biosciences	560593
CD8	FITC	1:200	BD Biosciences	553030
CD3	APC	1:100	BD Biosciences	565643
FOXP3	PE	1:50	BD Biosciences	560408
CD4	PerCP	1:100	BD Biosciences	553052

2.6 Immunohistochemistry and TEM Analysis

For CD31 immunostaining, paraffin-embedded tissue sections were deparaffinized by heating to 60ºC for 20 min, cleared via xylene and dehydrated in 100% ethanol. Sections were blocked for 10 minutes using Protein Block included in rabbit-specific HRP/DAB (ABC) Detection IHC kit (Abcam, ab64261) and slides were incubated overnight at 4ºC with primary anti- CD31 antibody (clone D8V9E, catalog no. 77699, Abcam, dilution 1:100). This was followed by incubation with a biotin-labeled anti-rabbit secondary antibody for 10 min, washing with PBS-Tween, and incubation with streptavidin-peroxidase for 10 min. The staining was then detected with DAB substrate by incubation for 5-6 min. Slides were counter-stained with hematoxylin for 2 min before dehydration, mounting, and imaging.

For IHC staining of kidney, tissues were paraffin embedded, sectioned, and stained using an antibody against CD31 as previously published[159]. In brief, tissue sections were blocked and

then incubated with CD31 primary antibody (catalog #553370, BD Biosciences) overnight. An anti-Rat ABC kit (catalog # PK-6104, Vector Laboratories) was utilized to visualize the stain, with sections then counterstained with hematoxylin. For Pfn1 IHC of RCC TMA, tissue sections were deparaffinized and rehydrated tissue sections were incubated overnight with the primary anti-Pfn1 antibody (clone EPR6304, catalog #ab124904, Abcam, dilution 1:100). For immunodetection of the primary antibody, a secondary biotin-labeled anti-rabbit antibody (catalog #ab97049, Abcam) and streptavidin-peroxidase conjugates (catalog #11089153001, Roche) were used. The staining was detected with the Pierce DAB Substrate Kit (catalog #34002, ThermoFisher). The slides were counterstained with hematoxylin before dehydration and mounting.

For hematoxylin and eosin (H&E) staining, the same initial steps were adopted before incubation of histosections with Mayer's hematoxylin (Lillie's modification) for 2-3 minutes. Slides were washed in deionized water, color adjusted with 5% glacial acetic acid, incubated with bluing reagent for 10-15 seconds, washed in DI, and stained with eosin for 2-3 minutes before dehydration and mounting. For apoptotic cell analysis, Click-IT TUNEL colorimetric kit (Invitrogen, Waltham, MA) staining was performed according to manufacturer-supplied protocol. Masson's Trichrome staining was performed by the McGowan Institute of Regenerative Medicine Histology Core at the University of Pittsburgh. Masson's trichrome staining of aortic root sections were conducted by the Children's Hospital of Pittsburgh histology core.

For TEM, tissues were harvested and immersion fixed in 2.5% glutaraldehyde, 2% paraformaldehyde in PBS overnight at 4^{o}C. Following fixation, tissue were washed 3x in PBS then post-fixed in aqueous 1% OsO4, 1% K3Fe(CN)6 for 1 hour. Following 3 PBS washes, the tissue was dehydrated through a graded series of 30-100% ethanol, 100% propylene oxide then infiltrated in 1:1 mixture of propylene oxide:Polybed 812 epoxy resin (Polysciences, Warrington, PA) for 1

hr. After several changes of 100% resin over 24 hrs, tissue was embedded in molds, cured at 37°C overnight, followed by additional hardening at 65°C for two more days. Ultrathin (60 nm) cross-sections of liver or kidney were collected on copper grids, stained with 1% uranyl acetate for 10 minutes, followed by 1% lead citrate for 7 min. Sections were imaged using a JEOL JEM 1400 Flash transmission electron microscope (Peabody, MA) at 80 kV with a bottom-mount AMT 2k digital camera (Advanced Microscopy Techniques, Danvers, MA).

Histology services were performed by University of Pittsburgh McGowan Institute for Regenerative Medicine histology core. Briefly, cardiac tissue was fixed overnight, maintained in 30% sucrose, and excess cardiac tissue was cut up to the aortic root and cleaned of excess tissue and embedded in OCT for sectioning. 5-10μM sections were cut until the aortic root could be appropriately visualized. These sections were stained for Oil Red-O to visualize lipid accumulation, and Masson's trichrome to visualize the fibrous cap and collagen deposition. These services were performed by the University of Pittsburgh histology core. Total plaque was identified by dark-red area present in Oil Red O staining. Fibrous cap was identified as darkly stained layer present around necrotic core (situated between vascular wall and fibrous cap).

2.7 Immunoblot

Total cell lysate (TCL) was collected using a modified RIPA buffer (25 mMTris- HCl, pH 7.5, 150 mM NaCl, 1% (v/v) Nonidet P-40, 5% (v/v) glycerol), 1 mM EDTA, 50 mM NaF, 1 mM sodium pervanadate, along with 6x sample buffer with SDS diluted to 2% in final buffer. TCL was run on an SDS-PAGE and immunoblotted using antibodies specific for Pfn1 (Abcam, ab124904;

1:3000)), IRF7 (Cell Signaling Technology, Danvers MA, 72073; 1:1000), p-IRF7 (Cell Signaling Technology, 24129; 1:1000), STAT1 (Cell Signaling Technology, 9172; 1:1000), p-STAT1 (Cell Signaling Technology, 9167; 1:1000) and GAPDH (Sigma-Aldrich, G9545; 1:2000).

Isolated liver was cut, digested, and sonicated in lysis buffer for 1 min and spun for 30 min at >8000g. Total tissue lysate was collected using a modified RIPA buffer (25 mMTris- HCl, pH 7.5, 150 mM NaCl, 1% (v/v) Nonidet P-40, 5% (v/v) glycerol), 1 mM EDTA, 50 mM NaF, 1 mM sodium pervanadate, along with 6x sample buffer with SDS diluted to 2% in final buffer. Liver protein lysate was run on an SDS-PAGE and immunoblotted using antibodies specific for LDLR (BioLegend, ab124904; 1:200), GFP (Living Colors, Takara Biotech, San Jose CA, 632375; 1:2000), and GAPDH (Sigma-Aldrich, G9545; 1:2000).

2.8 Gene Expression Analysis

For assessing Pfn1 expression in ECs in vivo, single cell isolate was collected by collagenase-mediated kidney digestion and labeled with MACS mouse CD31 magnetic beads (130-097-418, Miltenyi Biotec; Gaithersburg MD) prior to isolation using magnetic LS columns according to manufacturer's recommended protocol. Unlabeled effluent was collected as a negative control. To assess gene expression in circulating myeloid populations, whole blood was labeled with MACS mouse F4/80 beads (130-110-443, Miltenyi Biotec) and isolated using LS columns. Cellular RNA was extracted using Qiagen RNeasy Mini Kit (Qiagen, Valencia, CA) as per the manufacturer's protocol. Complementary DNA (cDNA) synthesis from the extracted RNA was then performed using the Qiagen QuantiTect Reverse Transcription kit (Qiagen, Germantown MD) using the Applied Biosystems Veriti Thermal Cycler (Applied Biosystems, Waltham MA) following the

manufacturer's instructions. Collected cDNA was amplified using SYBR Green Gene Expression Master Mix on the StepOnePlus real-time PCR system (Applied Biosystems) using primers for specific genes of interest. For product amplification, the plate was ramped to 50^{o}C for 4 min, followed by 2 min at 95oC pre-amplification cycling. Cycling conditions of 95^{o}C for 20s, 49.7^{o}C for 25s, and 95^{o}C for 50s were used for 60 cycles (see Table 2).

Table 2. Primer sequences for qRT-PCR analyses of genes of interest.

Gene	Primer sequence	Amplicon size
IL6	F: 5'— CTG CAA GAG ACT TCC ATC CAG—3' R: 5'— AGT GGT ATA GAC AGG TCT GTT GG—3'	131
Pfn1	F: 5'—CGA GAG CAG CCC CAG TAG CAG C—3' R: 5'—ACC AGG ACA CCC ACC TCA GCT G—3'	180
18S	F: 5'—GCA ATT ATT CCC CAT GAA CG—3' R: 5'—GGC CTC ACT AAA CCA TCC AA—3'	123
GAPDH	F: 5' – CGG AGT CAA CGG ATT TGG TCG TAT – 3' R: 5' – AGG CTT CTC CAT GGT GGT GAA GAC – 3'	307

2.9 RNA sequencing

Total RNA was submitted to Azenta Genewiz (Burlington, MA) for quality control analyses, preparation of multiplexed paired-end libraries, polyA selection, and sequencing on an Illumina platform with 20-30 million reads per sample. FASTQ data processing and downstream analyses are described in detail in our recent study[156].

2.10 Statistics

All statistical tests were performed using GraphPad Prism 9 software. Normality was assessed before statistical analysis to determine use of either standard parametric or in the case of non-normal data non-parametric statistical analysis. For experiments with small sample size and non-normal distribution of data, non-parametric Mann-Whitney u-test was used for statistical comparison of data between the groups. For experiments involving a larger sample size and normal sample distribution, an unpaired t-test was used. Two-way ANOVA was used for multiple group comparison in lipid panel analysis. A p-value less than 0.05 was considered to be statistically significant.

3.0 Vascular Endothelial Cell-Specific Disruption of the *profilin1* Gene Leads to Severe Multi-Organ Pathology and Inflammation Causing Mortality

All research content of this section is published excluding Figure 5. Figure 6 *is published in a separate article.*

Reference: **Abigail Allen-Gondringer**, David Gau, Christopher Varghese, David Boone, Donna Stolz, Adriana Larregina, Partha Roy. "Vascular endothelial cell-specific disruption of the profilin1 gene leads to severe multiorgan pathology and inflammation causing mortality", *PNAS Nexus*, Volume 2, Issue 10, October 2023, pgad305

Figure 6 *Reference*: **Abigail Allen,** David Gau, Paul Francoeur, Jordan Sturm, Yue Wang, Ryan Martin, Jodi Maranchie, Anette Duensing, Adam Kaczorowski, Stefan Duensing, Lily Wu, Michael T. Lotze, David Koes, Walter J. Storkus, Partha Roy "Actin-binding protein profilin1 promotes aggressiveness of clear-cell renal cell carcinoma cells", *Journal of Biological Chemistry*, Volume 295, Issue 46, November 2020, P15636-15649

Specific Aim 1: Investigate the immunomodulatory role of vascular endothelial loss of Pfn1 in adult mammals.

3.1 Introduction

Profilins (Pfn) make up a set of 14-17kDa proteins originally identified for their role in G-actin sequestration and regulation[2], [160]. While expression level varies per isoform, only Pfn1 is ubiquitously expressed in almost all (excluding skeletal) mammalian cell types, with Pfn2 typically present in neural cells and Pfn3 and Pfn4 present in further restricted quantities[161], [162]. In addition to Pfn1 regulation of actin dynamics, Pfn1 is known to interact with poly-L-proline (PLP) domains, as well as membrane-based phosphoinositides (PPIs), even branching into the regulation of microtubule dynamics.[163]–[166]. Outside of physiological regulation of actin,

PLP binding, and PPIs, preliminary investigation has supported roles for Pfn1 activity in health and disease.

Chronic inflammatory conditions can lead to elevated Pfn1 expression in both experimental and clinical settings[110]–[112], [114], [147]. For example, an increase in serum Pfn1 is observed as disease severity increases in atherosclerotic patients[111]. In a global single-allele Pfn1 depleted mouse model, features of atherosclerosis including reduced foam cell accumulation, plaque size, and cell-adhesion molecule (CAM) expression were dramatically decreased in Pfn1 depleted mice[110]. While reduced Pfn1 expression has been shown to improve endothelial activity, barrier function and reduce contractility in endothelial cells[50], perturbed Pfn1 expression has also been demonstrated in diseases affecting immune cell activity[110]. Elevated Pfn1 has previously been shown as a negative regulator of cytotoxic T lymphocyte (CTL) function[155], and elevated Pfn1 expression is present in myeloid dendritic cells collected from severe aplastic anemia patients, potentially contributing to disease severity[167]. As such, it is not clear whether reduced immune infiltration and inflammation present in pathology is due to Pfn1 depletion within myeloid cells, reduced endothelial dysfunction due to Pfn1 perturbation within the vasculature, or whether there is some other mechanism of cellular crosstalk, such as that present between endothelial cells and immune cells.

Previous research conducted in our lab has demonstrated that, while Pfn1 is typically localized to the cytoplasm, some amount can be exported to the extracellular space[54], [168]. Increased migration of renal cell carcinoma cells (RCC) toward Pfn1 overexpressing endothelial cells has also been detected, with the reverse observed for Pfn1 depleted endothelial cells[54]. In rat glomerular mesangial cells, elevated Pfn1 expression is excreted from the cell, and may interact with an unidentified cell-surface receptor leading to signal transduction and downstream DNA

synthesis[169]. These data support the possibility that cellular crosstalk may be mediated through some paracrine mechanism, underlining the importance of a model to investigate cell-type specific effect of Pfn1 expression.

Efforts to generate a double-allele deleted Pfn1 mouse have failed to produce viable homozygous pups[170], either in the global deleted case or in an endothelial cell specific model[154]. This has been observed in other models (*Drosophila* and *Dictyostelium*)[171], [172], underpinning a need for Pfn1 expression during prenatal development. Unfortunately, a constitutive Pfn1 depleted model is likely not accessible. To address this shortcoming, a novel conditional endothelial Pfn1 depleted model (CDH5 CreERT2$^{+/-}$ Pfn1$^{flox/flox}$) has been used to assess diabetic retinopathy in post-natal mouse pups[151]. Retinal vascularization was dramatically reduced in knockout (KO) versus wild-type (WT) pups, allowing study of Pfn1 loss on post-natal vascular development[151]. However, an evaluation of endothelial and immune cell populations in adult mice is required to advance this model's utility in further pathologies (cardiovascular disorders, solid cancers, and other highly vascularized diseases). A model with conditional Pfn1 KO specific to endothelial cells will help to elucidate potential mechanisms of cellular crosstalk.

In our studies, we evaluated the overall survival, health, and metabolic profile of wild-type (WT) versus endothelial Pfn1 knockout (KO) mice. These data revealed reduced kidney and liver function, alongside ascites production both inside and external to the peritoneal cavity. Histological evaluation was conducted on selected tissues (kidney, liver) to investigate immune infiltrate and endothelial and morphological characteristics of WT vs. KO mice. Based on immune profile data, we posit that endothelial Pfn1 KO may contribute to immune cell infiltration and a more inflammatory phenotype of myeloid cells. Preliminary studies conducted on monocytes and

M0 macrophages show an increase in pro-inflammatory characteristics in cells treated with Pfn1 depleted media, with commensurate elevation of IL-6 in both endothelial and myeloid compartments with co-culture studies revealing a potential paracrine regulatory mechanism. Paracrine crosstalk between Pfn1 deficient EC may contribute to immune cell population maturation with a more polarized/inflammatory phenotype, potentially due to upregulation of IRF7/STAT1 signaling. These studies pave the way for a potential mechanism of action of EC Pfn1 loss, influencing cell-cell crosstalk and immune maturation.

3.2 Results and Discussion

3.2.1 Endothelial Pfn1 Deletion Dramatically Reduces Neovascularization

To build upon existing studies utilizing a Tie2-Cre $Pfn1^{+/-}$ heterozygous (Het) mouse model, early investigations relevant to this project utilized a newly generated CDH5 Cre-$ERT2^{+/-}$ $Pfn1^{flox/flox}$ (termed $Pfn1^{EC\text{-}KO}$) conditional vascular $Pfn1^{EC\text{-}KO}$ mouse model. CDH5 Cre-$ERT2^{-/-}$ $Pfn1^{flox/flox}$ (termed $Pfn1^{WT}$) littermate controls were utilized as controls in all experiments. To circumvent embryonic lethality following total Pfn1 KO[170], tamoxifen (TMX) was intragastric injected from postnatal day 0 (P0) to P2, with kidney tissue collected between P8-10. Pfn1 gene excision was confirmed by presence of 700bp excision band (Figure 5A), and total and microvascularization were both visually (Figure 5B) and quantifiably (Figure 5C) reduced. As such, our early postnatal model provided *in vivo* support for vascular EC Pfn1 in regulating vascular networks, as its deletion limited neovascularization, that may suggest reducing EC Pfn1 as a potential target in highly vascular disease (solid cancers, cardiovascular disorders, endocrine

diseases, among others). However, pathological investigations classically require inciting inflammatory conditions conducted over a longer period in adult animals. Thus, we elected to conduct similar long-term studies in adult mice.

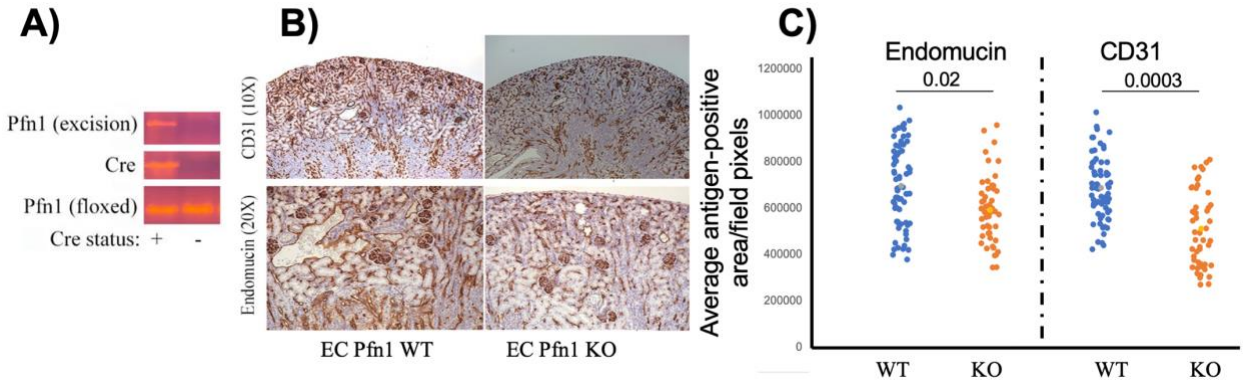

Figure 5. EC Pfn1 depletion in a post-natal (P8-10) mouse kidney model reduces total vascularization and microvascularization.

A) Pfn1 deletion at the gene expression level is validated by presence of 700bp Pfn1 excision band. B) CD31 (total vasculature) and endomucin (microvasculature) staining in EC Pfn1 WT and KO mouse kidney supports visual depletion of both vascular types. C) quantification of endomucin and CD31 staining provides statistical support for vascular depletion in in Pfn1^{EC-KO} mouse pups.

3.2.2 Endothelial Pfn1 Depletion Regulates Cancer Cell Migration Through Some Paracrine Mechanism

While an intrinsic cellular signaling role is apparent for EC Pfn1 in the context of vascular formation and regulation, a paracrine functionality for EC Pfn1 is not clear. To further investigate this possibility, a Transwell co-culture system consisting of RVN (RENCA-derive clear cell renal cell carcinoma cell line) in the upper well, with conditioned media collected from either Pfn1 OE (Figure 6A) or Pfn1 KD (Figure 6B) cultured ECs present in the lower well. Following overnight

transmigration, total cellular migration events were either elevated in the Pfn1 OE setting or reduced in the Pfn1 KD setting. This direct correlation between elevated Pfn1 and an activated migratory phenotype in renal cancer cells was intriguing, however, it did not directly support a regulatory role for extracellular Pfn1 or unveil its extracellular regulatory capabilities. To improve our understanding of the paracrine signaling function of EC Pfn1, we needed not only to improve our understanding of its function in the context of secreted factors, but also to investigate interaction potential in the context of other stromal cells (i.e. immune cell populations). While our available Transwell co-culture model illuminated a potential regulatory phenotype for EC Pfn1, it did not allow the opportunity to delve into heterogenous cell population analysis, secreted factors, tissue-specific and circulatory variation, and other parameters most effectively investigated in an *in vivo* model. Paired with our vascularization findings *in vivo*, as well as our preliminary *in vitro* findings in the Transwell setting, we elected to extend our studies to $Pfn1^{EC\text{-}KO}$ in adult mice to provide a complete picture of the inflammatory, immune, and tissue-specific setting present in the context of EC Pfn1 depletion.

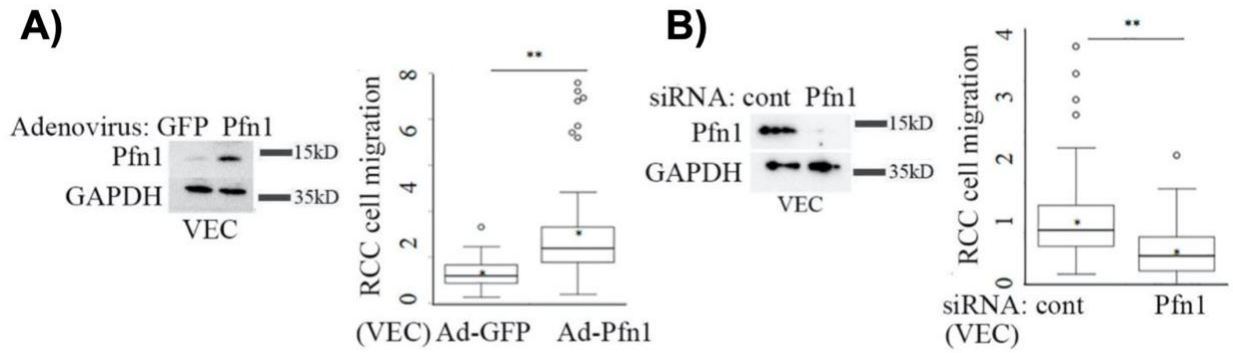

Figure 6. Effect of modulating Pfn1 expression in VEC on RCC cell migration.

A-B) Effects of conditioned media of Pfn1 overexpressing (A) and KD (B) cultures of VEC on chemotactic migration of RVN cells (migration data normalized to control adenovirus transduction or siRNA transfection condition). Pfn1 and GAPDH (loading control) immunoblots in panels C and E confirm Ad-Pfn1- and Pfn1-siRNA-mediated overexpression and KD of Pfn1, respectively (data summarized from 3 experiments). In the bar graphs, * and ** denote $p<0.05$ and $p<0.01$, respectively.

3.2.3 Endothelial Pfn1 is Effectively Depleted at the Gene Expression and Protein Levels

To substantiate EC Pfn1 depletion in an adult mouse *in vivo* model, we investigated Pfn1 depletion at the gene expression and protein levels in primary-derived endothelial cells collected from novel $Pfn1^{WT}$ and $Pfn1^{EC\text{-}KO}$ mice. CD31+ bead isolation of a single cell kidney isolates from mice 8-10 days following completion of 5-day TMX-injection course was conducted, with lysates collected for either RNA or total protein. qRT-PCR analysis revealed significant reduction of Pfn1 gene expression specifically in CD31+ sorted ECs as compared to effluent (CD31-) sorted controls (Figure 7A). This finding was further supported by Western blot analysis of CD31- effluent lysate versus CD31+ EC lysate, showing that Pfn1 is also specifically reduced at the protein level (Figure 7B). While incomplete EC Pfn1 depletion (at approximately 60% reduction) may seem

incongruous with complete gene KO expected for a Cre-flox model, this aligns with the expected level of gene depletion in kidney-specific tissue[173].

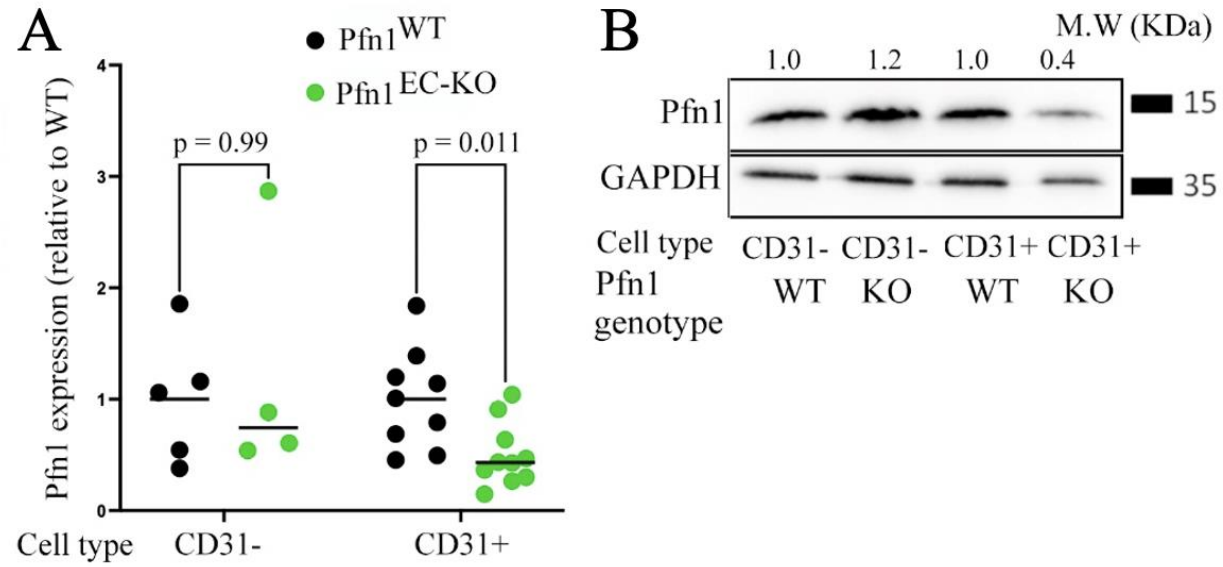

Figure 7. CDH5-CreERT2-driven Pfn1 depletion is selectively induced in endothelial cells.

A) Quantitative PCR-based evaluation of Pfn1 gene expression in CD31+ vs and CD31- (effluent sorted) single cell isolates from the kidney of $Pfn1^{EC\text{-}KO}$ mice relative to those from $Pfn1^{WT}$ mice. Each data point represents a single mouse. B) Immunoblot-based validation of downregulation of Pfn1 expression at the protein level in CD31+ but not in CD31- kidney cell isolates in $Pfn1^{EC\text{-}KO}$ mice (GAPDH blot serves as the loading control). The numbers indicate GAPDH-normalized Pfn1 band intensity in KO relative to the WT group for a given cell type.

3.2.4 Animal Survival is Dramatically Reduced Upon Endothelial Pfn1 Deletion

Prior to initiating long-term studies, we elected to observe general health markers, activity, and weight in our $Pfn1^{WT}$ vs. $Pfn1^{EC\text{-}KO}$ mice. We conducted a five-day time course of TMX injection, with first day of observation denoted as D1 (one day after completion of TMX injection).

From D1 onward, we attempted to collect weight data and general observations for up to 30 days. General observations of $Pfn1^{EC\text{-}KO}$ mice included scruffy coat, labored breathing, limited mobility in some cases requiring compassionate euthanasia only up to the 18-20 day mark. Intriguingly, at time of necropsy, $Pfn1^{WT}$ mice presented with normal size and coloration while $Pfn1^{EC\text{-}KO}$ mice presented jaundiced coloration and enlarged abdomen (Figure 8A) paired with elevated weight gain in $Pfn1^{EC\text{-}KO}$ mice up to approximately day 15 (Figure 8B). However, survival is dramatically reduced around 15 days post-TMX injection course (Figure 8C), in contrast to the apparent elevated weight gain and enlarged size of $Pfn1^{EC\text{-}KO}$ mice. At necropsy, gross observation of the extraperitoneal space revealed abdominal fluid accumulation indicative of ascites build-up and potential lipolysis[174], as well as hemorrhage (contributing factors to weight gain) in the thorax of $Pfn1^{EC\text{-}KO}$ mice in addition to cutaneous vascular bed perturbation (Figure 8D). Peritoneal cavity, GI tract, and liver were also notably reduced in size. While pathological features were clear, contributing tissue sources required further investigation. Isolation of liver from $Pfn1^{WT}$ and $Pfn1^{EC\text{-}KO}$ animals revealed significantly reduced liver weight, hemorrhage (Figure 8E-F, E right inset) alongside white threaded coloration and 3 to 5mm diameter yellow nodules (Figure 8E-F, E left inset), symptomatic of portal hypertension when paired with enlarged spleen. Similarly, kidney size was reduced in $Pfn1^{EC\text{-}KO}$ mice as compared to $Pfn1^{WT}$, supporting impaired kidney function (Figure 8E-F). As a result of these findings, a comprehensive metabolic panel was conducted on $Pfn1^{WT}$ and $Pfn1^{EC\text{-}KO}$ mice to unveil potential functional and metabolic defects in $Pfn1^{EC\text{-}KO}$ mice. A decrease in albumin, total protein, and globulin (metabolites contributing to kidney and liver function) support impaired function in $Pfn1^{EC\text{-}KO}$ mice as compared to $Pfn1^{WT}$, potentially due to reduced liver and kidney function (Figure 8G). Collectively, these findings suggest liver and

kidney as targets for deeper investigation and demonstrate an essential role for EC Pfn1 in retaining normal physiology and survival.

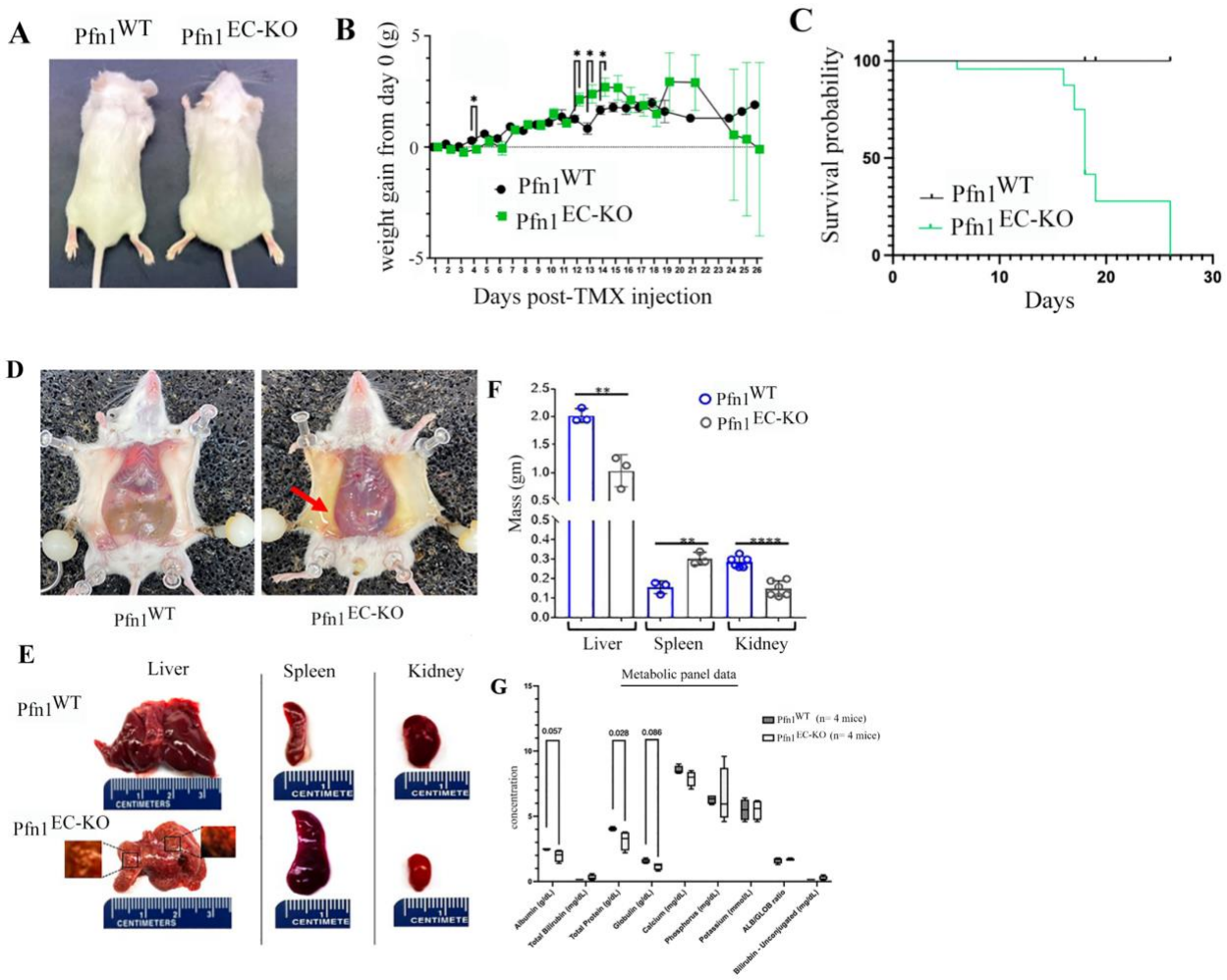

Figure 8. Loss of endothelial Pfn1 results in gross multi-organ pathology and compromises survival of mice. A) Representative images of Pfn1EC-KO and littermate control Pfn1WT mice on d18 following the last tamoxifen administration showing abdominal enlargement (indicative of ascites) in Pfn1^{EC-KO} mice. B) Relative weight gain profiles of Pfn1^{WT} (n=18) and Pfn1^{EC-KO} (n=20) mice until the day of sacrifice. C) Kaplan-Meir overall survival curves of Pfn1^{WT} (n= 7) and Pfn1^{EC-KO} (n=9) mice. D) Necropsy of mice on d18 revealing presence of peritoneal fluid (yellow) accumulation (arrow) in Pfn1^{EC-KO} mice. E) Liver, spleen, kidney, harvested from Pfn1^{EC-KO} and littermate control Pfn1^{WT} mice. The liver of Pfn1^{EC-KO} mouse is smaller than the one dissected from the littermate and presents pale nodules of 2-4 mm (*left inset*), which alternate

with areas of vascular congestion and sub-capsular hemorrhage (*right inset*). Middle panels show increase in size and congestion of the spleen from Pfn1^{EC-KO} mouse compared to that from the littermate. Right panels show a reduction in size of the kidney of Pfn1^{EC-KO} mouse compared to that from the littermate. F) Bar diagram illustrating the weight (means ± std. dev) of livers, spleens and kidneys from Pfn1^{EC-KO} and littermate control Pfn1^{WT} mice (n= 3 mice/genotype). G) Relative abundance of various serum analytes of Pfn1^{WT} and Pfn1^{EC-KO} mice based on the results of Idexx serum metabolic panel analyses. $^{**}p<0.01$, $^{***}p<0.001$, $^{****}p<0.0001$.

3.2.5 Histological Evaluation of EC Pfn1 KO Lung and Cardiac Tissue Reveals Mild Pathological Defects

In the gross histological analyses displayed in Figure 8, the main pathological features of Pfn1^{EC-KO} mice were observed in the heart, lung, liver, and kidney. Lung and cardiac tissue samples were collected between days 15 to 18 for Pfn1^{EC-KO} mice in comparison to their littermate controls. In Pfn1^{EC-KO} mice, lung tissue harvested on day 18 after the last TMX injection showed significant decrease of the airspaces, alveolar edema with extravasation of erythrocytes, capillaries filled with blood and cellular protrusion into the alveoli lumen without evident fibrosis (Figure 9A). Chronic disease features were more apparent in heart as compared to lung. In particular, the hearts from Pfn1^{EC-KO} mice showed areas of chronic infarcts by Masson's trichrome staining, with inflammatory infiltrate composed of mononuclear cells and extensive fibrosis apparent by way of H&E staining (Figure 9B). While cardiac tissue presented some sclerosis in Pfn1^{EC-KO}, developed histopathological features were not obvious in either tissue. It follows that more developed histological investigation was conducted in kidney and liver tissues due to metabolic panel results and gross histological evaluation.

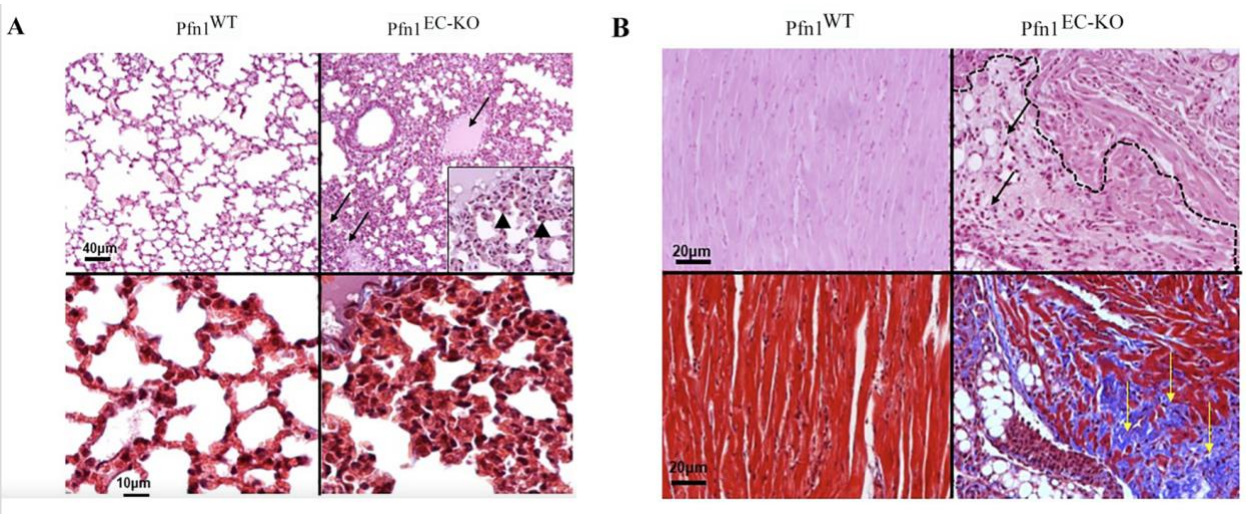

Figure 9. Histopathological findings in mouse lungs and hearts lacking endothelial Pfn1.

A) Upper panels are representative images of H&E staining sections from the lungs of Pfn1^{EC-KO} and littermate control Pfn1^{WT} mice harvested on d18 showing decrease of the airspace, alveolar edema (arrows), extravasation of erythrocytes and alveolar capillaries filled with blood and protruding in the alveoli (inset, arrowheads) in Pfn1^{EC-KO} lung. Lower panels are lung sections stained with Masson trichrome showing lack of fibrosis. B) Upper panels are representative images of H&E staining sections of the hearts of a littermate control Pfn1^{WT} mouse (left) showing healthy heart muscle, and a Pfn1^{EC-KO} mouse (right), with an area of chronic infarct (dotted line) with mononuclear cell inflammatory infiltrate (arrows). Lower panels are sections of the heart stained with Masson trichrome showing extensive fibrosis in the area of the heart infarct (arrows).

3.2.6 Histological Evaluation of Kidney Supports Late-Stage Perturbation of Tissue Function, Structure, and Immune Infiltration in EC Pfn1 KO Mice

Preliminary evaluation of gross histological features paired with reduced liver and kidney metabolites in Pfn1^{EC-KO} offered liver and kidney as tissues of interest for further investigation. First, H&E and Masson's trichrome histological analysis was conducted on kidney tissue. By H&E staining, histological analyses of the kidneys from Pfn1^{EC-KO} mice showed smaller glomeruli,

proliferation of mesangial cells and abundant deposit of mesangial matrix (Figure 10A) with no evidence for fibrosis (Figure 10B). Although relevant histopathological features are present, lack of sclerosis as evidenced by Masson's trichrome staining suggests later-stage or secondary defects in the $Pfn1^{EC\text{-}KO}$ kidney. CD31 immunostaining revealed a lack of capillaries in the cortical areas of the kidneys in $Pfn1^{EC\text{-}KO}$ mice; additionally, the glomeruli of $Pfn1^{EC\text{-}KO}$ kidneys showed a significant reduction in capillaries, and those that were present had the characteristics of immature neovessels (Figure 10C). To obtain a more granular understanding of endothelial cells and relevant stromal cells, transmission electron microscopy (TEM) was conducted to assess cellular characteristics. TEM analyses showed apoptosis of endothelial cells and podocytes, collapse of the urinary filtration space, and further confirmed increased number of mesangial cells and thickening of basal membranes observed by H&E staining (Figure 10D).

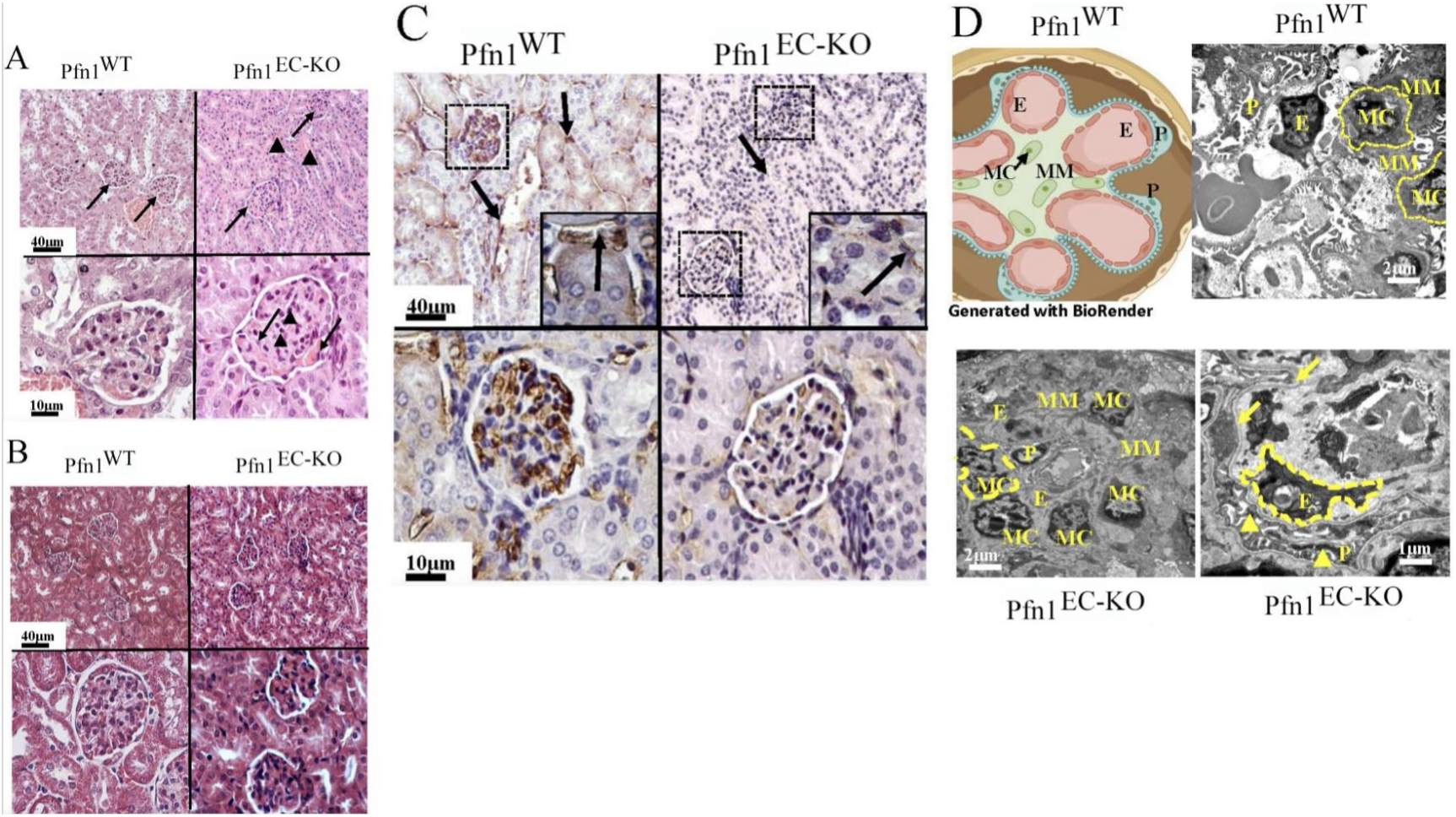

Figure 10. Histopathological findings in mouse kidneys lacking endothelial Pfn1.

A) H&E-stained sections of the kidneys of a littermate control Pfn1^{WT} (left) and a Pfn1^{EC-KO} mice (right). The glomeruli of Pfn1^{EC-KO} mice were smaller than those of the littermate controls (arrows), and the tubules showed apoptotic epithelial cells, edema and erythrocytes (arrowheads). Lower panels at higher magnification show proliferation of mesangial cells (arrowheads), eosinophil deposits and dead EC (arrows) in Pfn1^{EC-KO} mice. B) Masson

trichrome staining of kidney sections show absence of fibrosis. C) CD31 staining of kidney sections show normal vascularization of glomeruli (arrows) and surrounding the tubules (arrowheads) in littermate control $Pfn1^{WT}$ mouse (upper left panel). Upper right panel shows lack of mature capillaries in the glomeruli (arrows) and between tubules (arrowheads) in sections of kidneys from $Pfn1^{EC\text{-}KO}$ mice. Lower panels are high magnifications of glomeruli showing presence of mature blood vessels in the glomerulus of a $Pfn1^{WT}$ mouse (left) contrasting scarce endothelial cells with immature characteristics in the glomerulus of a $Pfn1^{EC\text{-}KO}$ mouse (right). D) Upper left: cartoon of a normal glomerulus (generated using the BioRender illustration software). Upper right panels are TEM images (X 5000) of a glomerulus from a $Pfn1^{WT}$ mouse showing normal endothelial cells (E), podocytes (P) and mesangial cells (Mc). Lower panels are images of a glomerulus from a $Pfn1^{EC\text{-}KO}$ mouse showing a high number of mesangial cells (arrows) and deposits of mesangial matrix (Mc) surrounding a collapsed capillary (dotted area). Lower right shows a capillary lined by apoptotic endothelial cells, thickening of the basal membrane (asterisk) and apoptotic podocytes.

3.2.7 Early Histopathological Features, Immune Infiltration, Sclerosis, and Necrosis Present in EC Pfn1 KO Liver

Following evaluation of cardiac, lung, and kidney tissue, liver offered an intriguing target of investigation for $Pfn1^{EC\text{-}KO}$ mice due to **1)** dramatic reduction in liver weight, **2)** developing portal hypertension, and **3)** reduction in functional liver metabolites. In the liver, the histopathological changes were observed only 10 days after the last TMX administration by H&E, which progressed significantly by day 18. On day 10, $Pfn1^{EC\text{-}KO}$ livers showed distorted acinar architecture (characteristic hexagonal portal vein structure) and collapsed sinusoids lacking both EC lining and Disse spaces. The hepatocytes were small and most of them presented cytoplasmic fat vesicles. There were areas of necrosis with inflammatory cellular infiltrates composed of mononuclear cells (Figure 11A). On day 18, EC Pfn1 KO livers showed extensive infarcts surrounded by fibrosis, vascular disturbance, and abundant centers of extramedullary hematopoiesis indicative of immature immune cell development (Figure 11A-B). There was a general defect in sinusoid development with several CD31-positive cells distributed throughout the hepatic functional tissue in a disorganized pattern and some of them with characteristics of immature vessels (Figure 11C). TEM analysis showed the presence of necrotic hepatocytes with cytoplasmic fat vesicles, extensive deposits of collagen, and isolated immature neovessels (Figure 11D). TUNEL staining further confirmed extensive apoptosis throughout the liver in $Pfn1^{EC\text{-}KO}$ mice (Figure 11E). Together, these microscopic and histological findings in $Pfn1^{EC\text{-}KO}$ mice demonstrate a severe defect in the development, expansion, and maturation of blood vessels. The expected defective blood circulation is consistent with pathological features including infarcts,

portal hypertension, neovessel formation, and inflammatory infiltrates, likely contributing to impaired liver and kidney function.

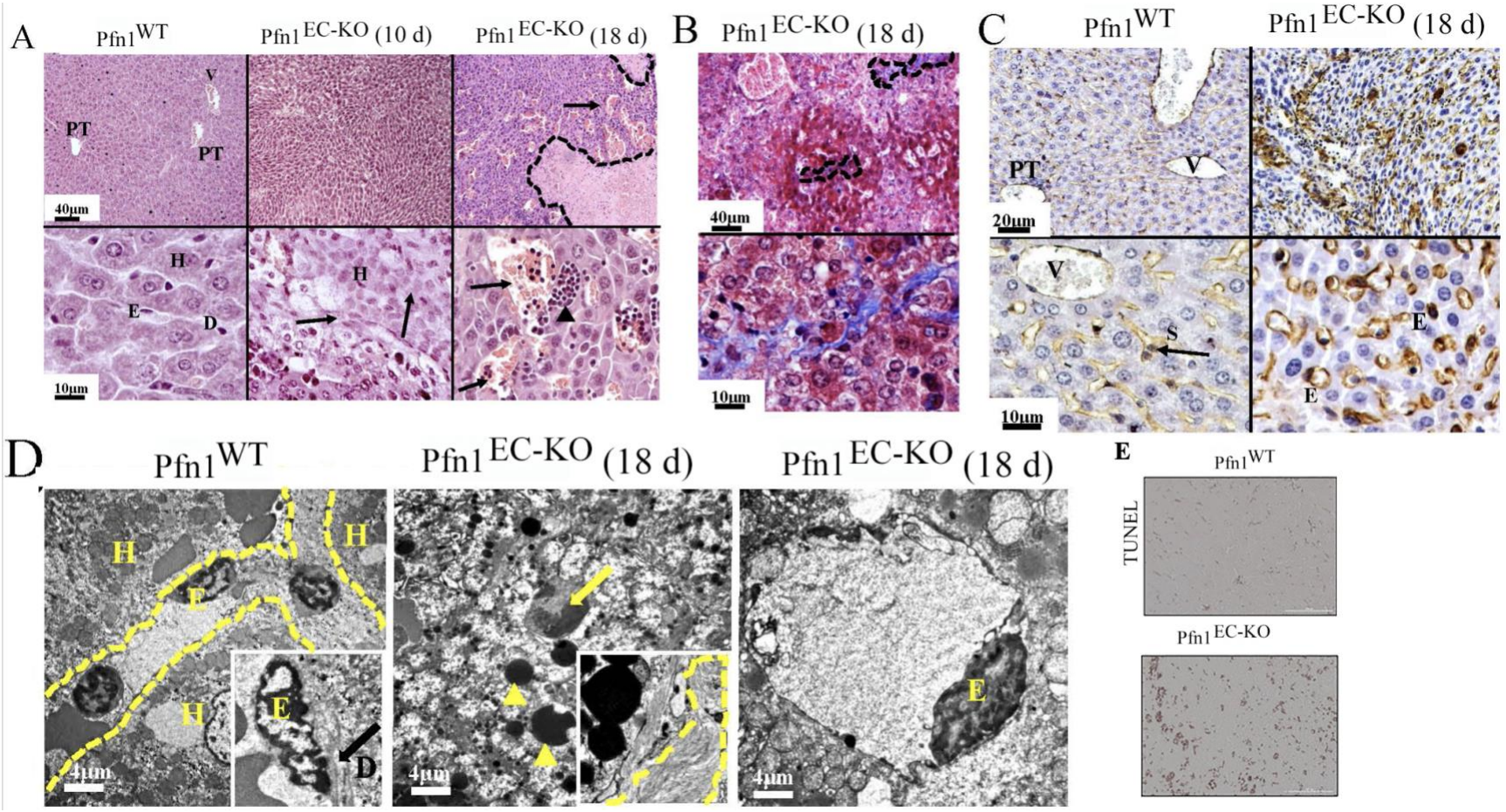

Figure 11. Histopathological findings in mouse livers lacking endothelial Pfn1.

A) Representative images showing normal liver histology (left) or the histopathological changes observed 10 d (center) or 18 d (right) after tamoxifen administration in $Pfn1^{EC\text{-}KO}$ mice. Upper left is a section of the liver from a littermate control $Pfn1^{WT}$ mouse illustrating the characteristic acinar units composed of the central vein, portal tracts and hepatocytes arranged radiating towards the central vein. Upper middle is a section of the liver of a $Pfn1^{EC\text{-}KO}$ mouse 10 d after administration of tamoxifen showing disruption of the acinar architecture, with areas devoid of central veins. Upper right is

a section of the liver of a Pfn1^{EC-KO} mouse 18 d after administration of tamoxifen showing ample areas of infarcts (dotted lines) with inflammatory infiltrates composed of mononuclear cells surrounded by angiectasias (arrow). Lower images at higher magnification. B) Representative sections stained with Masson trichrome of the livers in A, showing the presence of fibrosis in the liver of Pfn1^{EC-KO} mouse. C) Upper left, immunostaining with CD31 of a liver section from a littermate Pfn1^{WT} mouse showing the normal vascular architecture. Upper right immunostaining with CD31 of a liver section of a Pfn1^{EC-KO} mouse showing a disarrayed pattern that lacks the typical sinusoidal shape. Lower right is higher magnification of showing immature blood vessels without branches and lack of sinusoids. D) Upper left is a TEM image of the liver from a littermate Pfn1^{WT} mouse showing a sinusoid lined by EC and surrounded by alive hepatocytes. A higher magnification shows the nucleus of one endothelial cell, the space of Disse (arrow). Center is a TEM image of a liver from a Pfn1^{EC-KO} mouse showing necrotic hepatocytes and microvesicular fat accumulation. Right panels shows an isolated immature neovessel in the liver from a Pfn1^{EC-KO} mouse. E) TUNEL staining of day 18 liver tissue sections show extensive apoptotic cell death in Pfn1EC-KO liver (Scale bar – 100 mm) CV: central vein, D: Disse space, E: endothelial cells, H: hepatocyte, I: infarct, PT: portal tract, S: sinusoid

3.2.8 Examination of a Broad Immune Cell Population Panel Reveals Pro-Inflammatory Profile Following Late-Stage EC Pfn1 Depletion

Next, to determine potential global immunological impact of endothelial Pfn1 ablation *in vivo*, we performed comprehensive analyses of various immune cell subtype populations in peripheral blood and spleen harvested from mice at either the mid-stage (10-11 days after last TMX injection, generally normal histological findings) or the late-stage (18 days after last TMX injection, abnormal histopathology and maximum length of time for humane use) of EC Pfn1-depletion. A broad panel of immune cells (Table 1, further detail in methods) was used to assess immune cell development and maturation, granulocyte and T cell differentiation, and myeloid populations. When assessing total cell population levels, mid-stage immune profiling showed evidence for dramatically (up to ~10-fold) elevated total leukocytes, lymphocytes and monocytes in the peripheral blood but not spleen of $Pfn1^{EC\text{-}KO}$ relative to $Pfn1^{WT}$ mice (Figure 12A-B). End-stage immune profiling revealed a significant decrease in the total splenic counts of leukocytes and various sub-types of immune cells including neutrophils, macrophages, anti-inflammatory $Lys6C^{lo}$ monocytes, B cells and T-helper cells (Figure 12C), a finding that is consistent with portal hypertension and splenic dysfunction as observed in Figure 8. Although the total circulating leukocyte count normalized between the two groups in late-stage immune profiling, the total counts of $Lys6C^{lo}$ monocytes and adaptive immunity-associated cells (B cells and various T cells) showed a decline in $Pfn1^{EC\text{-}KO}$ animals (Figure 12D).

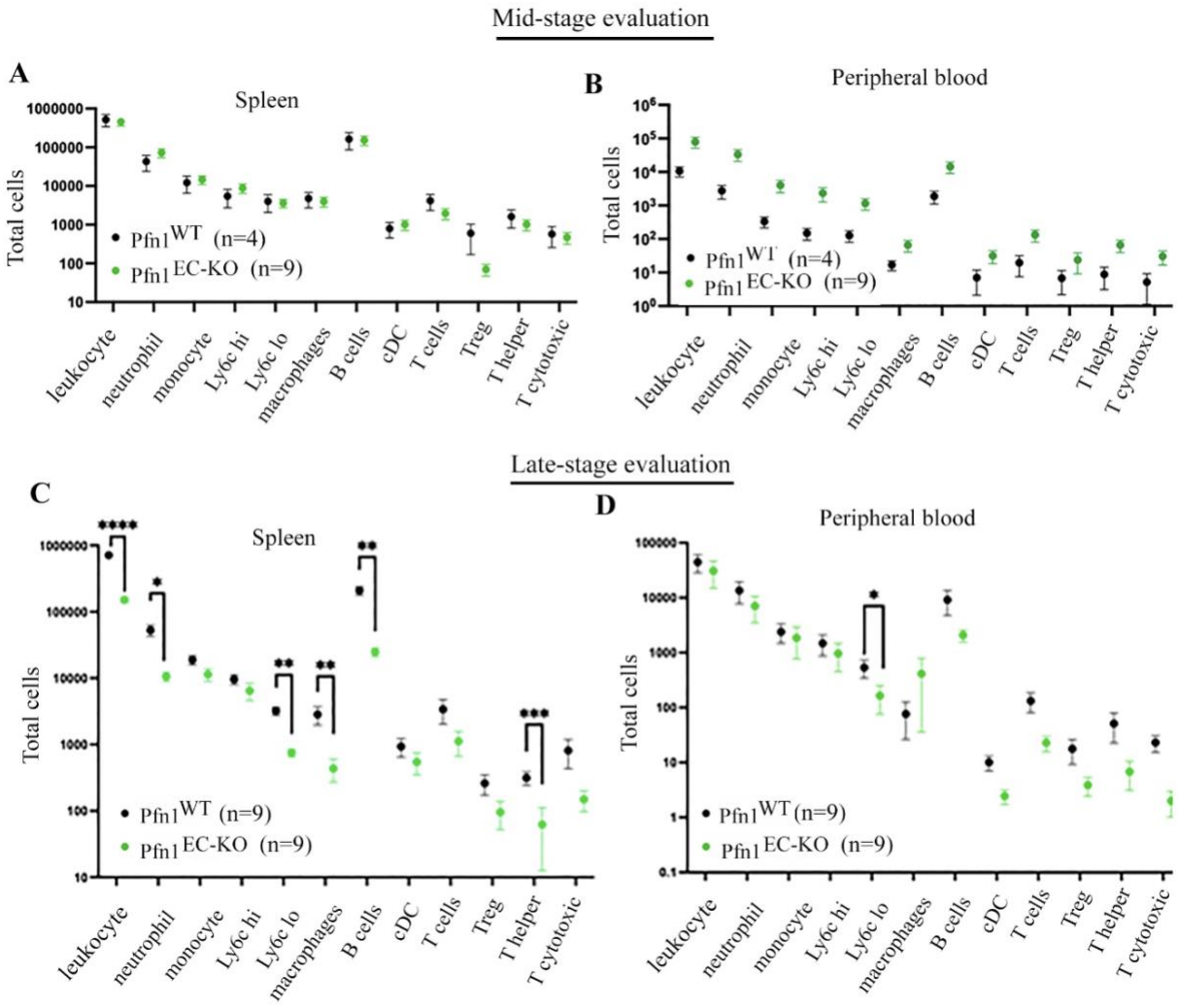

Figure 12. Flow cytometry-based assessment of total count of leukocytes and various immune cell subpopulations in the spleen and peripheral blood of Pfn1WT vs. Pfn1EC-KO mice at the indicated time-points ('n' indicates the number of animals in each group).

To compare across $Pfn1^{WT}$ and $Pfn1^{EC\text{-}KO}$ immune populations, individual immune cell subtype populations were normalized to total leukocytes quantified per mouse. When we specifically analyzed various subtypes of immune cells as a percent of total leukocytes, late-stage $Pfn1^{EC\text{-}KO}$ animals exhibited higher relative abundance of splenic monocytes (specifically $Ly6C^{hi}$ pro-inflammatory subtype) and circulating macrophages compared to $Pfn1^{WT}$ animals in a statistically significant manner (Figure 13). A greater proportion of pro-inflammatory $Lys6C^{hi}$

splenic monocytes, with concurrent reduction of anti-inflammatory Lys6C^{lo} pool in circulating monocytes alongside elevated macrophages, is further indicative of skewing of myeloid-derived sub-population of immune cells toward a pro-inflammatory phenotype in Pfn1^{EC-KO} animals. Given intriguing variation in myeloid population in Pfn1^{EC-KO} mice as compared to Pfn1^{WT}, we next elected to conduct a broad pro-inflammatory cytokine panel to investigate contributing inflammatory factors.

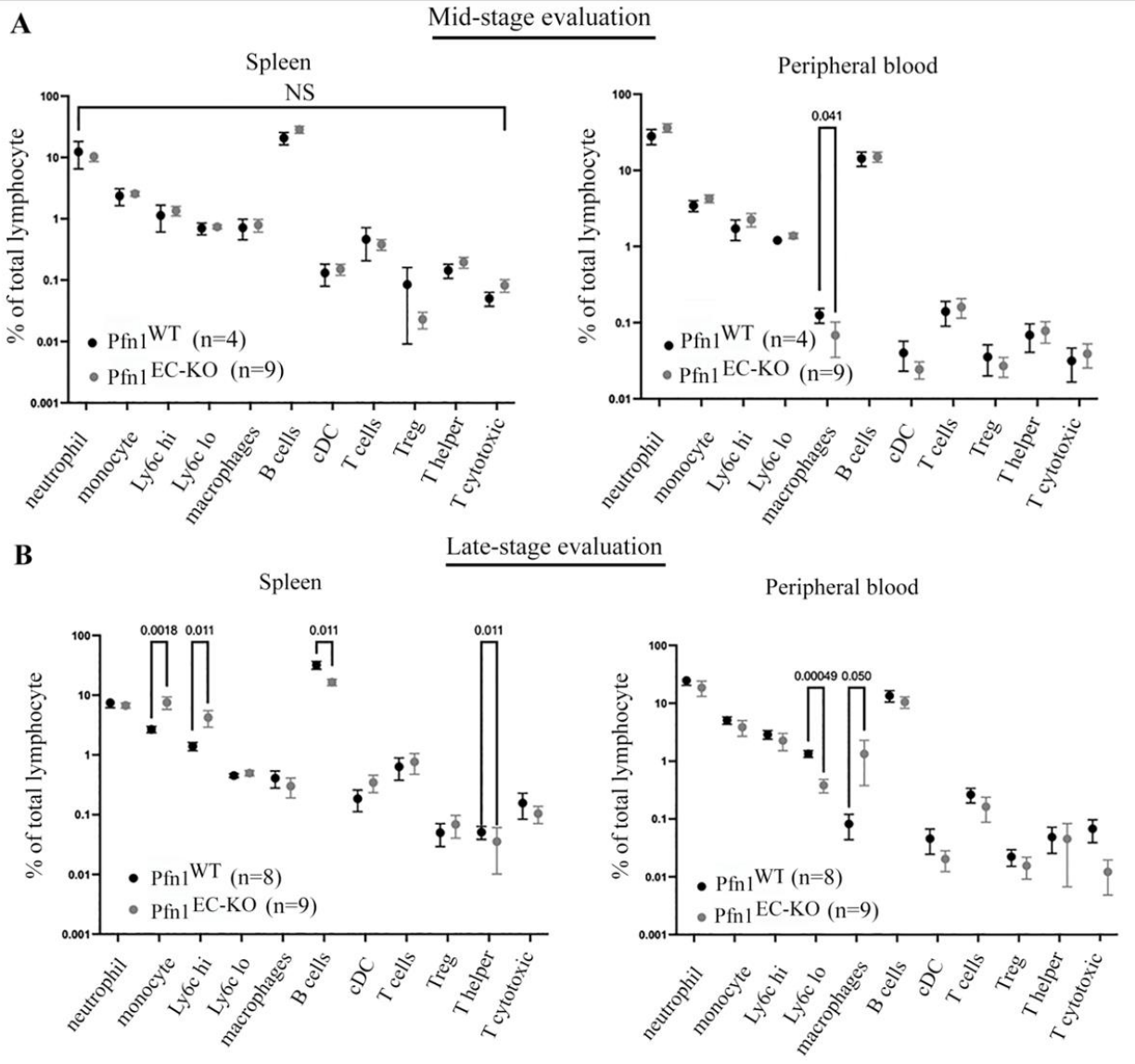

Figure 13. Effect of endothelial Pfn1 depletion on immunological profile in vivo.

Flow cytometry- based quantification of various subtypes of immune cells expressed as a percent of total lymphocytes in either spleen or peripheral blood of Pfn1WT vs Pfn1EC-KO mice either 8-10 days (mid-stage, *panel A*) or 15-18 days (late-stage, *panel B*) after last tamoxifen administration. Data representative of at least three separate litters with 'n' representing the total number of mice in each group pooled from different litters. The 'p' values, when significant (or close to being significant), are indicated above the comparison bar.

3.2.9 Cytokine Profiling Supports Elevated Levels of Pro-inflammatory Cytokines in the Circulation of Pfn1^{EC-KO} Mice with Elevated IL-6 in ECs and Myeloid Cells

Immune population findings led us to query whether endothelial Pfn1 depletion perturbs circulating levels of immunomodulatory cytokines and chemokines *in vivo* to promote immune cell population development. To address this question, we profiled serum of Pfn1^{WT} and Pfn1^{EC-KO} animals for a panel of 32 immunomodulatory cytokines and chemokines using a Luminex-based assay at either mid-stage or late-stage of endothelial Pfn1 depletion. Based on these analyses, mid-stage Pfn1^{EC-KO} mice showed a statistically significant 2.45-fold increase in the circulating level of pro-inflammatory cytokine IL6 ($p=0.015$) relative to Pfn1^{WT} mice (Figure 14A). Pfn1^{EC-KO} animals also presented a general increase in the circulating levels of GM-CSF, M-CSF, KC/CXCL1, and RANTES/CCL5 but these changes did not reach statistical significance due to large animal-to-animal variations observed. Changes in the immunomodulatory factors were more prominent at the late-stage evaluation. In addition to continued elevation of IL6 (increased by ~5 fold; $p=0.00016$), circulating levels of several other factors including VEGF, G-CSF, IL1β, IL9, IL10, IP10/CXCL10 and MCP-1/CCL2 increased in a statistically significant manner in late-stage Pfn1 $^{EC-KO}$ relative to Pfn1^{WT}animals (Figure 14B). A few additional cytokines including IL2, RANTES/CCL5, and LIF also exhibited a similar trend, but these changes did not reach statistical significance due to animal-to-animal variations. IL1α was the only circulating cytokine that appeared to show a reduction in both early and late-stage Pfn1^{EC-KO} animals relative to Pfn1^{WT} controls.

While several immunomodulatory factors were disrupted in circulation of Pfn1^{EC-KO} mice, contributing cellular sources are not clear from Luminex-based serum analysis. To address these

findings, we asked whether EC could be a potential cellular source for some of these elevated pro-inflammatory factors as seen in $Pfn1^{EC\text{-}KO}$ mice. To address this question, we transduced 2D cultures of our recently generated human telomerase reverse transcriptase (hTERT)-immortalized EC isolated from $Pfn1^{flox/flox}$ FVB mice (mouse endothelial cells, termed MEC) [152] with adenovirus encoding either Cre (Ad-Cre) or GFP (Ad-GFP) as control, and performed matched Luminex analyses of collected conditioned media (CM). Ad-Cre mediated acute loss of Pfn1 expression in cultured MEC cells was confirmed by both qRT-PCR and immunoblot analyses (Figure 14C-D). Although our *in vitro* experiments with cultured EC did not perfectly reiterate the *in vivo* findings, likely due to secretion of immunomodulatory factors from multiple different cell types *in vivo*, we were able to see some degree of qualitative concordance between our *in vitro* and *in vivo* results. For instance, similar to our findings in $Pfn1^{EC\text{-}KO}$ mice, secreted levels of IL-6, CXCL10, RANTES/CCL5 and IL1β were also elevated upon Pfn1 gene KO in EC (Figure 14E). However, a contrasting finding included detection of prominent elevation of CXCL9/MIG9 in Pfn1-depleted EC, that differed from a modest reduction of this chemokine in $Pfn1^{EC\text{-}KO}$ relative to $Pfn1^{WT}$ mice. Overall, these results suggest that EC could at least partly contribute to elevated levels of some of the circulating pro-inflammatory factors as seen upon loss of Pfn1 expression *in vivo*.

Although several immunomodulatory cytokines were upregulated in $Pfn1^{EC\text{-}KO}$ mice at the late-stage collection point, IL-6 was not only consistently and reproducibly upregulated at both mid- and late-stage collection points in a statistically significant manner but was also one of the most robustly elevated cytokines. Although our *in vitro* studies qualitatively recapitulated IL6 elevation in EC in response to loss of Pfn1 expression, the fold-change was not commensurate with that seen *in vivo*. As such, this begged the question of whether other types of cells could

further contribute to IL6 elevation in response to endothelial Pfn1 loss *in vivo*. Given macrophages are one of the major sources of circulating IL6[175], we next analyzed IL6 expression in bead-isolated F4/80+ circulating monocytes/macrophages populations isolated from $Pfn1^{WT}$ and $Pfn1^{EC\text{-}KO}$ mice by qRT-PCR analyses. Although the p-value (=0.09) did not reach statistical significance due to animal-to-animal variation, monocytes/macrophages from $Pfn1^{EC\text{-}KO}$ mice retained a trend of higher IL6 expression relative to those harvested from $Pfn1^{WT}$ mice (Figure 14F). To further determine whether loss of Pfn1 in EC could promote upregulation of IL6 expression in macrophages, we performed indirect co-culture experiments. Specifically, M0 macrophages derived from primary bone-marrow derived mouse monocytes (BMDMs) were exposed to conditioned media derived from Ad-GFP- vs Ad-Cre transduced MEC, either in the absence or presence of IFNγ stimulation (mimics a pro-inflammatory milieu). These indirect co-culture experiments showed that endothelial Pfn1 depletion potentiates IFNγ-dependent IL6 induction in macrophages (Figure 14G). These data further support a scenario that depletion of Pfn1 may enhances the ability of EC to crosstalk with myeloid lineage populations and upregulate IL6 expression through some paracrine mechanism requiring further cellular signaling validation.

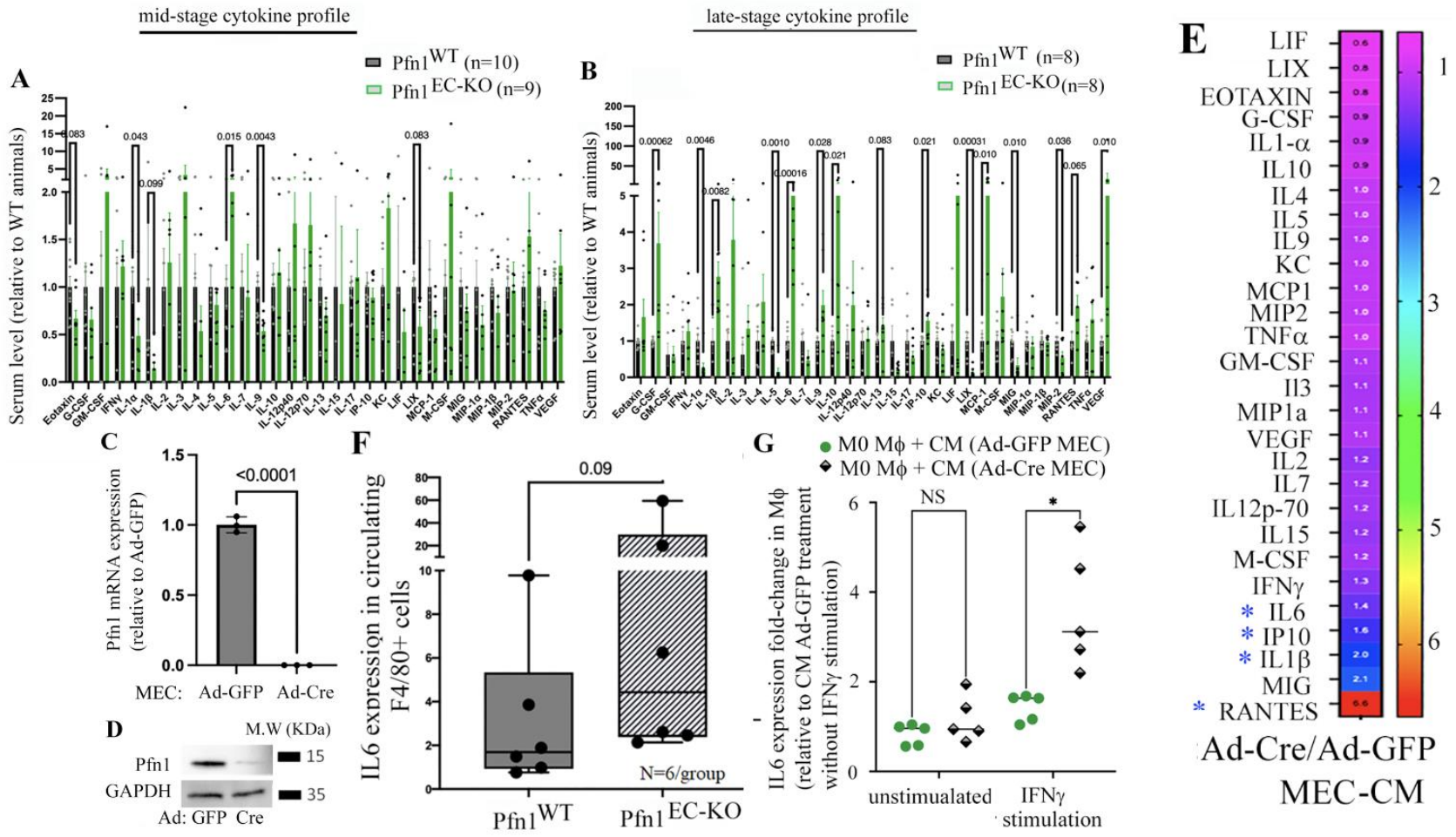

Figure 14. Endothelial Pfn1 depletion leads to increased levels of circulating pro-inflammatory cytokine/chemokines in vivo.

Relative abundance of the indicated cytokines/chemokines circulating in the serum of Pfn1WT vs Pfn1EC-KO mice collected either A) 8-10 days or B) 15-18 days after last tamoxifen administration. Data representative of at least three separate litters with 'n' representing the total number of mice in each group pooled from different litters. Validation of Pfn1 depletion following Ad-Cre infection (versus Ad-GFP control) at either the C) gene

expression or D) protein level in kidney-derived MECs. E) Ad-Cre infected MEC KO cell supernatant partially concurs with secreted cytokine/chemokine profile present in circulation-derived serum sample from EC Pfn1 KO mouse. F) IL-6 gene expression is elevated in EC Pfn1 KO-derived myeloid cells. G) IL-6 gene expression is elevated in EC-Pfn1 KO primary-derived circulatory myeloid cells following IFN-g stimulation.

$^{*}p<0.05$, $^{**}p<0.01$.

3.2.10 STAT1 and IRF7 Signaling is Activated Following Endothelial Pfn1 Deletion

While co-culture studies, immunomodulatory findings, and immune subtype population profiling support a regulatory role for endothelial Pfn1 in paracrine regulation of myeloid cell behavior, the regulatory mechanism is not clear. To gain mechanistic insights into biological and signaling pathway perturbation in EC upon loss of Pfn1 expression, we performed RNA-sequencing analyses to transcriptionally profile Ad-GFP vs Ad-Cre transduced EC in an acute setting ensuring that cell viability was not compromised. To elucidate a specific mechanism of action, RNA was isolated from AdGFP and AdCre MEC and processed for RNAseq preparation and analysis. Gene expression profiles were dramatically perturbed between AdGFP and AdCre MEC samples, and even with the absolute fold-change in expression and the false-discovery rate (FDR) set to >1.5 and <0.05, respectively, we found a total of 1035 differentially expressed genes (DEGs - 789 upregulated and 246 downregulated) in Pfn1 KO relative to control MEC (Figure 15A). When specifically probed for expression changes in immunomodulatory factor-encoding genes (specifically interleukins, CXC- and CC-family chemokines, and colony-stimulating factors (CSFs)), G-CSF/CSF3, CXCL10 and CCL5 were found to be robustly elevated (indicated by asterisks in Figure 15B) in Pfn1 KO MEC in agreement with our serum and/or CM Luminex data. Upstream Regulator Analysis (URA) of EC Pfn1-responsive genes in IPA predicted inhibition and activation of a wide range of transcriptional regulators as shown in the form of a volcano plot (Figure 15C). As per these analyses, transcription factors STAT1 and IRF7 (interferon regulatory factor 7) were predicted to be the most robustly activated transcription factors in EC under Pfn1-depleted condition (Figure 15C). Interestingly, TRIM24 (tripartite motif 24 – an inhibitor of STAT1 transcription[176]) was predicted to be most inhibited transcription factor in Pfn1 depleted

MEC. TRIM24-chromatin binding activates estrogen-associated genes, supporting a role for TRIM24 in sex-specific variability. While cytokine secretion was elevated in female as compared to male mice, there was not sufficient data collected from male mice to quantitatively assess against female mice. To validate gene expression-level findings, we investigated STAT1 and IRF7 activation and total protein levels. As an experimental validation, elevated total protein levels of both IRF7 and STAT1 were observed in Pfn1 KO MECs, with comparable or elevated phosphorylation (indicative of activation) in IRF7 and STAT1, respectively (Figure 15D). Overall, these results are consistent with a well-established role of IRF/STAT1 signaling in induction of pro-inflammatory cytokine/chemokine genes and classical activation of macrophages through some paracrine mechanism[177].

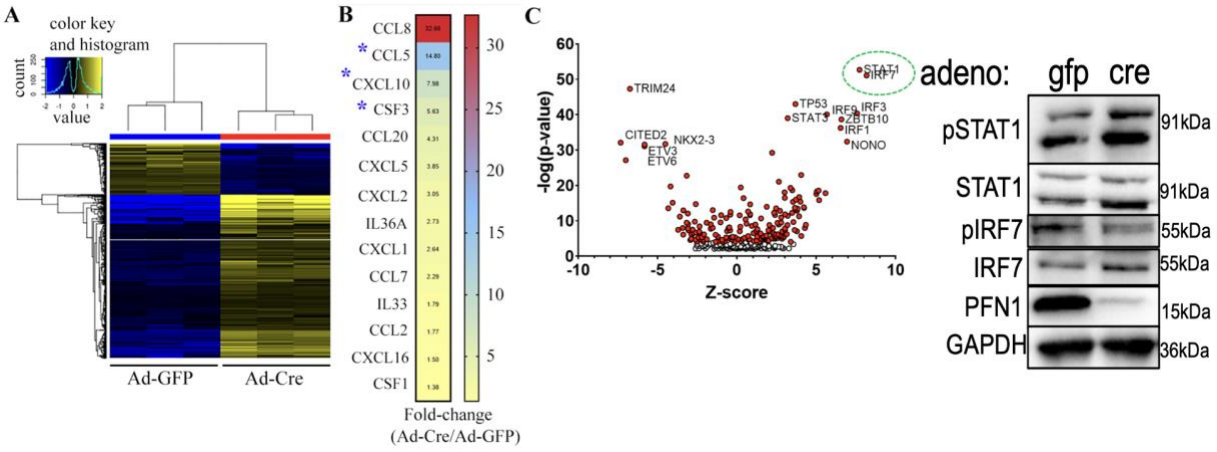

Figure 15. Impact of Pfn1 depletion on EC transcriptome.

A) Heat plot showing differentially expressed genes between Ad-GFP– and Ad-Cre–infected EC (genes color coded by blue and yellow denote transcriptionally downregulated and upregulated genes in Ad-Cre relative to Ad-GFP–infected cells; data summarized from three biological replicates). B) Heat plot showing transcriptionally altered cytokines/chemokines as a result of Pfn1 depletion in EC (numbers alongside indicate the average fold change in Ad-Cre relative Ad-GFP groups; asterisks denote robustly altered cytokines/chemokines that are in agreement with serum and/or CM Luminex data). C) A volcano plot (*P*-value vs *Z* score) displaying IPA-predicted activated and inhibited transcriptional regulators in Ad-Cre– vs Ad-GFP–infected cells. Top IPA-predicted activated transcription factors (based on the absolute *Z* score and negative log *P*-value) are outlined by a green oval. D) Representative immunoblots showing the relative levels of the total as well as phosphorylated forms of STAT1 and IRF7 between Ad-GFP– and Ad-Cre–infected cells (GAPDH blot serves as the loading control; Pfn1 blot confirms Ad-Cre–induced suppression of Pfn1 expression). RNAseq fastq analysis conducted by Dr. David Gau, with additional Western blot data collected by Christopher Varghese.

3.3 Conclusions

Originally identified as an actin shuttling protein, Pfn1's role in a variety of pathologies have been unveiled[18], [54], [110], [111], [111], [112], [145], [156]. While inhibitors are effective to study Pfn1:actin interaction[54], [151] a conditional Pfn1 KO model specific to EC can expand beyond this case. Loss of function (LOF) animal models, both constitutive and inducible, are a common tool in pathological studies. Though essential, LOF models are not always compatible with life. Efforts to generate a double-allele deleted Pfn1 mouse have failed to produce viable homozygous pups, either in a global deleted case[170] or in an endothelial cell specific model[154]. This has been observed in other models (*Drosophila* and *Dictyostelium*[171], [172]), underpinning a need for Pfn1 expression during prenatal development. To address this shortcoming, a novel conditional endothelial Pfn1 depleted model (CDH5 CreERT2$^{+/-}$ Pfn1$^{flox/flox}$) has been used to assess diabetic retinopathy in post-natal mouse pups[151], [152], with retinal vascularization dramatically reduced in Pfn1$^{EC\text{-}KO}$ versus Pfn1^{WT} pups, allowing study of Pfn1 loss on post-natal vascular development. Though mice were used effectively in short-term post-natal experiments, long-term viability was not assessed.

In our current study, we reported three novel findings. **First,** loss of endothelial Pfn1 over an extended period leads to dramatic reduction in animal health and mortality, underpinning the essential need for endothelial Pfn1 in long-term animal health and viability. This contrasts with existing conditional Pfn1 KO models that supported loss of Pfn1 in select cell-types and tissues while retaining animal viability. These findings will be critical to future studies on endothelial Pfn1 in vascularized disease, including cardiovascular disorders and solid cancers. **Second,** endothelial Pfn1 deletion promotes a pro-inflammatory response, including elevated immunomodulatory cytokine secretion in Pfn1$^{EC\text{-}KO}$ mice that in part promote elevated pro-

inflammatory myeloid populations. Collectively, these findings support a causative role for endothelial Pfn1 deletion in perturbing immune cell populations. **Third,** loss of endothelial Pfn1 leads to dramatic upregulation of pro-inflammatory IRF7/STAT1 signaling components specifically in ECs, while also promoting an inflammatory response (elevated IL-6 expression) in myeloid populations collected both *in vitro* and *in vivo*. These data suggest a paracrine regulatory mechanism mediated through endothelial Pfn1 factor secretion to promote pro-inflammatory macrophage activation, as schematized by Figure 16.

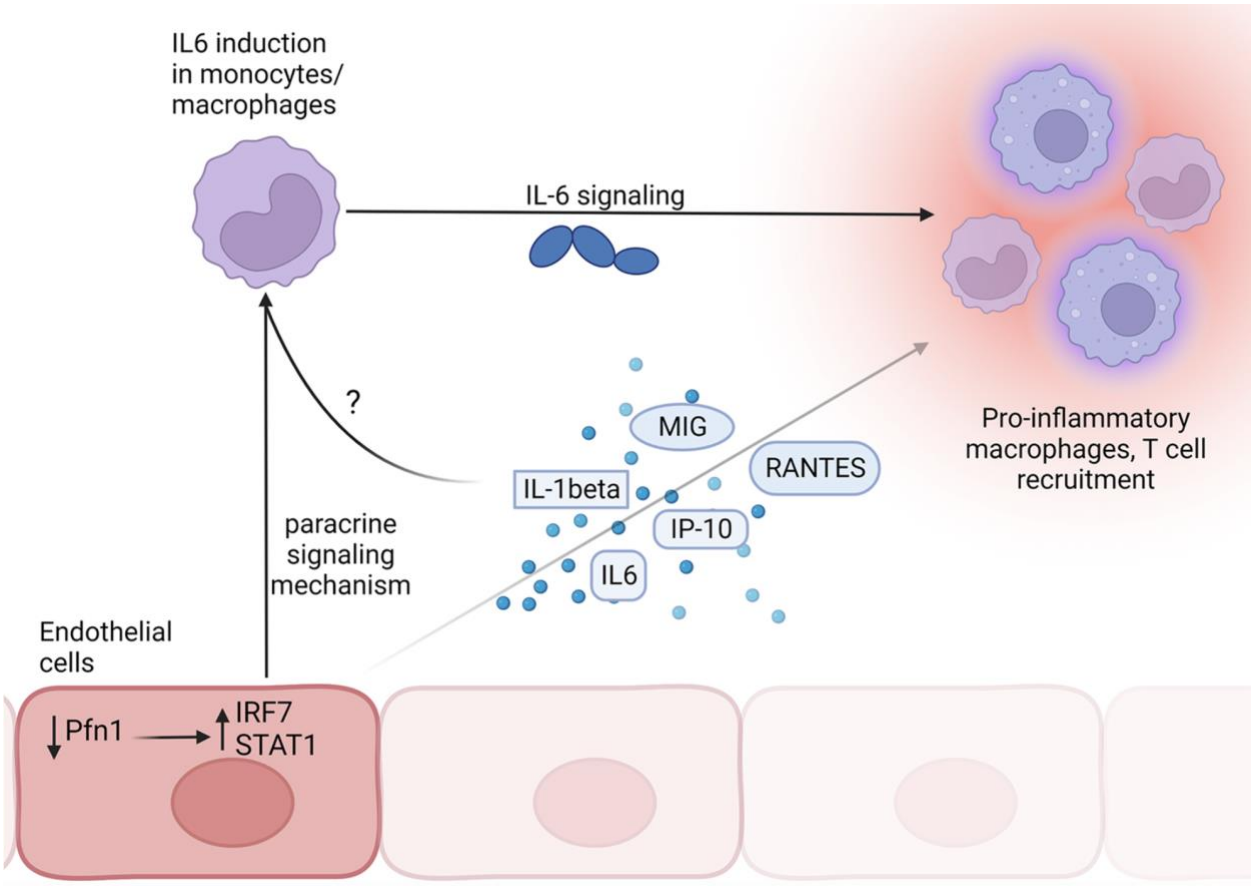

Figure 16. Schematic representation of potential mechanism of action of endothelial Pfn1 in regulating pro-inflammatory activation.

Endothelial intracellular signaling via Pfn1 deletion may promote activation and phosphorylation of IRF7 and STAT1. Inflammatory signaling activation in endothelial cells may directly promote cytokine and chemokine release leading to myeloid cell activation or may activate some unknown paracrine signaling mechanism due to IL-6 induction that leads to pro-inflammatory activation of myeloid cells, or some combination of both. Created with biorender.com.

Chronic inflammatory conditions can lead to elevated Pfn1 expression in both experimental and clinical settings[110], [111], [114]. For example, an increase in serum Pfn1 is observed as disease severity increases in atherosclerotic patients[111]. In a global single-allele Pfn1 depleted mouse model, features of atherosclerosis including reduced foam cell accumulation, plaque size, and cell-adhesion molecule (CAM) expression were dramatically decreased in single-allelic Pfn1 depleted mice[110]. Classically, these features appear to be attributed to restoration of endothelial function. This would be expected alongside previous findings from our group, indicating that Pfn1 loss leads to improved endothelial barrier and function. Though at first contradictory, impaired vascular integrity and function agrees with *in vitro* Pfn1 depletion experiments, as reduced proliferation and improved barrier junctions are observed in HUVEC[50]. While ideal in a static culture model, these conditions are not ideal to growth and proliferation in maturing vessels and capillaries.

Salient pathological features of $Pfn1^{EC\text{-}KO}$ mice at the organ level found in this study are disrupted vasculature, stunted weight gain and development, tissue infarct, fibrosis, sclerosis and immune cell infiltration. Disrupted vasculature in organs (most notable in kidney and liver) in $Pfn1^{EC\text{-}KO}$ mice is consistent with endothelial Pfn1-dependency for angiogenesis previously shown by our group in early post-natal developmental setting[151], and more recently, in a renal cancer model of tumor angiogenesis[152]. In the latter study, pro-angiogenic factor serpinE1 was most heavily downregulated in the tumor microenvironment in response to loss of endothelial Pfn1. In the current study, prominent tissue infarct is suggestive of severe defect in circulation due to impaired vascularization, which are expected to directly lead to some of the other observed histological changes including fibrosis and mononuclear immune cell infiltration. One of the striking features of $Pfn1^{EC\text{-}KO}$ mice is abnormal peritoneal fluid accumulation and abdominal

hemorrhage, the most likely cause of which is increased vascular permeability (supported by qualitatively elevated VEGF in late-stage Pfn1^{EC-KO} animals).

Endothelial barrier function requires integrity of actin cytoskeleton and intact junction tethering to the underlying cytoskeleton. A previous study showed that loss of Ena/VASP family of F-actin elongating proteins compromises cell-cell junctions, endothelial barrier dysfunction and hemorrhage in mice[178], similar to the phenotypes we observed in Pfn1^{EC-KO} mice. Ena/VASP proteins bind to Pfn1 to augment actin polymerization ability of Ena/VASP[179]. Therefore, Pfn1-Ena/VASP interaction may contribute to vascular leakiness in Pfn1^{EC-KO} mice due to cytoskeletal defects. Interestingly, we previously showed that acute silencing of Pfn1 expression in vascular EC stabilizes adherens and tight junctions conferring protection to VEGF-induced junctional disruption[50]. Another group also reported improved retinal vascular barrier function in mice when subjected to intravitreal administration of Pfn1-shRNA encoding adenovirus[143]. We attribute the apparent contradictions between those results and the in vivo phenotype of Pfn1^{EC-KO} mice to at least two possible reasons. First, gene silencing of Pfn1 in EC reduces but does not eliminate Pfn1 expression and does not cause cell death, unlike the effect of total absence of Pfn1 expression. Second, we saw a robust systemic elevation of VEGF (a key vascular permeability-inducing factor) in Pfn1^{EC-KO} mice. Therefore, VEGF upregulation (compounded by apoptotic cell death) could be a major driver for inducing vascular leakiness in Pfn1^{EC-KO} mice.

A key question derived from this study is whether the pro-inflammatory consequence of loss of endothelial Pfn1 is specific to some particular function of EC Pfn1 or a generic feature as could be expected due to loss of any other key actin polymerization regulatory proteins. Disruption of endothelial barrier function may contribute to local inflammation and cell death and could signal a common phenotypic consequence of disruption of actin polymerization regulators. However, our

cell culture-based studies showed that loss of endothelial Pfn1 leads to upregulation of pro-inflammatory factors not only in an EC-intrinsic manner but also in macrophages through a paracrine mechanism, supporting a direct interaction in our selected cell types. Furthermore, our RNAseq studies revealed that many of the biological pathways that are predicted to be activated in EC upon Pfn1 depletion are related to immunological functions. Therefore, we reason that there are additional cellular consequences capable of impacting immune response that are unique to the loss of Pfn1.

The most prominent immunological consequence of endothelial Pfn1 depletion is expanded pro-inflammatory myeloid-derived population of immune cells. This finding is consistent with the systemic elevation of several pro-inflammatory cytokines in $Pfn1^{EC\text{-}KO}$ mice. In the context of these data, it is interesting to note that in atherosclerosis setting, global heterozygous deletion of the Pfn1 gene reduces inflammation and macrophage activity conferring partial protection from the severity of atherosclerosis[110]. While those data may appear contradictory, a direct comparison cannot be made because **1)** global heterozygous KO mice have attenuation (but not complete loss) of Pfn1 expression in all cell types, and so a direct immunological consequence of Pfn1 heterozygous mice cannot be directly tied to endothelial Pfn1 expression, **2)** there is prior evidence for altered immune cell behavior (specifically cytotoxic T-cells) in response to perturbation of Pfn1 expression[155] and **3)** cell death and necrosis, features of $Pfn1^{EC\text{-}KO}$ but not of global Pfn1 heterozygous knockout mouse model, could be direct triggers of an inflammatory response *in vivo*.

Inflammatory macrophages with M1-like phenotype are characterized by high expressions of IL1β and IL6[180]. A recent study also supports IL1β signaling in transcriptional upregulation of VEGF in macrophages[181]. Macrophage-secreted IL6 can also stimulate the production of

CXCL10 (a potent chemokine for macrophages and T cells) in an autocrine manner suggesting a positive feedback loop[182]. Our cytokine profiling data show elevated levels of IL1β, IL6, VEGF and CXCL10 (M1-macrophage associated marker) in $Pfn1^{EC\text{-}KO}$ mice, with *in vitro* studies providing evidence for both EC and macrophages as potential sources of these factors. Though IL6 expression was moderately (1.4x) overexpressed specifically in endothelial cells, large animal-to-animal variability in IL6 expression was also present in primary-isolated myeloid lineage cells (Figure 14). While these findings support consistent upregulation of IL6, we must consider additional secretors of IL6. IL6 is produced by innate immune cells, B and some T cells, with expression of IL6 receptor (IL6R) predominantly restricted to hepatocytes and leukocytes[183]. As such, IL6 may interact directly with hepatocytes, supporting accelerated pathological features present in liver. Additionally, lung pneumocytes are a major secretor of IL6, and IL6 neutralizing antibody treatment ameliorates features of lung fibrosis[184]. Investigating IL6 expression profile in the lung and the liver tissues of $Pfn1^{WT}$ vs $Pfn1^{EC\text{-}KO}$ mice may reveal additional tissue secretion source of IL6. Additionally, STAT1 and IRF7 are key mediators of type I interferon response, regulated in a positive feedback loop controlling each other's expression in addition to acting as major transcriptional regulators of several pro-inflammatory factors (e.g. CXCL10, CCL5, CXCL9) that are elevated either *in vitro* or *in vivo* upon endothelial Pfn1 loss [185], [186]. Therefore, increased STAT1/IRF7 activation could offer a molecular basis for pro-inflammatory gene induction in EC triggered by loss of Pfn1. Interestingly, we recently reported suppression of STAT1 expression in a tumor microenvironment when Pfn1 is overexpressed in EC[152]. Although this study did not discern which cell type reflects Pfn1-induced suppression of STAT1 expression *in vivo*, elevated STAT1 expression in $Pfn1^{EC\text{-}KO}$ as demonstrated herein underpins these findings. How loss of Pfn1 increases STAT1/IRF7 expression/activation remains to be

elucidated, and future studies can be used to explore whether TRIM24 inactivation, DNA damage, and/or toll-like receptor signaling by certain damage-associated molecular patterns are responsible for hyper-activation of IRF-STAT signaling in EC when depleted of Pfn1.

4.0 Haplo-insufficiency of Profilin1 in Vascular Endothelial Cells is Beneficial but Not Sufficient to Confer Protection Against Experimentally Induced Atherosclerosis

Content in this chapter is currently under review for publication

Reference: **Abigail Allen-Gondringer**, Partha Dutta, Partha Roy. "Haplo-insufficiency of Profilin1 in vascular endothelial cells is beneficial but not sufficient to confer protection against experimentally induced atherosclerosis", (*under review)*

Specific Aim 2: Determine the consequence of partial vascular endothelial loss of Pfn1 on atherosclerosis development.

4.1 Introduction

Cardiovascular diseases are a leading cause of death world-wide, contributing to approximately 17.9 million deaths a year [187]. The most common form, ischemic heart disease, remains the leading cause of cardiovascular-related death, and develops due to atherosclerotic plaque formation [188]. Atherosclerosis begins with fatty streak deposition, appearing in clinically relevant locations including aortic, coronary, and cerebellar arteries as early as age 30-40 years in humans [97]. Over time, fatty streaks develop into fibrotic plaques composed of extracellular matrix and necrotic cellular deposits, smooth muscle cells (SMCs) and immune cells. Immune cell sub-populations are characterized by infiltration of lipid-rich macrophagic foam cells, cytotoxic T lymphocytes, granulocytes, and other antigen presenting cells (APCs) [96], [97]. An early contributor to fatty streaks and plaque development is EC dysfunction. In the healthy endothelium, atheroprotective nitric oxide (NO) released by constitutive endothelial nitric oxide synthase (eNOS)[189] regulates expression of endothelial cell adhesion molecules (CAMs, i.e. VCAM-1,

ICAM-1), while eNOS dysfunction in the vasculature (signified by a decrease in bioavailable nitric oxide (NO))[190] may enhance levels of VCAM-1 and ICAM-1, inciting local immune invasion and inflammation[191].

Actin cytoskeleton plays an important role in various aspects of atherosclerosis. For example, remodeling of actin cytoskeleton is largely responsible for pro-atherogenic morphological changes and dysfunction (characterized by impaired barrier function) of ECs in response to turbulent flow[192], [193]. Actin regulatory proteins control EC stiffness, in turn impacting clustering of cell surface adhesion molecules and transendothelial migration of immune cells [194]. Other aspects of atherosclerosis, such as polarization and lipid processing by macrophages, are sensitive to the state of actin cytoskeleton in immune cells [195], [196]. Overexpression of actin-binding protein Profilin1 (Pfn1 - an important promoter of actin polymerization in cells) in atherosclerotic plaques as well as increased circulating level of Pfn1 in the serum are features of human atherosclerosis[111]. In atherosclerotic plaques, Pfn1 abundance is elevated in both intracellular and extracellular spaces, and *in vitro* studies provide evidence for Pfn1's ability to stimulate vascular smooth muscle cell migration and proliferation (features of atherosclerosis) utilizing an extracellular mode of action. High-fat diet induced atherosclerosis in low-density lipoprotein receptor (LDLR) knockout ($LDLR^{-/-}$) knockout mice also leads to a trend of Pfn1 expression increase in atherosclerotic blood vessels mimicking the human disease. Furthermore, in the same mouse model of atherosclerosis, when Pfn1 expression is partially depleted globally in all cell types by heterozygous gene deletion, it results in reduced severity of atherosclerosis marked by smaller plaque size, lower VCAM-1 expression, and diminished vascular infiltration by macrophages [110]. However, since atherosclerosis involves altered activities of a number of different cell types including vascular EC, immune cells

(monocytes/macrophages, neutrophils and various subpopulation of T cells) and vascular smooth muscle cells Pfn1 downregulation in which specific cell type is primarily responsible for atheroprotective effect in $Pfn1^{+/-}$ mice remained unclear. Our recent studies show that triggering complete loss of vascular EC Pfn1 has a profound immunological consequence providing evidence for Pfn1 as an important mediator of vascular EC-immune cell crosstalk[156]. Given these findings, we sought to investigate whether haplo-insufficiency of Pfn1 in vascular ECs alone has any beneficial effect in experimentally induced atherosclerosis.

4.2 Results and Discussion

4.2.1 Atherosclerosis Progression Following PCSK9 Loss is Not Impeded Due to Partial EC Pfn1 Depletion

To assess the impact of EC-specific partial Pfn1 reduction ($Pfn1^{+/-(EC)}$), we backcrossed our available CDH5-$CreERT2^{+/-}$ $Pfn1^{flox/flox}$ BALBC/J mice onto the C57BL6/J background for use in atherosclerotic experiments. To evaluate the impact of EC-specific Pfn1 depletion on atherosclerosis, we used $Pfn1^{+/-(EC)}$ C57Bl/6 mice for two reasons. First, mortality is observed in total Pfn1 depleted mice, either globally[170], endothelial constitutive[154], or 3-weeks after conditional endothelial Pfn1 gene ablation[156], and since it takes several months to develop atherosclerosis in mouse models, $Pfn1^{-/-(EC)}$ mice are not suitable for atherosclerosis development studies. Secondly, use of $Pfn1^{+/-(EC)}$ animals (which are completely viable) allows for a direct evaluation of EC-specific partial depletion of Pfn1 vs previously published global Pfn1 heterozygous knockout mouse model-based findings in atherosclerosis setting[110]. Additionally,

ECs harvested from $Pfn1^{+/-(EC)}$ have ~50% downregulation of Pfn1 expression at the protein level and are morphologically indistinguishable from those harvested from $Pfn1^{+/+}$ mice (Figure 17**A-B**). As such, we elected to use an EC-partially depleted Pfn1 ($Pfn1^{+/-(EC)}$) mouse model to retain sufficient EC Pfn1 for survival while probing partial EC Pfn1 depletion in a chronic inflammatory setting.

Since generating $LDLR^{-/-}$ mice harboring additional cell-type-specific conditional knockout of gene of interest requires extensive breeding and is time consuming, we adopted use of AAV8-mPCSK9 combined with HCD to induce atherosclerosis[157], [158]. PCSK9 directly binds to hepatic LDLR promoting its degradation in the lysosomes, and consequently, induces hyperlipidemia[197]. To initially confirm the efficacy of AAV8-mPCSK9–induced depletion of hepatic LDLR, we probed for expression of LDLR in the liver in both $Pfn1^{+/+}$ and $Pfn1^{+/-(EC)}$ mice 3.5 months after a single intraperitoneal injection of AAV8-mPCSK9 vs AAV8-GFP (as control). Immunoblot analyses of liver extracts showed near complete depletion of LDLR in both $Pfn1^{+/+}$ and $Pfn1^{+/-(EC)}$ mice following administration of AAV8-mPCSK9 (Figure 17**C**). Lipid panel analyses of serum showed significant elevation of both total cholesterol and LDL (but not triglycerides and HDL) in HCD-fed $Pfn1^{+/+}$ and $Pfn1^{+/-(EC)}$ mice which were administered with AAV8-mPCSK9 relative to those receiving AAV8-GFP (Figure 17**D**). However, we did not find any significant difference in the serum level of either total cholesterol or LDL between $Pfn1^{+/+}$ and $Pfn1^{+/-(EC)}$ animals (Figure 17**D**) suggesting that partial loss of EC Pfn1 does not impact the severity of hyperlipidemia. Oil Red-O staining of aortic roots revealed presence of atherosclerotic plaques in both $Pfn1^{+/+}$ and $Pfn1^{+/-(EC)}$ mice (Figure 17**E**). However, when we compared multiple features of atherosclerosis including the areas of total plaque, fibrous cap and necrotic core measured at the aortic root, we did not find any statistically significant difference in any of these parameters

between the two Pfn1 genotypes of mice (Figure 17**F**). These data further suggest that partial depletion of Pfn1 in vascular EC alone is not sufficient to confer overall protection against experimentally induced atherosclerosis *in vivo*. Based on these findings, we elected to investigate the immunomodulatory profile present in both $Pfn1^{+/+}$ and $Pfn1^{+/-(EC)}$ mice in both the atherosclerotic and non-atherosclerotic settings.

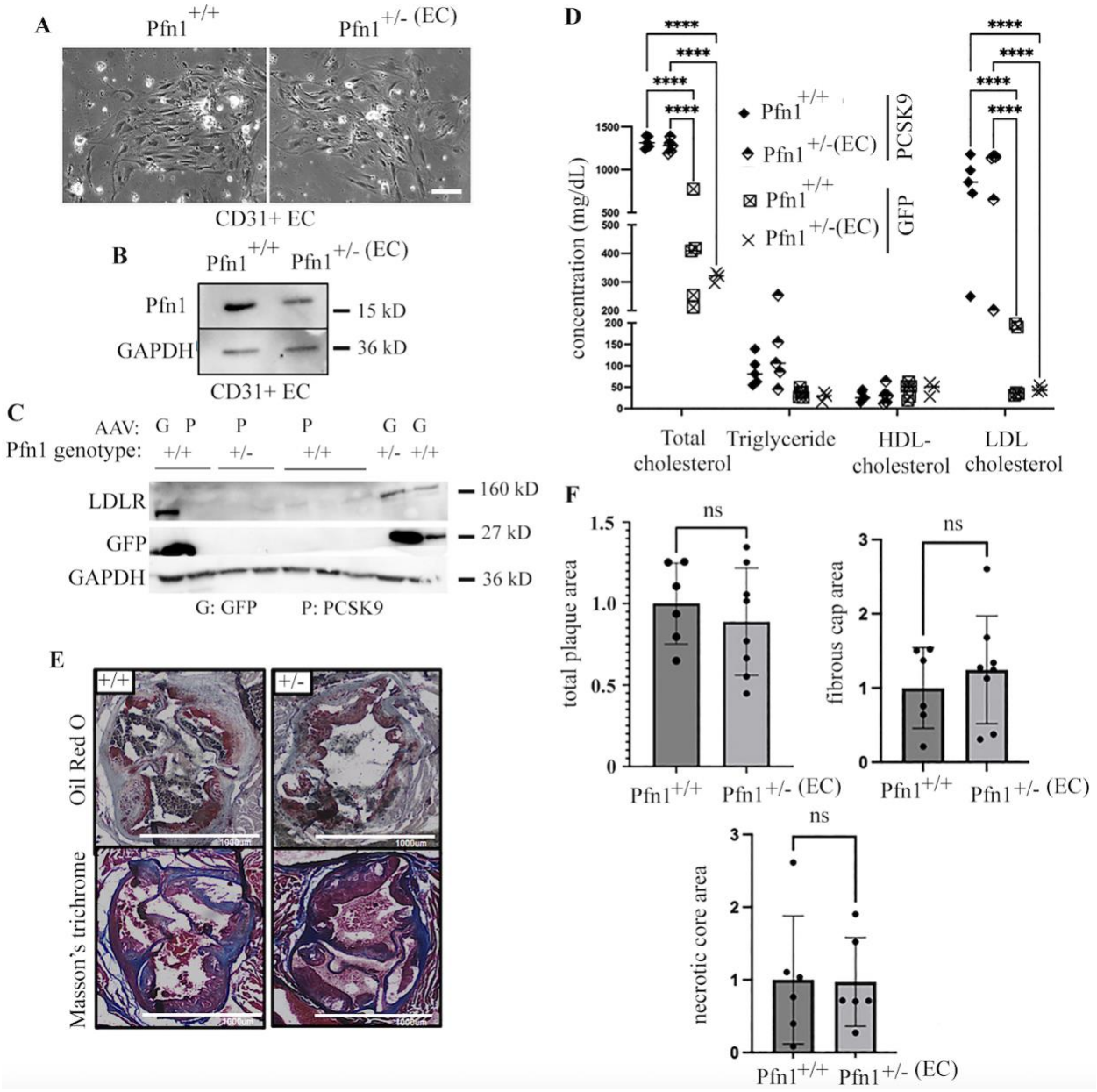

Figure 17. Pfn1 haplo-insufficiency in vascular EC is not sufficient to induce atheroprotection.

A-B) Immunoblot analyses of Pfn1 (panel B – GAPDH: loading control) and phase-contrast images (panel A) for CD31+ mouse kidney ECs isolated from $Pfn1^{+/+}$ and $Pfn1^{+/-(EC)}$ mice. C) Immunoblot anlsyses of liver extracts prepared from mice of indicated Pfn1 genotypes showing loss of LDLR expression in reponse to AAV8-mPCSK9 administration (samples from AAV8-GFP injected mice serve as control; GAPDH-loading control). D) Relative serum levels of total cholesterol, LDL, HDL and triglycerides in AAV8-mPCSK9 vs AAV8-GFP injected mice of indicated Pfn1 genotypes maintained on a high cholesterol diet. The number of animals for various groups for lipid panel analyses were: $Pfn1^{+/+}$/PCSK9 (n=5); $Pfn1^{+/-(EC)}$/PCSK9 (n=5);

$Pfn1^{+/+}$/GFP (n=5); $Pfn1^{+/-(EC)}$/GFP (n=3) E-F) Representative images of aortic roots prepared from atherosclerotic $Pfn1^{+/+}$ and $Pfn1^{+/-(EC)}$ mice stained with Oil Red-O and Masson's trichrome staining (panel E) along with quantifications of various atherosclerosis-related parameters (data normalized to the mean values of $Pfn1^{+/+}$ mice (panel F). Data were summarized from 6 $Pfn1^{+/+}$ and 8 $Pfn1^{+/-(EC)}$ atherosclerotic mice pooled from multiple experiments; *p<0.05, **p<0.01, ***p<0.001, ****p<0.0001; ns – not significant.

4.2.2 Broad Immune Cell Panel Reveals Reduced Cytotoxic T Cells and Elevated B Cells in EC Pfn1 Depleted Mice

Although our studies showed that partial depletion of EC Pfn1 alone does not ameliorate either hyperlipidemia or the severity of atherosclerosis, we asked whether haplo-insufficiency of vascular EC Pfn1 has any favorable immunological consequence in the setting of atherosclerosis. Therefore, we performed flow cytometric analysis to obtain immunological profile of spleen, bone marrow, thoracic aorta and whole blood isolated from atherosclerotic $Pfn1^{+/+}$ and $Pfn1^{+/-(EC)}$ mice and compared the findings from these studies to those obtained in a similar manner for non-atherosclerotic mice (these animals did not receive AAV8-mPCSK9 and were maintained on a normal diet). As summarized in Figure 18, we noticed a statistically significant decrease in circulatory cytotoxic $CD8^+$ T cell abundance in atherosclerotic $Pfn1^{+/-(EC)}$ vs $Pfn1^{+/+}$ mice. A similar trend was also observed in the aortic $CD8^+$ T cell population in atherosclerotic mice although the difference did not reach statistical significance likely because of large animal-to-animal variability. Given that this trend was not observed in splenic and bone marrow $CD8^+$ T cell population, it is likely that $CD8^+$ T cell mobilization from lymphoid organs rather than their development was negatively impacted in atherosclerotic $Pfn1^{+/-(EC)}$ mice.

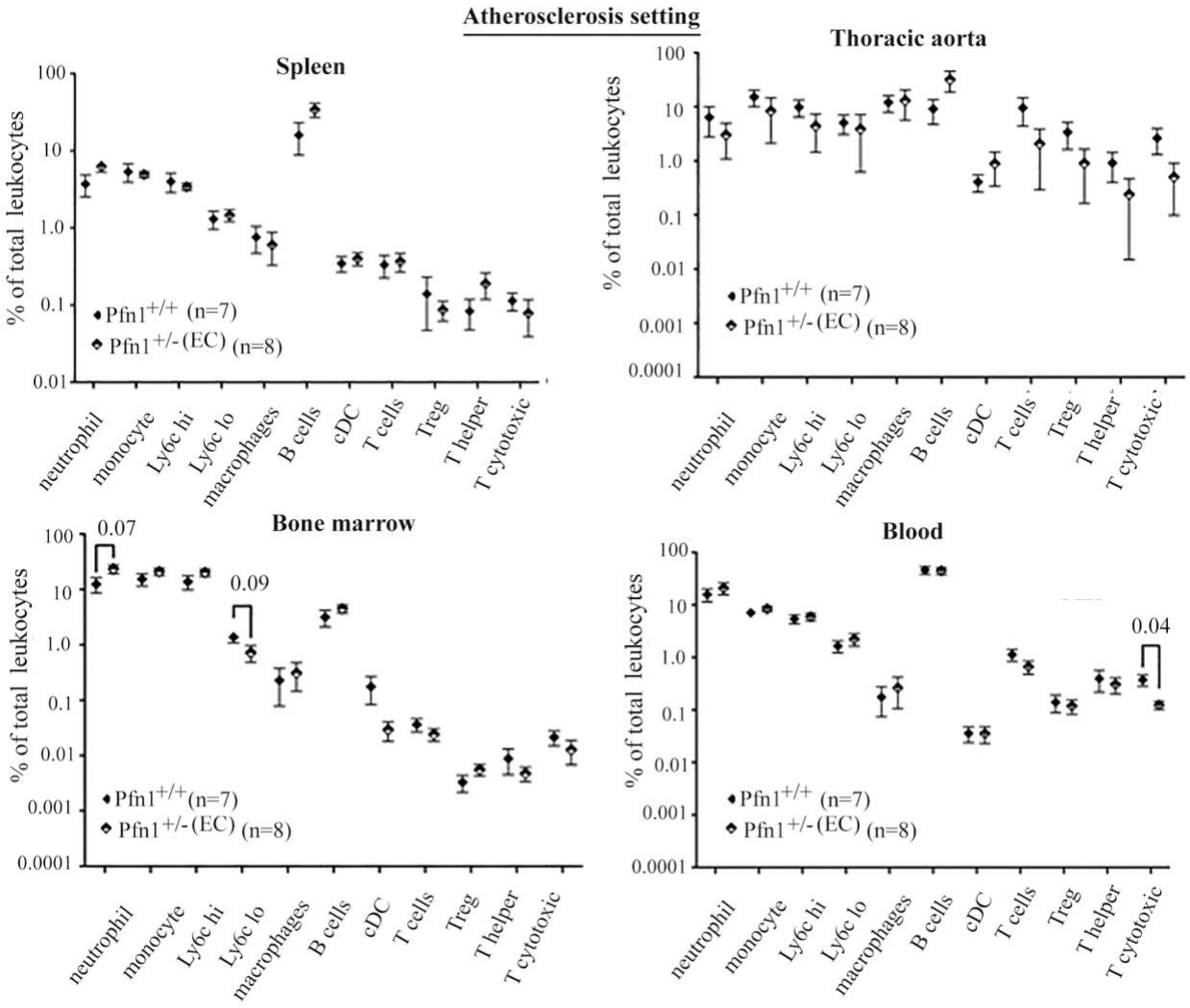

Figure 18. Immuneprofiling of atherosclerotic Pfn1$^{+/+}$ and Pfn1$^{+/-(EC)}$ mice.

Flow cytometry-based analyses of the relative abundance of various immune cell subtypes (as % of total leukocytes) in the circulation (whole blood) and various organs/tisssues (spleen, aorta and bone marrow) of atherosclerotic Pfn1$^{+/+}$ and Pfn1$^{+/-(EC)}$ ('n' indicates the number of animals in each group pooled from mutiple experiments; 'p' values when significant or close to being significant are indicated).

It is important to note that non-atherosclerotic mice did not show any effect of partial loss of EC Pfn1 on circulatory and aortic CD8^{+} T cell abundance (Figure 19). When analyzed for relative content of B cells between the two groups of animals, both splenic and aortic B cell content

in atherosclerotic $Pfn1^{+/-(EC)}$ mice showed signs of elevation relative to $Pfn1^{+/+}$ animals although the difference did not reach statistical significance because of large animal-to-animal variability (Figure 18). Somewhat consistent with these findings, non-atherosclerotic $Pfn1^{+/-(EC)}$ mice also exhibited a sign of elevated circulating B cells relative to $Pfn1^{+/+}$ mice with the p-value close to being significant (p=0.07); however, a reverse trend was found when splenic B cell content was compared between the two groups of animals in non-atherosclerosis setting (Figure 19). We recently showed that complete loss of vascular EC Pfn1 induces a selective bias of myeloid-derived cells (monocytes/macrophages) toward a pro-inflammatory phenotype *in vivo*[156]. Consistent with these findings, anti-inflammatory $Ly6C^{lo}$ monocytes were present at a lower level in atherosclerotic bone marrow and non-atherosclerotic spleen isolates of $Pfn1^{+/-(EC)}$ relative to $Pfn1^{+/+}$ mice; however, these changes were not preserved in the aortic immune cell compositional analyses (Figure 18). In summary, these immunological profiling studies demonstrate that the most noteworthy changes in the immune cell composition of the aorta (the main pathologic tissue of interest) elicited by partial loss of EC Pfn1 in atherosclerosis setting are trends of diminished and elevated $CD8^+$ T cells and B cells, respectively.

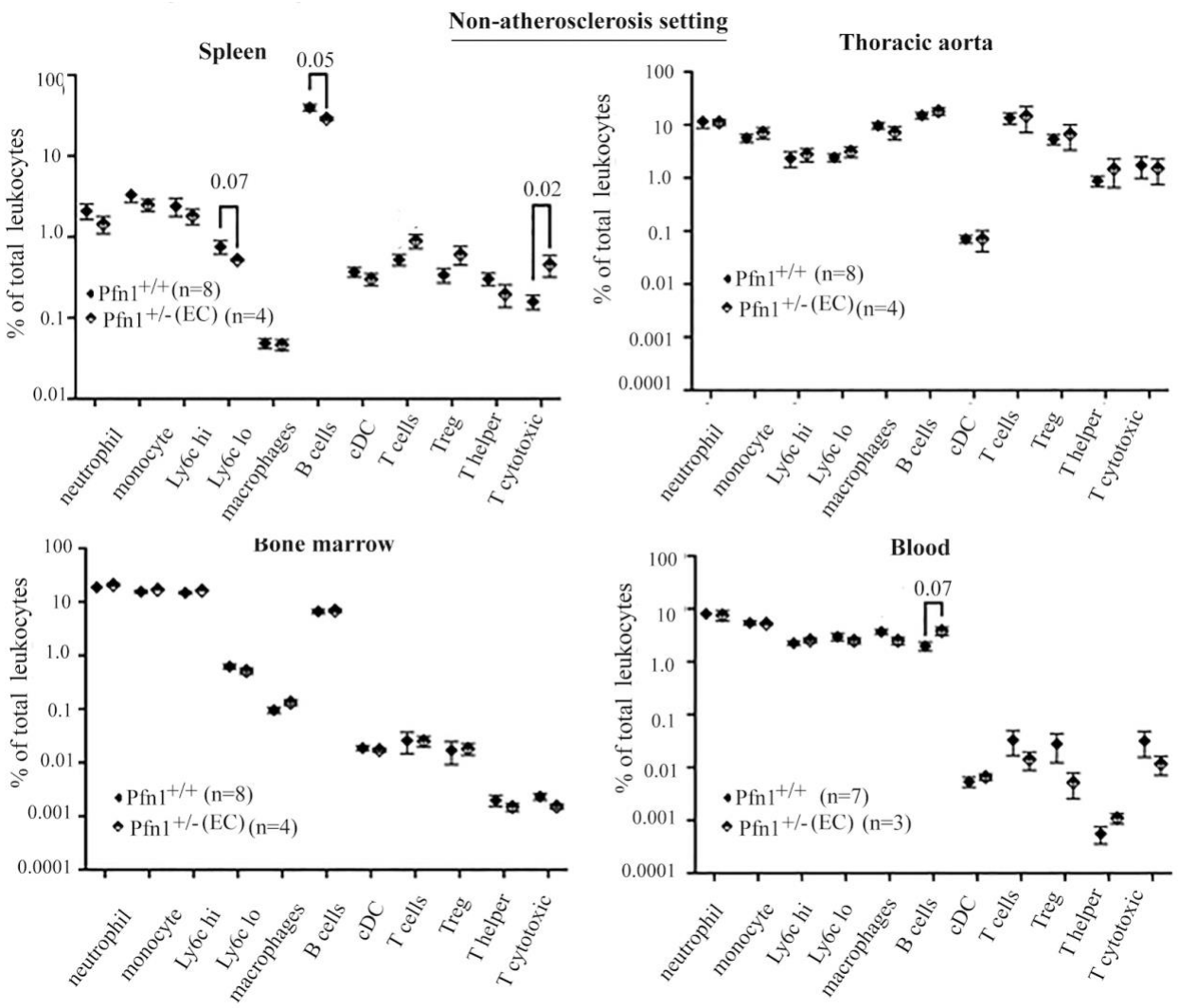

Figure 19. Immuneprofiling of non-atherosclerotic Pfn1$^{+/+}$ and Pfn1$^{+/-(EC)}$ mice.

Flow cytometry-based analyses of the relative abundance of various immune cell subtypes (as % of total leukocytes) in the circulation (whole blood) and various organs/tisssues (spleen, aorta and bone marrow) of non-atherosclerotic Pfn1$^{+/+}$ and Pfn1$^{+/-(EC)}$ ('n' indicates the number of animals in each group pooled from mutiple experiments; 'p' values when significant or close to being significant are indicated).

4.2.3 Limited but Specific Depletion of Pro-inflammatory Cytokines in EC Pfn1 Depleted Mice

To gain further mechanistic insights into how partial loss of EC Pfn1 may alter circulating/aortic composition of select immune cell sub-types in atherosclerosis setting, we performed a broad assessment of circulating cytokine/chemokines in the two groups of animals utilizing a Luminex assay probing for a panel of 32 immunomodulatory factors. As per these analyses, IP-10/CXCL10 and IL7 are the only two immunomodulatory factors that were differentially abundant within statistical significance with the average circulating CXCL10 and IL7 levels being ~40% and ~70% lower, respectively, in $Pfn1^{+/-(EC)}$ relative to $Pfn1^{+/+}$ atherosclerotic animals. (Figure 20**A-B**). Similar Luminex analyses performed with serum of non-atherosclerotic animals did not reveal any significant difference in circulating level of either CXCL10 or IL7 between the two groups, suggesting that the effect of partial loss of EC Pfn1 on these cytokines is specific to atherosclerosis setting (Figure 20**A-B**).

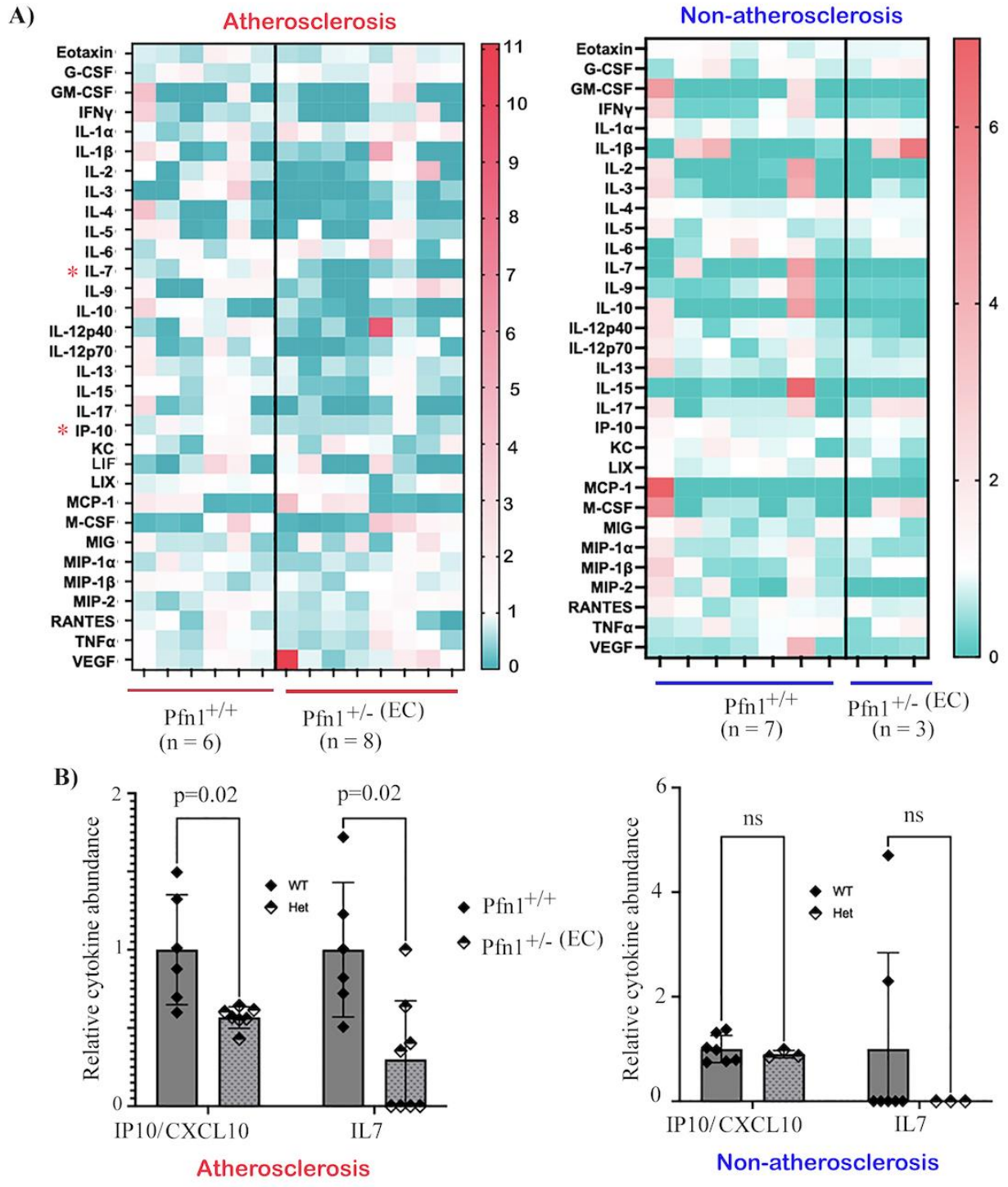

Figure 20. Luminex based profiling of circulating cytokines and chemokines of atherosclerotic vs non-atherosclerotic Pfn1$^{+/+}$ and Pfn1$^{+/-(EC)}$ mice.

A-B) Heat-plots showing relative abundance of indicated cytokines and chemokines in the serum of atherosclerotic (panel A) and non-atherosclerotic (panel B) mice of indicated genotypes (data for each analyte

normalized to the corresponding mean value calculated of $Pfn1^{+/+}$ mice; immunomodulatory factor(s) that are differentially abundant within statistical significance are indicated by asterisk. B) Relative serum abundance of CXCL10 and IL7 between the two groups of animals in atherosclerosis vs non-atherosclerosis settings ('n' indicates the number of animals in each group pooled from mutiple experiments; ns – not significant).

4.3 Conclusions

In the current study, the role of partial EC Pfn1 depletion was probed in the context of the atherosclerotic and non-atherosclerotic settings. Our findings validated the utility of an AAV8-mPCSK9 mediated $Pfn1^{+/-(EC)}$ atherosclerotic model as elevated LDL and total cholesterol profile and elevated plaque accumulation were present in both $Pfn1^{+/-(EC)}$ and $Pfn1^{+/+}$ mice (Figure 17). Although plaque formation was indistunguishable between $Pfn1^{+/-(EC)}$ and $Pfn1^{+/+}$ mice (Figure 17D), we posited that $Pfn1^{+/-(EC)}$ mice may still present some broader immunomodulatory changes. Of the assayed cytokines/chemokines, CXCL10 and IL7 were the only significantly reduced cytokines specifically in the atherosclerotic setting (**Figure 18**C). Comparable change in depletion of cytotoxic lymphocytes and elevated B cell populations in the atherosclerotic setting are supported in part by CXCL10/IL7 findings, as these cytokines regulate T lymphocytes and myeloid populations, respectively (**Figure 18**, **Figure 19**).

Vascular infiltration of both innate and adaptive immune cells is a key feature of atherosclerosis. In particular, presence of pro-inflammatory M1 macrophages exacerbates disease progression[198], [199]. The role of cytotoxic $CD8^+$ T cells in atherosclerosis has been debatable in the literature. $CD8^+$ T cell activity induces growth and promote instability (i.e. rupture-prone) of atherosclerotic lesions through lysis of EC and smooth muscle cells[200]. These findings correlate with increased abundance of $CD8^+$ T cells in advanced atherosclerotic lesions[201], and

higher circulatory level of $CD8^+$ T cells linked to atherosclerosis development[202] in humans. These results support a pro-atherosclerotic role of $CD8^+$ T cells. However, an inverse correlation between $CD8^+$ T cell and macrophage content in human atherosclerotic aortas, taken together with preclinical evidence for antibody-mediated depletion of $CD8^+$ T cells resulting in reduced plaque stability and increased necrosis and macrophage content in advanced-stage $LDLR^{-/-}$ atherosclerotic animals support a protective role of $CD8^+$ T cells in late-stage atherosclerosis [203]. In general, immunosuppressive action of regulatory T cells (Tregs) inhibits atherosclerosis[204]. Furthermore, B cell-driven antibody response to oxidized LDL (driver of chronic inflammation), and cooperation between B and T cells have been demonstrated to contribute to athero-protective immunity in $ApoE^{-/-}$ mouse model of atherosclerosis [205]. These findings support moderate athero-protective effect in $Pfn1^{+/-(EC)}$ mice due to reduced cytotoxic T cell populations.

Further, CXCL10 is associated with pro-inflammatory immune cell activation, specifically playing a prominent role T cell recruitment in chronic inflammation [206], [207]. A previous study found that genetic ablation of CXCL10 leads to reduced $CD8^+$ T cell accumulation and enhanced Treg activity resulting in a prominent two-fold reduction in atherosclerotic lesion formation in $ApoE^{-/-}$ mice [206]. Reduced circulating CXCL10 level in $Pfn1^{+/-(EC)}$ relative to $Pfn1^{+/+}$ animals specifically in atherosclerosis setting may partly explain diminished circulating and aortic $CD8^+$ T cell abundance as a consequence of partial loss of EC Pfn1. Interestingly, these CXCL10-associated data diverges from our recently published findings of prominent CXCL10 elevation in response to complete loss of EC Pfn1 *in vitro* and *in vivo*[156]. While at first confounding, some part of the pro-inflammatory effect present in the aforementioned study may be due to cellular and tissue death not present in $Pfn1^{+/-(EC)}$ mice, leading to elevated CXCL10 secretion in total EC Pfn1 depleted mice. Separate from CXCL10, IL7, a cytokine that triggers Th1 and Th17 response [208],

has pro-atherogenic function[209]. Interestingly, IL7 is downregulated in both a totally and partially EC Pfn1 depleted setting[156], underscoring its potential as a target for further investigation in vascular disorders in which Pfn1 plays an essential role. Overall, these cytokine profiling data demonstrate that partial depletion of EC Pfn1 leads to reduction of select pro-atherogenic cytokines and chemokines in atherosclerosis setting.

Several lines of investigation are revealed based on the current study. **First**, though not significant, quantification of plaque components in $Pfn1^{+/-(EC)}$ mice as compared to $Pfn1^{+/+}$ at minimum supports probing of alternative stromal cells present in/near the atherosclerotic plaque (i.e. VSMCs) as a separate target of investigation. Pfn1 depletion in VSMCs may be especially promising, as Pfn1 KD reduced VSMC proliferation and migration[134], and a small molecule Pfn1:actin interaction inhibitor also presented with similar reduction in VSMC proliferation[210], offering a potential therapeutic option for further investigation. In addition to VSMCs, future studies to investigate Pfn1 reduction specific to either myeloid or lymphoid lineage immune cells is supported in part by reduced pro-atherogenic factors IL7 (myeloid associated) and CXCL10 (T lymphocyte associated) (Figure 20) as well as reduced cytotoxic T lymphocytes observed in flow cytometric analyses (Figure 18). Prior research has specifically investigated EC Pfn1 and global Pfn1 depletion[110], respectively, so alternative stromal cells may offer a promising point of investigation for Pfn1 depletion in future *in vitro* and *in vivo* studies (Figure 21). We must also consider sex-specific differences in atherosclerosis progression, as limited sample number did not reveal significant reduction of disease features in $Pfn1^{+/-(EC)}$ mice following male-female bifurcation of data. Future studies with increased sample number may reveal a sex-specific contribution in atherosclerotic $Pfn1^{+/-(EC)}$ mice. **Second**, while partial EC Pfn1 depletion only moderately impacts inflammatory and pathogenic features of atherosclerosis, further investigation

to create a viable $Pfn1^{EC\text{-}KO}$ mouse model may lead to dramatic change in atherosclerotic disease features. In $Pfn1^{EC\text{-}KO}$ mice, IL-6 was consistently upregulated in both endothelial and myeloid compartments following Pfn1 loss, though the precise paracrine mechanism is not clear[156]. Antibody-mediated IL-6 blockade may then offer a potential target to limit mortality as a consequence of EC Pfn1 depletion. We must also consider extending use of a Pfn1:actin interaction inhibitor into an *in vivo* atherosclerosis model, as small molecule treatment not only offers a potential therapeutic treatment modality, but will also facilitate granular study of Pfn1:actin abrogation by scaling supplied dosage of the inhibitor itself in the disease setting. **Third**, generation of an adenoviral-inducible $Pfn1^{flox/flox}$ model (no nascent Cre expression) paired with myeloid-specific, lymphocyte-specific, or VSMC-specific Ad-Cre-mediated Pfn1 gene KO may offer an easy-to-use model to investigate the effect of Pfn1 loss in specific cell-types and compartments without extensive backcrossing needed. As such, the current study offers many potential opportunities to further investigate the cell-type specific role of Pfn1 in atherosclerosis.

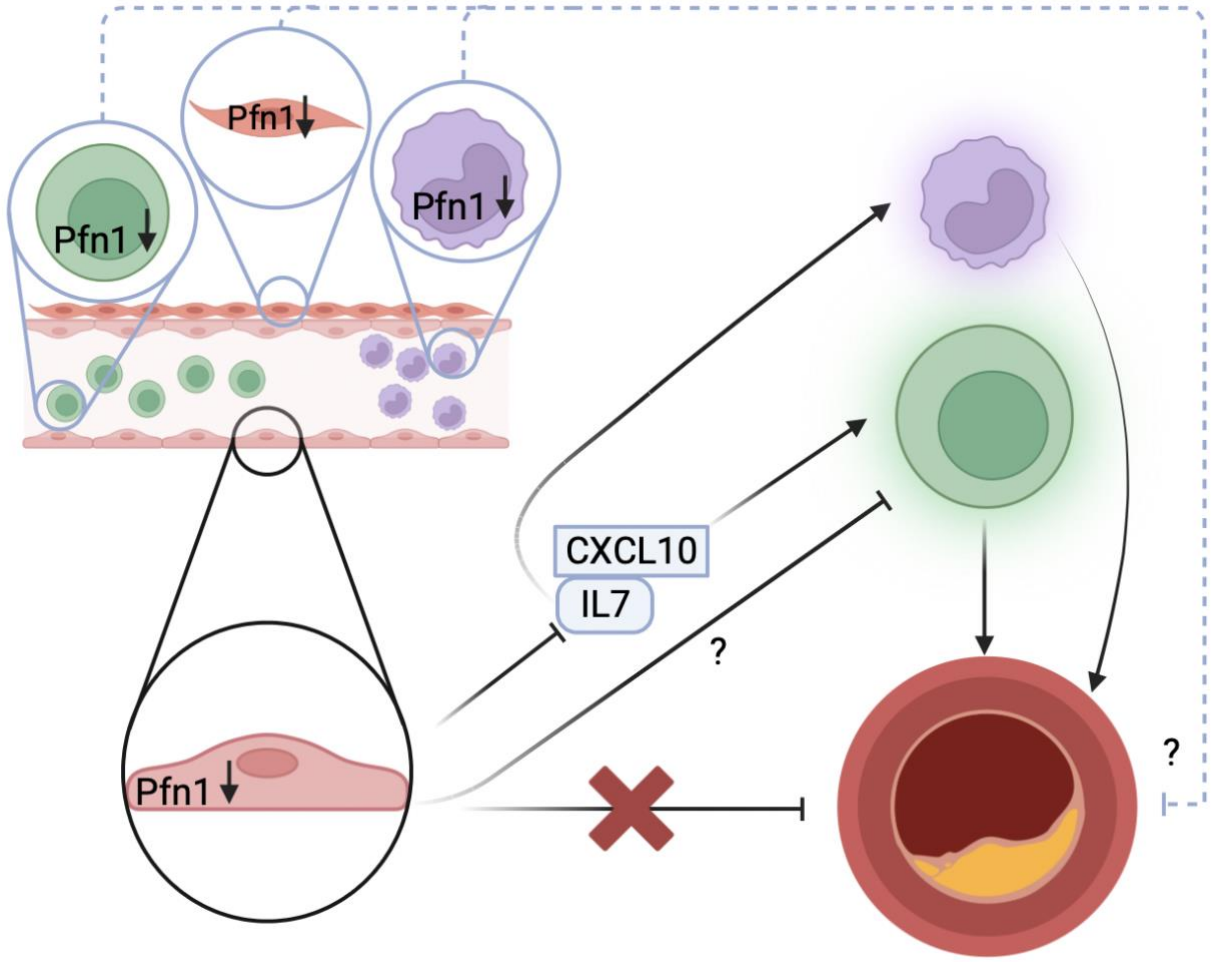

Figure 21. Endothelial Pfn1 partial reduction provides some benefit against atherosclerosis. Reduced levels of pro-atherogenic cytokines IL7 and CXCL10 may reduce activation of myeloid (blue) and lymphoid (green) lineage cells, respectively. Further investigation of Pfn1 depletion in myeloid and lymphoid lineage cells, as well as in VSMCs (orange), may reveal some atheroprotective effect,. Created with biorender.com.

In conclusion, this study for the first time investigates the impact of cell-type-specific partial loss of Pfn1 expression on atherosclerosis development. Although changes in EC play a key role in the initiation of atherosclerosis, our studies show that partial loss of Pfn1 expression selectively in ECs has certain beneficial effects (such as dampening of select pro-atherogenic

cytokines/chemokines with concomitant reduction in cytotoxic T cell abundance) but is not sufficient to confer atheroprotection *in vivo* (Figure 21). In light of these findings, we conclude that previously reported atheroprotective phenotype of global $Pfn1^{+/-}$ mice [110] is attributed to combined effects of Pfn1 depletion in additional cell types that are relevant for atherosclerosis progression. Therefore, it will be interesting to investigate in the future whether attenuated Pfn1 expression in monocytes/macrophages and/or smooth muscle cells offer additional benefits that could potentially explain atheroprotection conferred by global Pfn1 haplo-insufficiency.

5.0 Conclusions

Functional vascular structure and integrity is critical to tissue regulation on both the micro (cellular) and macro (tissues, whole organism) levels. While vascular regulation is tightly controlled by cell-cell interaction, as well as by intracellular protein and tissue regulation, dysregulation can lead to development of various pathologies. A contributor to this dysfunction is the actin-binding protein Pfn1. Actin cytoskeletal dysfunction can perturb cellular function not only on the level of vascularized disease (cardiovascular, endocrine disorders), but other Pfn isoforms can also contribute to other diseases, such as neurological disorders. In the context of endothelial dysfunction, the contributing role of Pfn1 is not clear. An *in vivo* model fully investigating total endothelial Pfn1 KO is not available, stunting development of a suitable model for further studies and improved clarification of the role of endothelial Pfn1 in pathology. Given our focus on vascularized diseases, we elected to further investigate endothelial Pfn1 in the acute (non-atherosclerotic, only EC Pfn1 KO) and chronic (atherosclerotic) settings. In this dissertation, we proposed that endothelial Pfn1 deletion will regulate pro-inflammatory response in both non-atherosclerotic and chronic inflammatory studies. This hypothesis was partially supported in Chapter 3 in the non-atherosclerotic setting by dramatic upregulation of pro-inflammatory cytokines both *in vitro* and *in* vivo following endothelial Pfn1 depletion as well as elevated pro-inflammatory myeloid cell populations. Gene expression analyses supported a role for IL-6 upregulation in myeloid cells, potentially tied to STAT1/IRF7 pathway activation in endothelial cells. Chapter 4 offered some additional support, as lymphocyte and myeloid specific factors (CXCL10, IL7, lymphocyte populations) were driven to a less inflammatory phenotype.

This work, while of importance in illuminating the mechanism of action of EC Pfn1 in inflammatory activation and signaling, also raises the question of how EC Pfn1 depletion influences the chronic inflammatory setting. Given mortality of Pfn1 depletion in the bi-allelic setting in all cell types[170], in a constitutive endothelial setting[154], and in an inducible endothelial setting[156], we elected to use a single-allelic deleted EC Pfn1 model in Chapter 4. In Chapter 4, we investigated partial EC Pfn1 depletion in the chronic inflammatory setting of atherosclerosis. Prior research has supported a role for Pfn1 depletion in abrogating the progression of atherosclerosis in a pre-clinical model[110]. However, this model was a single-allelic depleted Pfn1 model due to bi-allelic mortality at embryonic level[170], and did not reveal a cell-type specific effect for Pfn1 in atherosclerosis progression. While lipid profile and plaque development were not significantly impacted in the partial EC Pfn1 depleted setting, we see concurrence in depleted IL-7 and CXCL10 cytokines in the EC partial depleted setting for both non-atherosclerotic and chronic-collected samples. We also see some perturbation in $Ly6c^{lo}$ in both settings, as well as in T and B cell lineages. To parse a role for myeloid versus endothelial Pfn1, we conducted static co-culture studies that show elevated adhesion in Pfn1 depleted macrophages (indicative of early/late stage disease progression). This study demonstrated that EC Pfn1 may have a role in chronic inflammation, though further investigation in the context of myeloid, lymphoid and VSMC populations as well as in a total EC Pfn1 depleted model is required.

6.0 Future Directions

While several Pfn1 depleted models have been found successful in maintaining viability and facilitating the study of select genes of interest[42], [153], [211]–[215], this dissertation revealed that this approach is not necessarily relevant to all cell types and compartments, in addition to revelations related to an immunomodulatory and cell-signaling specific role for EC Pfn1. In addition to a technical standpoint, further work is needed to understand the role of endothelial Pfn1 in a variety of pathological conditions. Promising new targets of investigation have been revealed by the current findings of this dissertation, that are further illuminated below.

6.1 Determine a Role for Cell-type Specific Pfn1 in Chronic Inflammation

While we were able to conduct a preliminary investigation into EC Pfn1 in an acute (non-atherosclerotic) and chronic (atherosclerotic) setting, a greater understanding is required at both the **1)** cellular signaling level and **2)** in the chronic inflammatory setting. However, $Pfn1^{+/-(EC)}$ depletion in the chronic atherosclerotic setting revealed CXCL10 and IL7 downregulation and depleted lymphocyte/myeloid populations paired with a trend of upregulated B cell populations. Though of limited utility in their current form, perturbations in secreted cytokines and immune populations offer several targets of investigation. Namely, future studies can be conducted in an optimized *in vivo* model utilizing adenoviral-mediated Pfn1 deletion in cell types of interest. Specifically, an adenoviral vector targeted to the bone marrow or specific to the hepatocytic vascular lineage (most histologically perturbed in Chapter 4) would allow utilization of our fully

backcrossed C57BL6/J $Cre^{+/-}$ $Pfn1^{flox/flox}$ to immediately probe these factors without need for additional backcrossing. Available Ad(MBP) and Ad(RGD) adenoviral vectors could be modified and extended for *in vivo* use to target immune cell populations including myeloid cells[216], [217]. Following induction of atherosclerosis and disease progression, similar evaluation measures (lipids, plaque development, and immunomodulatory profile) can be used to assess potential remediation of atherosclerosis in mice with Pfn1 depletion in cell compartments of interest. Prior to these studies, additional extensive static and flow-based adhesion studies with Pfn1 WT or KO ECs exposed to Pfn1 WT or KO macrophages and lymphocytes ($CD8^+$ and $CD4^+$ subtypes) will aid in streamlining future atherosclerosis studies. Further investigation of pathway signaling may also provide a method to stunt pro-inflammatory signaling.

6.2 Investigate Cell-Type Specific Role of Pfn1 in Cellular Signaling

While current studies have conducted a preliminary investigation into cellular signaling, we do not yet have an understanding of cellular signaling in the single and multi-cellular context. Current findings support an intracellular signaling role for Pfn1 KO ECs in upregulating IRF7/STAT1 signaling. However, it is not clear whether this directly promotes a pro-inflammatory phenotype in myeloid derived populations, if secreted factors promote IL6 signaling in macrophages leading to pro-inflammatory activation, or some combination of both. Additional studies to assess the impact of Pfn1 depletion in myeloid lineage cells are required. In part, RNA isolation and RNAseq pathway analysis will illuminate pathways perturbed following Pfn1 KO in monocytes/macrophages. To improve the resolution of this study, we would investigate Pfn1 depletion in a mono-culture setting containing only WT and Pfn1 KO myeloid cells, in myeloid

cells incubated with conditioned media isolated from WT or Pfn1 KO ECs, as well as WT or Pfn1 KO myeloid co-cultured with WT or Pfn1 KO ECs in direct contact (total lysate collected). Significantly perturbed pathways can then be validated at the protein and RNA levels and used as potential signaling targets in developing a later stage therapeutic approach.

6.3 Elucidate a Role for Pfn1 in Other Endothelial-Derived Pathologies

We found that EC Pfn1 contributed to pro-inflammatory activation in the non-atherosclerotic setting, with some tempering of chronic inflammation in the partial EC Pfn1 depleted atherosclerotic setting. It would be of interest to conduct further investigations in the context of EC Pfn1 depletion with some moderator to reduce pro-inflammatory signaling. We saw major contributions of IL-6 in non-atherosclerotic total EC Pfn1 deletion, which could be due to inflammatory signaling due to IL-6 activation. Delving into a method that can reduce pro-inflammatory signaling would pave the way to use our total EC Pfn1 depleted model to specifically and selectively delete EC Pfn1 to elucidate its role in chronic inflammation. One possibility is to employ an endothelial cell-specific adenoviral Cre construct that can be targeted to our cell type and tissue of interest. A more directed model would not only limit off-target effects due to total vascular EC Pfn1 deletion as observed in Chapter 4, but it would also offer the opportunity to investigate specific tissues in different pathological contexts, opening the door to investigate a wide range of vascular and other endothelial-derived disorders in a targeted manner.

6.4 Utilize an Available Pfn1:actin Interaction Inhibitor in Atherosclerosis Studies

While not investigated in our studies, a Pfn1:actin interaction inhibitor (termed Pfn1i) developed in our lab offers an interesting tool for future pathological studies. Pfn1i has proven effective in reducing tumor size in an *in vivo* renal cell carcinoma model[54], and diminishes retinal neovascularization in an *in vivo* model of diabetic retinopathy[218]. Preliminary investigations of novel structural perturbations to the base structure of Pfn1i suggest even greater promise of these novel Pfn1i in limiting endothelial vascularization. Future studies utilizing either continuous mini-pump facilitated Pfn1i delivery or injection and microbubble-mediated delivery of Pfn1i will allow us to tune Pfn1i delivery and response effectively and specifically and unveil possible therapeutic effect.

Bibliography

[1] R. Valenta *et al.*, “Identification of profilin as an actin-binding protein in higher plants.,” *J. Biol. Chem.*, vol. 268, no. 30, pp. 22777–22781, Oct. 1993.

[2] L. Carlsson, L.-E. Nyström, I. Sundkvist, F. Markey, and U. Lindberg, “Actin polymerizability is influenced by profilin, a low molecular weight protein in non-muscle cells,” *J. Mol. Biol.*, vol. 115, no. 3, pp. 465–483, Sep. 1977, doi: 10.1016/0022-2836(77)90166-8.

[3] J. S. Widada, C. Ferraz, and J. P. Liautard, “Total coding sequence of profilin cDNA from Mus musculus macrophage,” *Nucleic Acids Res.*, vol. 17, no. 7, p. 2855, Apr. 1989, doi: 10.1093/nar/17.7.2855.

[4] D. J. Kwiatkowski and G. A. Bruns, “Human profilin. Molecular cloning, sequence comparison, and chromosomal analysis.,” *J. Biol. Chem.*, vol. 263, no. 12, pp. 5910–5915, Apr. 1988.

[5] E. Reichstein and E. D. Korn, “Acanthamoeba profilin. A protein of low molecular weight from Acanpthamoeba castellanii that inhibits actin nucleation.,” *J. Biol. Chem.*, vol. 254, no. 13, pp. 6174–6179, Jul. 1979.

[6] K.-H. Pyo, Y.-W. Lee, S. M. Lim, and E.-H. Shin, “Immune adjuvant effect of a Toxoplasma gondii profilin-like protein in autologous whole-tumor-cell vaccination in mice,” *Oncotarget*, vol. 7, no. 45, pp. 74107–74119, Sep. 2016, doi: 10.18632/oncotarget.12316.

[7] F. C. Mansilla *et al.*, “Immunization with Neospora caninum profilin induces limited protection and a regulatory T-cell response in mice,” *Exp. Parasitol.*, vol. 160, pp. 1–10, Jan. 2016, doi: 10.1016/j.exppara.2015.10.008.

[8] D. R. Kovar, P. Yang, W. S. Sale, B. K. Drobak, and C. J. Staiger, “Chlamydomonas reinhardtii produces a profilin with unusual biochemical properties,” *J. Cell Sci.*, vol. 114, no. 23, pp. 4293–4305, Dec. 2001.

[9] M. Edamatsu, M. Hirono, T. Takemasa, and Y. Watanabe, “The primary structure of Tetrahymena profilin,” *Biochem. Biophys. Res. Commun.*, vol. 175, no. 2, pp. 543–550, Mar. 1991, doi: 10.1016/0006-291X(91)91599-8.

[10] L. M. Machesky, N. B. Cole, B. Moss, and T. D. Pollard, “Vaccinia virus expresses a novel profilin with a higher affinity for polyphosphoinositides than actin,” *Biochemistry*, vol. 33, no. 35, pp. 10815–10824, Sep. 1994, doi: 10.1021/bi00201a032.

[11] V. Bitko, A. Oldenburg, N. E. Garmon, and S. Barik, “Profilin is required for viral morphogenesis, syncytium formation, and cell-specific stress fiber induction by respiratory syncytial virus,” *BMC Microbiol.*, vol. 3, p. 9, May 2003, doi: 10.1186/1471-2180-3-9.

[12] D. A. Kaiser, M. Sato, R. F. Ebert, and T. D. Pollard, “Purification and characterization of two isoforms of Acanthamoeba profilin,” *J. Cell Biol.*, vol. 102, no. 1, pp. 221–226, Jan. 1986, doi: 10.1083/jcb.102.1.221.

[13] R. Gieselmann, D. J. Kwiatkowski, P. A. Janmey, and W. Witke, “Distinct Biochemical Characteristics of the Two Human Profilin Isoforms,” *Eur. J. Biochem.*, vol. 229, no. 3, pp. 621–628, 1995, doi: 10.1111/j.1432-1033.1995.0621j.x.

[14] K. Krishnan and P. D. J. Moens, “Structure and functions of profilins,” *Biophys. Rev.*, vol. 1, no. 2, pp. 71–81, Jun. 2009, doi: 10.1007/s12551-009-0010-y.

[15] D. Polet, A. Lambrechts, K. Vandepoele, J. Vandekerckhove, and C. Ampe, “On the origin and evolution of vertebrate and viral profilins,” *FEBS Lett.*, vol. 581, no. 2, pp. 211–217, Jan. 2007, doi: 10.1016/j.febslet.2006.12.013.

[16] Z. Ding and P. Roy, “Profilin-1 versus profilin-2: two faces of the same coin?,” *Breast Cancer Res. BCR*, vol. 15, no. 3, p. 311, Jun. 2013, doi: 10.1186/bcr3433.

[17] A. Lambrechts *et al.*, “Profilin II Is Alternatively Spliced, Resulting in Profilin Isoforms That Are Differentially Expressed and Have Distinct Biochemical Properties,” *Mol. Cell. Biol.*, vol. 20, no. 21, pp. 8209–8219, Nov. 2000.

[18] K. Michaelsen *et al.*, “Fine-tuning of neuronal architecture requires two profilin isoforms,” *Proc. Natl. Acad. Sci.*, vol. 107, no. 36, pp. 15780–15785, Sep. 2010, doi: 10.1073/pnas.1004406107.

[19] E. Hu, Z. Chen, T. Fredrickson, and Y. Zhu, “Molecular cloning and characterization of profilin-3: a novel cytoskeleton-associated gene expressed in rat kidney and testes,” *Exp. Nephrol.*, vol. 9, no. 4, pp. 265–274, 2001, doi: 10.1159/000052621.

[20] N. Umer *et al.*, “PFN4 is required for manchette development and acrosome biogenesis during mouse spermiogenesis,” *Development*, vol. 149, no. 16, p. dev200499, Aug. 2022, doi: 10.1242/dev.200499.

[21] N. Umer *et al.*, “Loss of Profilin3 Impairs Spermiogenesis by Affecting Acrosome Biogenesis, Autophagy, Manchette Development and Mitochondrial Organization,” *Front. Cell Dev. Biol.*, vol. 9, 2021, Accessed: Oct. 22, 2023. [Online]. Available: https://www.frontiersin.org/articles/10.3389/fcell.2021.749559

[22] M. Behnen *et al.*, “Testis-expressed profilins 3 and 4 show distinct functional characteristics and localize in the acroplaxome-manchette complex in spermatids,” *BMC Cell Biol.*, vol. 10, p. 34, May 2009, doi: 10.1186/1471-2121-10-34.

[23] Y.-S. J. Ho, L. M. Burden, and J. H. Hurley, “Structure of the GAF domain, a ubiquitous signaling motif and a new class of cyclic GMP receptor,” *EMBO J.*, vol. 19, no. 20, pp. 5288–5299, Oct. 2000, doi: 10.1093/emboj/19.20.5288.

[24] N. Courtemanche and T. D. Pollard, “Interaction of profilin with the barbed end of actin filaments,” *Biochemistry*, vol. 52, no. 37, Sep. 2013, doi: 10.1021/bi400682n.

[25] E. Korenbaum, P. Nordberg, C. Björkegren-Sjögren, C. E. Schutt, U. Lindberg, and R. Karlsson, “The Role of Profilin in Actin Polymerization and Nucleotide Exchange,” *Biochemistry*, vol. 37, no. 26, pp. 9274–9283, Jun. 1998, doi: 10.1021/bi9803675.

[26] K.-K. Wen, M. McKane, E. Stokasimov, and P. A. Rubenstein, “Mutant Profilin Suppresses Mutant Actin-dependent Mitochondrial Phenotype in Saccharomyces cerevisiae,” *J. Biol. Chem.*, vol. 286, no. 48, pp. 41745–41757, Dec. 2011, doi: 10.1074/jbc.M110.217661.

[27] M. Tanaka and H. Shibata, “Poly(l-proline)-binding proteins from chick embryos are a profilin and a profilactin,” *Eur. J. Biochem.*, vol. 151, no. 2, pp. 291–297, 1985, doi: 10.1111/j.1432-1033.1985.tb09099.x.

[28] W. J. Metzler, A. J. Bell, E. Ernst, T. B. Lavoie, and L. Mueller, “Identification of the poly-L-proline-binding site on human profilin.,” *J. Biol. Chem.*, vol. 269, no. 6, pp. 4620–4625, Feb. 1994.

[29] I. Lassing and U. Lindberg, “Specific interaction between phosphatidylinositol 4,5-bisphosphate and profilactin,” *Nature*, vol. 314, no. 6010, Art. no. 6010, Apr. 1985, doi: 10.1038/314472a0.

[30] A. Lambrechts, V. Jonckheere, D. Dewitte, J. Vandekerckhove, and C. Ampe, “Mutational analysis of human profilin I reveals a second PI(4,5)-P2 binding site neighbouring the poly(L-proline) binding site,” *BMC Biochem.*, vol. 3, p. 12, May 2002, doi: 10.1186/1471-2091-3-12.

[31] P. J. Goldschmidt-Clermont, L. M. Machesky, J. J. Baldassare, and T. D. Pollard, “The actin-binding protein profilin binds to PIP2 and inhibits its hydrolysis by phospholipase C,” *Science*, vol. 247, no. 4950, pp. 1575–1578, Mar. 1990, doi: 10.1126/science.2157283.

[32] J. Funk *et al.*, “Profilin and formin constitute a pacemaker system for robust actin filament growth,” *eLife*, vol. 8, 24 2019, doi: 10.7554/eLife.50963.

[33] T. Finkel, J. A. Theriot, K. R. Dise, G. F. Tomaselli, and P. J. Goldschmidt-Clermont, “Dynamic actin structures stabilized by profilin.,” *Proc. Natl. Acad. Sci.*, vol. 91, no. 4, pp. 1510–1514, Feb. 1994, doi: 10.1073/pnas.91.4.1510.

[34] R. Lamprecht, C. R. Farb, S. M. Rodrigues, and J. E. LeDoux, “Fear conditioning drives profilin into amygdala dendritic spines,” *Nat. Neurosci.*, vol. 9, no. 4, Art. no. 4, Apr. 2006, doi: 10.1038/nn1672.

[35] M. R. Bennett, L. Farnell, and W. G. Gibson, “A Model of NMDA Receptor Control of F-actin Treadmilling in Synaptic Spines and Their Growth,” *Bull. Math. Biol.*, vol. 73, no. 9, pp. 2109–2131, Sep. 2011, doi: 10.1007/s11538-010-9614-4.

[36] K. Michaelsen-Preusse *et al.*, “Neuronal profilins in health and disease: Relevance for spine plasticity and Fragile X syndrome,” *Proc. Natl. Acad. Sci.*, vol. 113, no. 12, pp. 3365–3370, Mar. 2016, doi: 10.1073/pnas.1516697113.

[37] F. Wu *et al.*, “Urokinase-Type Plasminogen Activator Promotes Dendritic Spine Recovery and Improves Neurological Outcome Following Ischemic Stroke,” *J. Neurosci.*, vol. 34, no. 43, pp. 14219–14232, Oct. 2014, doi: 10.1523/JNEUROSCI.5309-13.2014.

[38] D. Wagh *et al.*, “Piccolo Directs Activity Dependent F-Actin Assembly from Presynaptic Active Zones via Daam1,” *PLoS ONE*, vol. 10, no. 4, Apr. 2015, doi: 10.1371/journal.pone.0120093.

[39] Y. Fukazawa, Y. Saitoh, F. Ozawa, Y. Ohta, K. Mizuno, and K. Inokuchi, “Hippocampal LTP Is Accompanied by Enhanced F-Actin Content within the Dendritic Spine that Is Essential for Late LTP Maintenance In Vivo,” *Neuron*, vol. 38, no. 3, pp. 447–460, May 2003, doi: 10.1016/S0896-6273(03)00206-X.

[40] W. Lei, K. R. Myers, Y. Rui, S. Hladyshau, D. Tsygankov, and J. Q. Zheng, “Phosphoinositide-dependent enrichment of actin monomers in dendritic spines regulates synapse development and plasticity,” *J. Cell Biol.*, vol. 216, no. 8, pp. 2551–2564, Aug. 2017, doi: 10.1083/jcb.201612042.

[41] Z. Wills, L. Marr, K. Zinn, C. S. Goodman, and D. Van Vactor, “Profilin and the Abl Tyrosine Kinase Are Required for Motor Axon Outgrowth in the Drosophila Embryo,” *Neuron*, vol. 22, no. 2, pp. 291–299, Feb. 1999, doi: 10.1016/S0896-6273(00)81090-9.

[42] R. Pinto-Costa *et al.*, “Profilin 1 delivery tunes cytoskeletal dynamics toward CNS axon regeneration,” *J. Clin. Invest.*, vol. 130, no. 4, pp. 2024–2040, Apr. 2020, doi: 10.1172/JCI125771.

[43] S. Palmgren, M. Vartiainen, and P. Lappalainen, “Twinfilin, a molecular mailman for actin monomers,” *J. Cell Sci.*, vol. 115, no. 5, pp. 881–886, Mar. 2002.

[44] R. Gareus, A. Di Nardo, V. Rybin, and W. Witke, “Mouse profilin 2 regulates endocytosis and competes with SH3 ligand binding to dynamin 1,” *J. Biol. Chem.*, vol. 281, no. 5, pp. 2803–2811, Feb. 2006, doi: 10.1074/jbc.M503528200.

[45] Y. Tanaka, “lntegrin activation by chemokines: Relevance to inflammatory adhesion cascade during T cell migration,” *Histol. Histopathol.*, vol. 15, no. 4, Art. no. 4, 2000.

[46] K. J. Ishii, S. Uematsu, and S. Akira, “‘Toll’ gates for future immunotherapy,” *Curr. Pharm. Des.*, vol. 12, no. 32, pp. 4135–4142, 2006, doi: 10.2174/138161206778743484.

[47] L. M. Neal and L. J. Knoll, “Toxoplasma gondii Profilin Promotes Recruitment of Ly6Chi CCR2+ Inflammatory Monocytes That Can Confer Resistance to Bacterial Infection,” *PLOS Pathog.*, vol. 10, no. 6, p. e1004203, Jun. 2014, doi: 10.1371/journal.ppat.1004203.

[48] A. A. Koblansky *et al.*, “Recognition of Profilin by Toll-like Receptor 12 Is Critical for Host Resistance to Toxoplasma gondii,” *Immunity*, vol. 38, no. 1, pp. 119–130, Jan. 2013, doi: 10.1016/j.immuni.2012.09.016.

[49] S. G. Rm *et al.*, “Toxoplasma gondii- derived profilin triggers human toll-like receptor 5-dependent cytokine production,” *J. Innate Immun.*, vol. 6, no. 5, 2014, doi: 10.1159/000362367.

[50] Z. Ding, A. Lambrechts, M. Parepally, and P. Roy, “Silencing profilin-1 inhibits endothelial cell proliferation, migration and cord morphogenesis,” *J. Cell Sci.*, vol. 119, no. 19, pp. 4127–4137, Oct. 2006, doi: 10.1242/jcs.03178.

[51] A. R. Brock *et al.*, “Transcriptional regulation of Profilin during wound closure in Drosophila larvae,” *J. Cell Sci.*, vol. 125, no. 23, pp. 5667–5676, Dec. 2012, doi: 10.1242/jcs.107490.

[52] H. Jasper *et al.*, “The genomic response of the Drosophila embryo to JNK signaling,” *Dev. Cell*, vol. 1, no. 4, pp. 579–586, Oct. 2001, doi: 10.1016/s1534-5807(01)00045-4.

[53] C. Jiang *et al.*, “A balanced level of profilin-1 promotes stemness and tumor-initiating potential of breast cancer cells,” *Cell Cycle Georget. Tex*, vol. 16, no. 24, pp. 2366–2373, 2017, doi: 10.1080/15384101.2017.1346759.

[54] A. Allen *et al.*, “Actin-binding protein profilin1 promotes aggressiveness of clear-cell renal cell carcinoma cells,” *J. Biol. Chem.*, vol. 295, no. 46, pp. 15636–15649, Nov. 2020, doi: 10.1074/jbc.RA120.013963.

[55] J. R. Karamchandani *et al.*, “Profilin-1 expression is associated with high grade and stage and decreased disease-free survival in renal cell carcinoma,” *Hum. Pathol.*, vol. 46, pp. 673–680, 2015, doi: http://dx.doi.org/10.1016/j.humpath.2014.11.007.

[56] O. Masui *et al.*, “Quantitative Proteomic Analysis in Metastatic Renal Cell Carcinoma Reveals a Unique Set of Proteins with Potential Prognostic Significance,” *Mol. Cell. Proteomics MCP*, vol. 12, no. 1, pp. 132–144, Jan. 2013, doi: 10.1074/mcp.M112.020701.

[57] B. A. Neely *et al.*, “Proteotranscriptomic Analysis Reveals Stage Specific Changes in the Molecular Landscape of Clear-Cell Renal Cell Carcinoma,” *PloS One*, vol. 11, no. 4, p. e0154074, 2016, doi: 10.1371/journal.pone.0154074.

[58] S. Minamida *et al.*, “Profilin 1 overexpression in renal cell carcinoma,” *Int. J. Urol.*, vol. 18, no. 1, pp. 63–71, 2011, doi: 10.1111/j.1442-2042.2010.02670.x.

[59] W. Rizwani, A. Fasim, D. Sharma, D. J. Reddy, N. A. M. B. Omar, and S. S. Singh, “S137 Phosphorylation of Profilin 1 Is an Important Signaling Event in Breast Cancer Progression,” *PLOS ONE*, vol. 9, no. 8, p. e103868, Aug. 2014, doi: 10.1371/journal.pone.0103868.

[60] C. R. Tessier and K. Broadie, “Drosophila fragile X mental retardation protein developmentally regulates activity-dependent axon pruning,” *Development*, vol. 135, no. 8, pp. 1547–1557, Apr. 2008, doi: 10.1242/dev.015867.

[61] M. Basso, S. Giraudo, D. Corpillo, B. Bergamasco, L. Lopiano, and M. Fasano, “Proteome analysis of human substantia nigra in Parkinson’s disease,” *Proteomics*, vol. 4, no. 12, pp. 3943–3952, Dec. 2004, doi: 10.1002/pmic.200400848.

[62] T. Zhao *et al.*, “Loss of nuclear activity of the FBXO7 protein in patients with parkinsonian-pyramidal syndrome (PARK15),” *PloS One*, vol. 6, no. 2, p. e16983, Feb. 2011, doi: 10.1371/journal.pone.0016983.

[63] M. Juneja *et al.*, “PFN2 and GAMT as common molecular determinants of axonal Charcot-Marie-Tooth disease,” *J. Neurol. Neurosurg. Psychiatry*, vol. 89, no. 8, pp. 870–878, 2018, doi: 10.1136/jnnp-2017-317562.

[64] C.-H. Wu *et al.*, “Mutations in the Profilin 1 Gene Cause Familial Amyotrophic Lateral Sclerosis,” *Nature*, vol. 488, no. 7412, pp. 499–503, Aug. 2012, doi: 10.1038/nature11280.

[65] B. N. Smith *et al.*, “Novel mutations support a role for Profilin 1 in the pathogenesis of ALS,” *Neurobiol. Aging*, vol. 36, no. 3, p. 1602.e17-1602.e27, Mar. 2015, doi: 10.1016/j.neurobiolaging.2014.10.032.

[66] C. Tiloca *et al.*, “Screening of the PFN1 gene in sporadic ALS and in FTD,” *Neurobiol. Aging*, vol. 34, no. 5, p. 1517.e9-1517.e10, May 2013, doi: 10.1016/j.neurobiolaging.2012.09.016.

[67] C. Ingre *et al.*, “A novel phosphorylation site mutation in profilin 1 revealed in a large screen of US, Nordic, and German amyotrophic lateral sclerosis/frontotemporal dementia cohorts,” *Neurobiol. Aging*, vol. 34, no. 6, p. 1708.e1-1708.e6, Jun. 2013, doi: 10.1016/j.neurobiolaging.2012.10.009.

[68] Y. Chen *et al.*, “PFN1 mutations are rare in Han Chinese populations with amyotrophic lateral sclerosis,” *Neurobiol. Aging*, vol. 34, no. 7, p. 1922.e1–5, Jul. 2013, doi: 10.1016/j.neurobiolaging.2013.01.013.

[69] S. Yang *et al.*, “Mutation analysis and immunopathological studies of PFN1 in familial and sporadic amyotrophic lateral sclerosis,” *Neurobiol. Aging*, vol. 34, no. 9, p. 2235.e7–10, Sep. 2013, doi: 10.1016/j.neurobiolaging.2013.04.003.

[70] S. Boopathy *et al.*, “Structural basis for mutation-induced destabilization of profilin 1 in ALS,” *Proc. Natl. Acad. Sci.*, vol. 112, no. 26, pp. 7984–7989, Jun. 2015, doi: 10.1073/pnas.1424108112.

[71] L. Dillen *et al.*, “Explorative genetic study of UBQLN2 and PFN1 in an extended Flanders-Belgian cohort of frontotemporal lobar degeneration patients,” *Neurobiol. Aging*, vol. 34, no. 6, p. 1711.e1-1711.e5, Jun. 2013, doi: 10.1016/j.neurobiolaging.2012.12.007.

[72] M. van Blitterswijk *et al.*, “Profilin-1 mutations are rare in patients with amyotrophic lateral sclerosis and frontotemporal dementia,” *Amyotroph. Lateral Scler. Front. Degener.*, vol. 14, no. 0, pp. 463–469, Sep. 2013, doi: 10.3109/21678421.2013.787630.

[73] P. Fratta *et al.*, “Profilin1 E117G is a moderate risk factor for amyotrophic lateral sclerosis,” *J. Neurol. Neurosurg. Psychiatry*, vol. 85, no. 5, pp. 506–508, May 2014, doi: 10.1136/jnnp-2013-306761.

[74] M. Brettle, A. K. Suchowerska, S. W. Chua, L. M. Ittner, and T. Fath, “Amyotrophic lateral sclerosis-associated mutant profilin 1 increases dendritic arborisation and spine formation in primary hippocampal neurons,” *Neurosci. Lett.*, vol. 609, pp. 223–228, Nov. 2015, doi: 10.1016/j.neulet.2015.09.034.

[75] D. Fil *et al.*, “Mutant Profilin1 transgenic mice recapitulate cardinal features of motor neuron disease,” *Hum. Mol. Genet.*, vol. 26, no. 4, Feb. 2017, doi: 10.1093/hmg/ddw429.

[76] C. Barham, D. Fil, S. D. Byrum, Y. Rahmatallah, G. Glazko, and M. Kiaei, “RNA-Seq Analysis of Spinal Cord Tissues from hPFN1 G118V Transgenic Mouse Model of ALS at Pre-symptomatic and End-Stages of Disease,” *Sci. Rep.*, vol. 8, no. 1, Art. no. 1, Sep. 2018, doi: 10.1038/s41598-018-31132-y.

[77] C. Yang *et al.*, “Mutant PFN1 causes ALS phenotypes and progressive motor neuron degeneration in mice by a gain of toxicity,” *Proc. Natl. Acad. Sci.*, vol. 113, no. 41, pp. E6209–E6218, Oct. 2016, doi: 10.1073/pnas.1605964113.

[78] M. Brettle *et al.*, “Developmental Expression of Mutant PFN1 in Motor Neurons Impacts Neuronal Growth and Motor Performance of Young and Adult Mice,” *Front. Mol. Neurosci.*, vol. 12, 2019, doi: 10.3389/fnmol.2019.00231.

[79] E. D. Poggetto *et al.*, “Stability of an aggregation-prone partially folded state of human profilin-1 correlates with aggregation propensity,” *J. Biol. Chem.*, vol. 293, no. 26, pp. 10303–10313, Jun. 2018, doi: 10.1074/jbc.RA118.002087.

[80] A. Freischmidt, M. Schöpflin, M. S. Feiler, A.-K. Fleck, A. C. Ludolph, and J. H. Weishaupt, “Profilin 1 with the amyotrophic lateral sclerosis associated mutation T109M displays unaltered actin binding and does not affect the actin cytoskeleton,” *BMC Neurosci.*, vol. 16, no. 1, p. 77, Nov. 2015, doi: 10.1186/s12868-015-0214-y.

[81] G. R. C. Pereira, G. H. A. S. Tellini, and J. F. D. Mesquita, “In silico analysis of PFN1 related to amyotrophic lateral sclerosis,” *PLOS ONE*, vol. 14, no. 6, p. e0215723, Jun. 2019, doi: 10.1371/journal.pone.0215723.

[82] M. Kiaei, M. Balasubramaniam, V. Govind Kumar, R. J. Shmookler Reis, M. Moradi, and K. I. Varughese, “ALS-causing mutations in profilin-1 alter its conformational dynamics: A computational approach to explain propensity for aggregation,” *Sci. Rep.*, vol. 8, no. 1, Art. no. 1, Aug. 2018, doi: 10.1038/s41598-018-31199-7.

[83] C.-H. Wu, A. Giampetruzzi, H. Tran, C. Fallini, F.-B. Gao, and J. E. Landers, "A Drosophila model of ALS reveals a partial loss of function of causative human PFN1 mutants," *Hum. Mol. Genet.*, vol. 26, no. 11, pp. 2146–2155, Jun. 2017, doi: 10.1093/hmg/ddx112.

[84] B. G. Burnett, J. Andrews, S. Ranganathan, K. H. Fischbeck, and N. A. Di Prospero, "Expression of expanded polyglutamine targets profilin for degradation and alters actin dynamics," *Neurobiol. Dis.*, vol. 30, no. 3, pp. 365–374, Jun. 2008, doi: 10.1016/j.nbd.2008.02.007.

[85] A. Ceccon, V. Tugarinov, R. Ghirlando, and G. M. Clore, "Abrogation of prenucleation, transient oligomerization of the Huntingtin exon 1 protein by human profilin I," *Proc. Natl. Acad. Sci.*, vol. 117, no. 11, pp. 5844–5852, Mar. 2020, doi: 10.1073/pnas.1922264117.

[86] J. Chakraborty *et al.*, "Profilin-2 increased expression and its altered interaction with β-actin in the striatum of 3-nitropropionic acid-induced Huntington's disease in rats," *Neuroscience*, vol. 281, pp. 216–228, Dec. 2014, doi: 10.1016/j.neuroscience.2014.09.035.

[87] H. Goehler *et al.*, "A Protein Interaction Network Links GIT1, an Enhancer of Huntingtin Aggregation, to Huntington's Disease," *Mol. Cell*, vol. 15, no. 6, pp. 853–865, Sep. 2004, doi: 10.1016/j.molcel.2004.09.016.

[88] M. Antoine *et al.*, "Splicing Defects of the Profilin Gene Alter Actin Dynamics in an S. pombe SMN Mutant," *iScience*, vol. 23, no. 1, Jan. 2020, doi: 10.1016/j.isci.2019.100809.

[89] M. Bowerman, D. Shafey, and R. Kothary, "Smn depletion alters profilin II expression and leads to upregulation of the RhoA/ROCK pathway and defects in neuronal integrity," *J. Mol. Neurosci. MN*, vol. 32, no. 2, pp. 120–131, 2007, doi: 10.1007/s12031-007-0024-5.

[90] T. Giesemann *et al.*, "A Role for Polyproline Motifs in the Spinal Muscular Atrophy Protein SMN PROFILINS BIND TO AND COLOCALIZE WITH SMN IN NUCLEAR GEMS," *J. Biol. Chem.*, vol. 274, no. 53, pp. 37908–37914, Dec. 1999, doi: 10.1074/jbc.274.53.37908.

[91] A. Nölle *et al.*, "The spinal muscular atrophy disease protein SMN is linked to the rho-kinase pathway via profilin," *Hum. Mol. Genet.*, vol. 20, no. 24, pp. 4865–4878, Dec. 2011, doi: 10.1093/hmg/ddr425.

[92] A. Sharma *et al.*, "A role for complexes of survival of motor neurons (SMN) protein with gemins and profilin in neurite-like cytoplasmic extensions of cultured nerve cells," *Exp. Cell Res.*, vol. 309, no. 1, pp. 185–197, Sep. 2005, doi: 10.1016/j.yexcr.2005.05.014.

[93] V. Caraballo-Miralles *et al.*, "SMN deficiency attenuates migration of U87MG astroglioma cells through the activation of RhoA," *Mol. Cell. Neurosci.*, vol. 49, no. 3, pp. 282–289, Mar. 2012, doi: 10.1016/j.mcn.2011.12.003.

[94] C. Camaré, M. Pucelle, A. Nègre-Salvayre, and R. Salvayre, "Angiogenesis in the atherosclerotic plaque," *Redox Biol.*, vol. 12, pp. 18–34, Feb. 2017, doi: 10.1016/j.redox.2017.01.007.

[95] M. A. Gimbrone Jr. and G. García-Cardeña, "Endothelial Cell Dysfunction and the Pathobiology of Atherosclerosis," *Circ. Res.*, vol. 118, no. 4, pp. 620–636, Feb. 2016, doi: 10.1161/CIRCRESAHA.115.306301.

[96] R. Ross, "The pathogenesis of atherosclerosis: a perspective for the 1990s," *Nature*, vol. 362, no. 6423, pp. 801–809, Apr. 1993, doi: 10.1038/362801a0.

[97] A. J. Lusis, "Atherosclerosis," *Nature*, vol. 407, no. 6801, pp. 233–241, Sep. 2000, doi: 10.1038/35025203.

[98] W. Herrington, B. Lacey, P. Sherliker, J. Arimtage, and S. Lewington, "Epidemiology of Atherosclerosis and the Potential to Reduce the Global Burden of Atherothrombotic Disease," *Circ. Res.*, vol. 118, no. 4, pp. 535–546, 2016, doi: https://doi.org/10.1161/CIRCRESAHA.115.307611.

[99] GBD, "Global, regional, and national age-sex specific all-cause and cause-specific mortality for 240 causes of death, 1990-2013: a systematic analysis for the Global Burden of Disease Study 2013," *Lancet*, vol. 385, no. 9963, pp. 117–171, Jan. 2015, doi: 10.1016/S0140-6736(14)61682-2.

[100] N. M. van Popele *et al.*, "Aortic stiffness is associated with atherosclerosis of the coronary arteries in older adults: the Rotterdam Study," *J. Hypertens.*, vol. 24, no. 12, pp. 2371–2376, Dec. 2006, doi: 10.1097/01.hjh.0000251896.62873.c4.

[101] S. S. Meyrelles, V. A. Peotta, T. M. C. Pereira, and E. C. Vasquez, "Endothelial dysfunction in the apolipoprotein E-deficient mouse: insights into the influence of diet, gender and aging," *Lipids Health Dis.*, vol. 10, p. 211, Nov. 2011, doi: 10.1186/1476-511X-10-211.

[102] H. N. Hayenga, A. Trache, J. Trzeciakowski, and J. D. Humphrey, "Regional Atherosclerotic Plaque Properties in ApoE–/– Mice Quantified by Atomic Force, Immunofluorescence, and Light Microscopy," *J. Vasc. Res.*, vol. 48, no. 6, pp. 495–504, 2011, doi: 10.1159/000329586.

[103] C. M. Warboys, N. Amini, A. de Luca, and P. C. Evans, "The role of blood flow in determining the sites of atherosclerotic plaques," *F1000 Med. Rep.*, vol. 3, p. 5, Mar. 2011, doi: 10.3410/M3-5.

[104] K.-C. Wang *et al.*, "Flow-dependent YAP/TAZ activities regulate endothelial phenotypes and atherosclerosis," *Proc. Natl. Acad. Sci. U. S. A.*, vol. 113, no. 41, pp. 11525–11530, 11 2016, doi: 10.1073/pnas.1613121113.

[105] H.-J. Choi, N.-E. Kim, B. M. Kim, M. Seo, and J. H. Heo, "TNF-α-Induced YAP/TAZ Activity Mediates Leukocyte-Endothelial Adhesion by Regulating VCAM1 Expression in Endothelial Cells," *Int. J. Mol. Sci.*, vol. 19, no. 11, Nov. 2018, doi: 10.3390/ijms19113428.

[106] A. Farina *et al.*, "Proteomic profiling of medial degeneration in human ascending aorta," *Clin. Biochem.*, vol. 43, no. 4–5, pp. 387–396, Mar. 2010, doi: 10.1016/j.clinbiochem.2009.10.015.

[107]R. Liu and J.-P. Jin, “Deletion of calponin 2 in macrophages alters cytoskeleton-based functions and attenuates the development of atherosclerosis,” *J. Mol. Cell. Cardiol.*, vol. 99, pp. 87–99, Oct. 2016, doi: 10.1016/j.yjmcc.2016.08.019.

[108]M. Zhang *et al.*, “BMP-2 Overexpression Augments Vascular Smooth Muscle Cell Motility by Upregulating Myosin Va via Erk Signaling,” *Oxid. Med. Cell. Longev.*, vol. 2014, p. 294150, 2014, doi: 10.1155/2014/294150.

[109]M. Yang *et al.*, “BMP-2 enhances the migration and proliferation of hypoxia-induced VSMCs via actin cytoskeleton, CD44 and matrix metalloproteinase linkage,” *Exp. Cell Res.*, vol. 368, no. 2, pp. 248–257, Jul. 2018, doi: 10.1016/j.yexcr.2018.05.004.

[110]G. R. Romeo, K. S. Moulton, and A. Kazlauskas, “Attenuated Expression of Profilin-1 Confers Protection From Atherosclerosis in the LDL Receptor–Null Mouse,” *Circ. Res.*, vol. 101, pp. 357–367, Jun. 2007, doi: 10.1161/CIRCRESAHA.107.151399.

[111]E. Caglayan *et al.*, “Profilin-1 is expressed in human atherosclerotic plaques and induces atherogenic effects on vascular smooth muscle cells,” *PloS One*, vol. 5, no. 10, p. e13608, Oct. 2010, doi: 10.1371/journal.pone.0013608.

[112]G. R. Romeo, M. Pae, D. Eberlé, J. Lee, and S. E. Shoelson, “Profilin-1 haploinsufficiency protects against obesity-associated glucose intolerance and preserves adipose tissue immune homeostasis,” *Diabetes*, vol. 62, no. 11, pp. 3718–3726, Nov. 2013, doi: 10.2337/db13-0050.

[113]J. Rahimzadeh, F. Meng, F. Sachs, J. Wang, D. Verma, and S. Z. Hua, “Real-time observation of flow-induced cytoskeletal stress in living cells,” *Am. J. Physiol.-Cell Physiol.*, vol. 301, no. 3, pp. C646–C652, Jun. 2011, doi: 10.1152/ajpcell.00099.2011.

[114]R. Dardik, N. Savion, N. Gal, and D. Varon, “Flow Conditions Modulate Homocysteine Induced Changes in the Expression of Endothelial Cell Genes Associated with Cell-Cell Interaction and Cytoskeletal Rearrangement,” *Thromb. Haemost.*, vol. 88, no. 6, pp. 1047–1053, 2002, doi: 10.1055/s-0037-1613353.

[115]Z. Chen *et al.*, “Blood pressure in relation to general and central adiposity among 500 000 adult Chinese men and women,” *Int. J. Epidemiol.*, vol. 44, no. 4, pp. 1305–1319, Aug. 2015, doi: 10.1093/ije/dyv012.

[116]T. R. Dawber, W. B. Kannel, N. Revotskie, J. Stokes, A. Kagan, and T. Gordon, “Some factors associated with the development of coronary heart disease: six years’ follow-up experience in the Framingham study,” *Am. J. Public Health Nations Health*, vol. 49, no. 10, pp. 1349–1356, Oct. 1959, doi: 10.2105/ajph.49.10.1349.

[117]R. S. Vasan *et al.*, “Impact of High-Normal Blood Pressure on the Risk of Cardiovascular Disease,” *N. Engl. J. Med.*, vol. 345, no. 18, pp. 1291–1297, Nov. 2001, doi: 10.1056/NEJMoa003417.

[118]W. B. Kannel, T. Gordon, and M. J. Schwartz, “Systolic versus diastolic blood pressure and risk of coronary heart disease. The Framingham study,” *Am. J. Cardiol.*, vol. 27, no. 4, pp. 335–346, Apr. 1971, doi: 10.1016/0002-9149(71)90428-0.

[119]S. S. Franklin and N. D. Wong, “Hypertension and cardiovascular disease: contributions of the framingham heart study,” *Glob. Heart*, vol. 8, no. 1, pp. 49–57, Mar. 2013, doi: 10.1016/j.gheart.2012.12.004.

[120]M. Moustafa-Bayoumi *et al.*, “Vascular hypertrophy and hypertension caused by transgenic overexpression of profilin 1,” *J. Biol. Chem.*, vol. 282, no. 52, pp. 37632–37639, Dec. 2007, doi: 10.1074/jbc.M703227200.

[121]S. Yang *et al.*, “Association Study of Common Variants in PFN1 With Hypertension in a Han Chinese Population: A Case–Control Study and A Follow-up Study,” *Am. J. Hypertens.*, vol. 30, no. 10, pp. 1024–1031, Oct. 2017, doi: 10.1093/ajh/hpx089.

[122]J.-M. Chen, R.-R. Guo, Y. Gao, C.-X. Wang, and P.-N. Yuan, “Mechanism of action of Profilin-1 and Fibulin-3 in vascular remodeling in hypertensive rats,” *Eur. Rev. Med. Pharmacol. Sci.*, vol. 23, no. 18, pp. 8101–8108, Sep. 2019, doi: 10.26355/eurrev_201909_19028.

[123]S. Zhao *et al.*, “Profilin-1 promotes the development of hypertension-induced cardiac hypertrophy,” *J. Hypertens.*, vol. 31, no. 3, pp. 576–586, Mar. 2013, doi: 10.1097/HJH.0b013e32835d6a56.

[124]V. Kooij *et al.*, “Profilin modulates sarcomeric organization and mediates cardiomyocyte hypertrophy,” *Cardiovasc. Res.*, vol. 110, no. 2, pp. 238–248, May 2016, doi: 10.1093/cvr/cvw050.

[125]L.-H. Xia, T. Chen, B. Zhang, and M. Chen, “Mechanism of Profilin-1 in regulating eNOS/NO signaling pathway and its role in hypertensive myocardial hypertension,” *Asian Pac. J. Trop. Med.*, vol. 8, no. 5, pp. 399–404, May 2015, doi: 10.1016/S1995-7645(14)60351-5.

[126]S. Zhao *et al.*, “Effect of ouabain on myocardial ultrastructure and cytoskeleton during the development of ventricular hypertrophy,” *Heart Vessels*, vol. 28, no. 1, pp. 101–113, Jan. 2013, doi: 10.1007/s00380-011-0219-0.

[127]J.-P. Hao *et al.*, “Role of GSPE in improving early cerebral vascular damage by inhibition of Profilin-1 expression in a ouabain-induced hypertension model,” *Eur. Rev. Med. Pharmacol. Sci.*, vol. 22, no. 20, pp. 6999–7012, 2018, doi: 10.26355/eurrev_201810_16171.

[128]Y. Wang *et al.*, “Profilin-1 Promotes the Development of Hypertension-induced Artery Remodeling,” *J. Histochem. Cytochem.*, vol. 62, no. 4, pp. 298–310, Apr. 2014, doi: 10.1369/0022155414520978.

[129]M. T. Elnakish, H. H. Hassanain, and P. M. L. Janssen, “Vascular remodeling-associated hypertension leads to left ventricular hypertrophy and contractile dysfunction in profilin-1

transgenic mice," *J. Cardiovasc. Pharmacol.*, vol. 60, no. 6, pp. 544–552, Dec. 2012, doi: 10.1097/FJC.0b013e318271225d.

[130]M. D. H. Hassona *et al.*, "Vascular hypertrophy-associated hypertension of profilin1 transgenic mouse model leads to functional remodeling of peripheral arteries," *Am. J. Physiol.-Heart Circ. Physiol.*, vol. 298, no. 6, pp. H2112–H2120, Apr. 2010, doi: 10.1152/ajpheart.00016.2010.

[131]I. Ramaiola *et al.*, "Changes in thrombus composition and profilin-1 release in acute myocardial infarction," *Eur. Heart J.*, vol. 36, no. 16, pp. 965–975, Apr. 2015, doi: 10.1093/eurheartj/ehu356.

[132]J.-F. Cheng *et al.*, "Involvement of profilin-1 in angiotensin II-induced vascular smooth muscle cell proliferation," *Vascul. Pharmacol.*, vol. 55, no. 1–3, pp. 34–41, Sep. 2011, doi: 10.1016/j.vph.2011.04.003.

[133]H.-Y. Jin *et al.*, "ACE2 deficiency enhances angiotensin II-mediated aortic profilin-1 expression, inflammation and peroxynitrite production," *PloS One*, vol. 7, no. 6, p. e38502, 2012, doi: 10.1371/journal.pone.0038502.

[134]B. Song *et al.*, "Angiotensin-converting enzyme 2 attenuates oxidative stress and VSMC proliferation via the JAK2/STAT3/SOCS3 and profilin-1/MAPK signaling pathways," *Regul. Pept.*, vol. 185, pp. 44–51, Aug. 2013, doi: 10.1016/j.regpep.2013.06.007.

[135]K. M. Flegal, M. D. Carroll, B. K. Kit, and C. L. Ogden, "Prevalence of Obesity and Trends in the Distribution of Body Mass Index Among US Adults, 1999-2010," *JAMA*, vol. 307, no. 5, pp. 491–497, Feb. 2012, doi: 10.1001/jama.2012.39.

[136]A. Menke, S. Casagrande, L. Geiss, and C. C. Cowie, "Prevalence of and Trends in Diabetes Among Adults in the United States, 1988-2012," *JAMA*, vol. 314, no. 10, pp. 1021–1029, Sep. 2015, doi: 10.1001/jama.2015.10029.

[137]J. A. Beckman, M. A. Creager, and P. Libby, "Diabetes and atherosclerosis: epidemiology, pathophysiology, and management," *JAMA*, vol. 287, no. 19, pp. 2570–2581, May 2002, doi: 10.1001/jama.287.19.2570.

[138]P. Dandona, A. Aljada, A. Chaudhuri, and A. Bandyopadhyay, "The Potential Influence of Inflammation and Insulin Resistance on the Pathogenesis and Treatment of Atherosclerosis-Related Complications in Type 2 Diabetes," *J. Clin. Endocrinol. Metab.*, vol. 88, no. 6, pp. 2422–2429, Jun. 2003, doi: 10.1210/jc.2003-030178.

[139]M. Ahmed, J. Forsberg, and P. Bergsten, "Protein Profiling of Human Pancreatic Islets by Two-Dimensional Gel Electrophoresis and Mass Spectrometry," *J. Proteome Res.*, vol. 4, no. 3, pp. 931–940, Jun. 2005, doi: 10.1021/pr050024a.

[140]N. A. A. Wahab, N. Abdullah, and N. Aminudin, "Characterisation of potential antidiabetic-related proteins from Pleurotus pulmonarius (Fr.) Quél. (grey oyster mushroom) by MALDI-

TOF/TOF mass spectrometry," *BioMed Res. Int.*, vol. 2014, p. 131607, 2014, doi: 10.1155/2014/131607.

[141]A. A. Alfadda *et al.*, "Proteomic analysis of mature adipocytes from obese patients in relation to aging," *Exp. Gerontol.*, vol. 48, no. 11, pp. 1196–1203, Nov. 2013, doi: 10.1016/j.exger.2013.07.008.

[142]M. R. Clarkson *et al.*, "High Glucose-altered Gene Expression in Mesangial Cells ACTIN-REGULATORY PROTEIN GENE EXPRESSION IS TRIGGERED BY OXIDATIVE STRESS AND CYTOSKELETAL DISASSEMBLY," *J. Biol. Chem.*, vol. 277, no. 12, pp. 9707–9712, Mar. 2002, doi: 10.1074/jbc.M109172200.

[143]H. Ding, B. Chen, Q. Lu, and J. Wang, "Profilin-1 mediates microvascular endothelial dysfunction in diabetic retinopathy through HIF-1α-dependent pathway," *Int. J. Clin. Exp. Pathol.*, vol. 11, no. 3, pp. 1247–1255, 2018.

[144]Q. Lu, P. Lu, W. Chen, L. Lu, and Z. Zheng, "ANGPTL-4 induces diabetic retinal inflammation by activating Profilin-1," *Exp. Eye Res.*, vol. 166, pp. 140–150, 2018, doi: 10.1016/j.exer.2017.10.009.

[145]G. R. Romeo and A. Kazlauskas, "Oxysterol and diabetes activate STAT3 and control endothelial expression of profilin-1 via OSBP1," *J. Biol. Chem.*, vol. 283, no. 15, pp. 9595–9605, Apr. 2008, doi: 10.1074/jbc.M710092200.

[146]D. Yang *et al.*, "Downregulation of Profilin-1 Expression Attenuates Cardiomyocytes Hypertrophy and Apoptosis Induced by Advanced Glycation End Products in H9c2 Cells," BioMed Research International. Accessed: Apr. 06, 2020. [Online]. Available: https://www.hindawi.com/journals/bmri/2017/9716087/

[147]G. Romeo, J. Frangioni, and A. Kazlauskas, "Profilin acts downstream of LDL to mediate diabetic endothelial cell dysfunction," *FASEB J.*, vol. 18, no. 6, pp. 725–7, Feb. 2004, doi: 10.1096/fj.03-0841fje.

[148]D. Yang *et al.*, "Profilin-1 contributes to cardiac injury induced by advanced glycation end-products in rats," *Mol. Med. Rep.*, vol. 16, no. 5, pp. 6634–6641, Nov. 2017, doi: 10.3892/mmr.2017.7446.

[149]X. Li, J. Liu, B. Chen, and L. Fan, "A Positive Feedback Loop of Profilin-1 and RhoA/ROCK1 Promotes Endothelial Dysfunction and Oxidative Stress," Oxidative Medicine and Cellular Longevity. Accessed: Apr. 20, 2020. [Online]. Available: https://www.hindawi.com/journals/omcl/2018/4169575/

[150]Q. Lu, L. Lu, W. Chen, H. Chen, X. Xu, and Z. Zheng, "RhoA/mDia-1/profilin-1 signaling targets microvascular endothelial dysfunction in diabetic retinopathy," *Graefes Arch. Clin. Exp. Ophthalmol. Albrecht Von Graefes Arch. Klin. Exp. Ophthalmol.*, vol. 253, no. 5, pp. 669–680, May 2015, doi: 10.1007/s00417-015-2985-3.

[151]D. Gau *et al.*, “Disruption of profilin1 function suppresses developmental and pathological retinal neovascularization,” *J. Biol. Chem.*, vol. 295, no. 28, pp. 9618–9629, Jul. 2020, doi: 10.1074/jbc.RA120.012613.

[152]D. Gau *et al.*, “Vascular endothelial profilin-1 drives a pro-tumorigenic tumor microenvironment and tumor progression in renal cancer,” *J. Biol. Chem.*, p. 105044, Jul. 2023, doi: 10.1016/j.jbc.2023.105044.

[153]F. Scotto di Carlo, L. Pazzaglia, T. Esposito, and F. Gianfrancesco, “The Loss of Profilin 1 Causes Early Onset Paget’s Disease of Bone,” *J. Bone Miner. Res. Off. J. Am. Soc. Bone Miner. Res.*, Jan. 2020, doi: 10.1002/jbmr.3964.

[154]D. Gau *et al.*, “Pharmacological intervention of MKL/SRF signaling by CCG-1423 impedes endothelial cell migration and angiogenesis,” *Angiogenesis*, vol. 20, no. 4, pp. 663–672, Nov. 2017, doi: 10.1007/s10456-017-9560-y.

[155]R. Schoppmeyer *et al.*, “Human profilin 1 is a negative regulator of CTL mediated cell-killing and migration,” *Eur. J. Immunol.*, vol. 47, no. 9, pp. 1562–1572, Jul. 2017, doi: 10.1002/eji.201747124.

[156]A. Allen-Gondringer *et al.*, “Vascular endothelial cell-specific disruption of the profilin1 gene leads to severe multiorgan pathology and inflammation causing mortality,” *PNAS Nexus*, vol. 2, no. 10, p. pgad305, Sep. 2023, doi: 10.1093/pnasnexus/pgad305.

[157]S. Kumar, D.-W. Kang, A. Rezvan, and H. Jo, “Accelerated atherosclerosis development in C57Bl6 mice by overexpressing AAV-mediated PCSK9 and partial carotid ligation,” *Lab. Invest.*, vol. 97, no. 8, Art. no. 8, Aug. 2017, doi: 10.1038/labinvest.2017.47.

[158]N. Zelcer and M. Westerterp, “Adeno-Associated Viruses as a Method to Induce Atherosclerosis in Mice and Hamsters,” *Circ. Res.*, vol. 114, no. 11, pp. 1672–1674, May 2014, doi: 10.1161/CIRCRESAHA.114.304067.

[159]E. Mukherjee *et al.*, “Endothelial marker-expressing stromal cells are critical for kidney formation,” *Am. J. Physiol. - Ren. Physiol.*, vol. 313, no. 3, pp. F611–F620, Sep. 2017, doi: 10.1152/ajprenal.00136.2017.

[160]K. Murk, M. Ornaghi, and J. Schiweck, “Profilin Isoforms in Health and Disease – All the Same but Different,” *Front. Cell Dev. Biol.*, vol. 9, 2021, Accessed: Oct. 12, 2023. [Online]. Available: https://www.frontiersin.org/articles/10.3389/fcell.2021.681122

[161]E. Hu, Z. Chen, T. Fredrickson, and Y. Zhu, “Molecular Cloning and Characterization of Profilin-3: A Novel Cytoskeleton-Associated Gene Expressed in Rat Kidney and Testes,” *Exp. Nephrol.*, vol. 9, no. 4, pp. 265–274, Jun. 2001, doi: 10.1159/000052621.

[162]H. Obermann, I. Raabe, M. Balvers, B. Brunswig, W. Schulze, and C. Kirchhoff, “Novel testis-expressed profilin IV associated with acrosome biogenesis and spermatid elongation,” *Mol. Hum. Reprod.*, vol. 11, no. 1, pp. 53–64, Jan. 2005, doi: 10.1093/molehr/gah132.

[163]M. Nejedla *et al.*, “Profilin connects actin assembly with microtubule dynamics,” *Mol. Biol. Cell*, vol. 27, no. 15, pp. 2381–2393, Aug. 2016, doi: 10.1091/mbc.E15-11-0799.

[164]R. Pinto-Costa and M. M. Sousa, “Profilin as a dual regulator of actin and microtubule dynamics,” *Cytoskeleton*, vol. 77, no. 3–4, pp. 76–83, 2020, doi: 10.1002/cm.21586.

[165]J. L. Henty-Ridilla, M. A. Juanes, and B. L. Goode, “Profilin Directly Promotes Microtubule Growth through Residues Mutated in Amyotrophic Lateral Sclerosis,” *Curr. Biol.*, vol. 27, no. 22, pp. 3535-3543.e4, Nov. 2017, doi: 10.1016/j.cub.2017.10.002.

[166]D. B. Ostrander, J. A. Gorman, and G. M. Carman, “Regulation of Profilin Localization in Saccharomyces cerevisiae by Phosphoinositide Metabolism (*),” *J. Biol. Chem.*, vol. 270, no. 45, pp. 27045–27050, Nov. 1995, doi: 10.1074/jbc.270.45.27045.

[167]H. Yu, Y. Zhao, X. Pan, C. Liu, and R. Fu, “Upregulated Expression of Profilin1 on Dendritic Cells in Patients With Severe Aplastic Anemia,” *Front. Immunol.*, vol. 12, p. 631954, 2021, doi: 10.3389/fimmu.2021.631954.

[168]M. Joy, D. Gau, N. Castellucci, R. Prywes, and P. Roy, “The myocardin-related transcription factor MKL co-regulates the cellular levels of two profilin isoforms,” *J. Biol. Chem.*, vol. 292, no. 28, pp. 11777–11791, Jul. 2017, doi: 10.1074/jbc.M117.781104.

[169]M. Tamura *et al.*, “Activation of DNA synthesis and AP-1 by profilin, an actin-binding protein, via binding to a cell surface receptor in cultured rat mesangial cells,” *J. Am. Soc. Nephrol. JASN*, vol. 11, no. 9, pp. 1620–1630, Sep. 2000, doi: 10.1681/ASN.V1191620.

[170]W. Witke, J. D. Sutherland, A. Sharpe, M. Arai, and D. J. Kwiatkowski, “Profilin I is essential for cell survival and cell division in early mouse development,” *Proc. Natl. Acad. Sci.*, vol. 98, no. 7, pp. 3832–3836, Mar. 2001, doi: 10.1073/pnas.051515498.

[171]M. Haugwitz, A. A. Noegel, J. Karakesisoglou, and M. Schleicher, “Dictyostelium amoebae that lack G-actin-sequestering profilins show defects in F-actin content, cytokinesis, and development,” *Cell*, vol. 79, no. 2, pp. 303–314, Oct. 1994, doi: 10.1016/0092-8674(94)90199-6.

[172]E. M. Verheyen and L. Cooley, “Profilin mutations disrupt multiple actin-dependent processes during Drosophila development,” *Dev. Camb. Engl.*, vol. 120, no. 4, pp. 717–728, Apr. 1994, doi: 10.1242/dev.120.4.717.

[173]B. Kilani *et al.*, “Comparison of endothelial promoter efficiency and specificity in mice reveals a subset of Pdgfb-positive hematopoietic cells,” *J. Thromb. Haemost. JTH*, vol. 17, no. 5, pp. 827–840, May 2019, doi: 10.1111/jth.14417.

[174]G. F. Grabner, H. Xie, M. Schweiger, and R. Zechner, “Lipolysis: cellular mechanisms for lipid mobilization from fat stores,” *Nat. Metab.*, vol. 3, no. 11, Art. no. 11, Nov. 2021, doi: 10.1038/s42255-021-00493-6.

[175]E. O. Gubernatorova *et al.*, “Non-redundant Functions of IL-6 Produced by Macrophages and Dendritic Cells in Allergic Airway Inflammation,” *Front. Immunol.*, vol. 9, p. 2718, Nov. 2018, doi: 10.3389/fimmu.2018.02718.

[176]K. Anderson *et al.*, “STAT1 is regulated by TRIM24 and promotes immunosuppression in head and neck squamous carcinoma cells, but enhances T cell antitumour immunity in the tumour microenvironment,” *Br. J. Cancer*, vol. 127, no. 4, pp. 624–636, Sep. 2022, doi: 10.1038/s41416-022-01853-z.

[177]E. Platanitis and T. Decker, “Regulatory Networks Involving STATs, IRFs, and NFκB in Inflammation,” *Front. Immunol.*, vol. 9, 2018, Accessed: Oct. 23, 2023. [Online]. Available: https://www.frontiersin.org/articles/10.3389/fimmu.2018.02542

[178]C. Furman *et al.*, “Ena/VASP is required for endothelial barrier function in vivo,” *J. Cell Biol.*, vol. 179, no. 4, pp. 761–775, Nov. 2007, doi: 10.1083/jcb.200705002.

[179]D. Gau, W. Veon, S. G. Shroff, and P. Roy, “The VASP-profilin1 (Pfn1) interaction is critical for efficient cell migration and is regulated by cell-substrate adhesion in a PKA-dependent manner,” *J. Biol. Chem.*, vol. 294, no. 17, pp. 6972–6985, Apr. 2019, doi: 10.1074/jbc.RA118.005255.

[180]S. Willenborg *et al.*, “CCR2 recruits an inflammatory macrophage subpopulation critical for angiogenesis in tissue repair,” *Blood*, vol. 120, no. 3, pp. 613–625, Jul. 2012, doi: 10.1182/blood-2012-01-403386.

[181]C. S. Mantsounga *et al.*, “Macrophage IL-1β promotes arteriogenesis by autocrine STAT3- and NF-κB-mediated transcription of pro-angiogenic VEGF-A,” *Cell Rep.*, vol. 38, no. 5, p. 110309, Feb. 2022, doi: 10.1016/j.celrep.2022.110309.

[182]F. Coperchini, L. Chiovato, and M. Rotondi, “Interleukin-6, CXCL10 and Infiltrating Macrophages in COVID-19-Related Cytokine Storm: Not One for All But All for One!,” *Front. Immunol.*, vol. 12, p. 668507, 2021, doi: 10.3389/fimmu.2021.668507.

[183]M. Rincon and C. G. Irvin, “Role of IL-6 in Asthma and Other Inflammatory Pulmonary Diseases,” *Int. J. Biol. Sci.*, vol. 8, no. 9, pp. 1281–1290, Oct. 2012, doi: 10.7150/ijbs.4874.

[184]T. Kobayashi *et al.*, “Bidirectional role of IL-6 signal in pathogenesis of lung fibrosis,” *Respir. Res.*, vol. 16, no. 1, p. 99, Aug. 2015, doi: 10.1186/s12931-015-0261-z.

[185]S. Chmielewski *et al.*, “STAT1-dependent signal integration between IFNγ and TLR4 in vascular cells reflect pro-atherogenic responses in human atherosclerosis,” *PloS One*, vol. 9, no. 12, p. e113318, 2014, doi: 10.1371/journal.pone.0113318.

[186]P. M. Colonne, M. E. Eremeeva, and S. K. Sahni, “Beta interferon-mediated activation of signal transducer and activator of transcription protein 1 interferes with Rickettsia conorii replication in human endothelial cells,” *Infect. Immun.*, vol. 79, no. 9, pp. 3733–3743, Sep. 2011, doi: 10.1128/IAI.05008-11.

[187]World Health Organization, “Cardiovascular diseases.” Accessed: Aug. 04, 2023. [Online]. Available: https://www.who.int/health-topics/cardiovascular-diseases

[188]D. Shepard, A. VanderZanden, A. Moran, M. Naghavi, C. Murray, and G. Roth, “Ischemic Heart Disease Worldwide, 1990 to 2013,” *Circ. Cardiovasc. Qual. Outcomes*, vol. 8, no. 4, pp. 455–456, Jul. 2015, doi: 10.1161/CIRCOUTCOMES.115.002007.

[189]A. Sharma *et al.*, “Direct Endothelial Nitric Oxide Synthase Activation Provides Atheroprotection in Diabetes-Accelerated Atherosclerosis,” *Diabetes*, vol. 64, no. 11, pp. 3937–50, Jun. 2015, doi: 10.2337/db15-0472.

[190]S. Kawashima and M. Yokoyama, “Dysfunction of endothelial nitric oxide synthase and atherosclerosis,” *Arterioscler. Thromb. Vasc. Biol.*, vol. 24, no. 6, pp. 998–1005, Mar. 2004, doi: 10.1161/01.ATV.0000125114.88079.96.

[191]S. Cejkova, I. Kralova-Lesna, and R. Poledne, “Monocyte adhesion to the endothelium is an initial stage of atherosclerosis development,” *Cor Vasa*, vol. 58, no. 4, pp. e419–e425, Aug. 2016, doi: https://doi.org/10.1016/j.crvasa.2015.08.002.

[192]B. O. Oluwole, W. Du, I. Mills, and B. E. Sumpio, “Gene regulation by mechanical forces,” *Endothel. J. Endothel. Cell Res.*, vol. 5, no. 2, pp. 85–93, 1997, doi: 10.3109/10623329709079866.

[193]T. N. Dear, N. T. Meier, M. Hunn, and T. Boehm, “Gene structure, chromosomal localization, and expression pattern of Capn12, a new member of the calpain large subunit gene family,” *Genomics*, vol. 68, no. 2, pp. 152–160, Sep. 2000, doi: 10.1006/geno.2000.6289.

[194]A. Schaefer *et al.*, “Actin-binding proteins differentially regulate endothelial cell stiffness, ICAM-1 function and neutrophil transmigration,” *J. Cell Sci.*, vol. 127, no. 20, pp. 4470–4482, Oct. 2014, doi: 10.1242/jcs.154708.

[195]I. Tabas, X. Zha, N. Beatini, J. N. Myers, and F. R. Maxfield, “The actin cytoskeleton is important for the stimulation of cholesterol esterification by atherogenic lipoproteins in macrophages.,” *J. Biol. Chem.*, vol. 269, no. 36, pp. 22547–22556, Sep. 1994, doi: 10.1016/S0021-9258(17)31681-2.

[196]F. Y. McWhorter, T. Wang, P. Nguyen, T. Chung, and W. F. Liu, “Modulation of macrophage phenotype by cell shape,” *Proc. Natl. Acad. Sci. U. S. A.*, vol. 110, no. 43, pp. 17253–17258, Oct. 2013, doi: 10.1073/pnas.1308887110.

[197]E. Yurtseven, D. Ural, K. Baysal, and L. Tokgözoğlu, “An Update on the Role of PCSK9 in Atherosclerosis,” *J. Atheroscler. Thromb.*, vol. 27, no. 9, pp. 909–918, Sep. 2020, doi: 10.5551/jat.55400.

[198]M. J. Davies, “Stability and instability: two faces of coronary atherosclerosis. The Paul Dudley White Lecture 1995,” *Circulation*, vol. 94, no. 8, pp. 2013–2020, Oct. 1996, doi: 10.1161/01.cir.94.8.2013.

[199]E. K. Koltsova *et al.*, "Dynamic T cell–APC interactions sustain chronic inflammation in atherosclerosis," *J. Clin. Invest.*, vol. 122, no. 9, pp. 3114–3126, Sep. 2012, doi: 10.1172/JCI61758.

[200]T. Kyaw *et al.*, "Cytotoxic and proinflammatory CD8+ T lymphocytes promote development of vulnerable atherosclerotic plaques in apoE-deficient mice," *Circulation*, vol. 127, no. 9, pp. 1028–1039, Mar. 2013, doi: 10.1161/CIRCULATIONAHA.112.001347.

[201]J. Gewaltig, M. Kummer, C. Koella, G. Cathomas, and B. C. Biedermann, "Requirements for CD8 T-cell migration into the human arterial wall," *Hum. Pathol.*, vol. 39, no. 12, pp. 1756–1762, Dec. 2008, doi: 10.1016/j.humpath.2008.04.018.

[202]J. Podolec *et al.*, "Higher levels of circulating naïve CD8+CD45RA+ cells are associated with lower extent of coronary atherosclerosis and vascular dysfunction," *Int. J. Cardiol.*, vol. 259, pp. 26–30, May 2018, doi: 10.1016/j.ijcard.2018.01.079.

[203]J. van Duijn *et al.*, "CD8+ T-cells contribute to lesion stabilization in advanced atherosclerosis by limiting macrophage content and CD4+ T-cell responses," *Cardiovasc. Res.*, vol. 115, no. 4, pp. 729–738, Apr. 2019, doi: 10.1093/cvr/cvy261.

[204]A. C. Foks, A. H. Lichtman, and J. Kuiper, "Treating atherosclerosis with regulatory T cells," *Arterioscler. Thromb. Vasc. Biol.*, vol. 35, no. 2, pp. 280–287, Feb. 2015, doi: 10.1161/ATVBAHA.114.303568.

[205]G. Caligiuri, A. Nicoletti, B. Poirier, and G. K. Hansson, "Protective immunity against atherosclerosis carried by B cells of hypercholesterolemic mice," *J. Clin. Invest.*, vol. 109, no. 6, pp. 745–753, Mar. 2002, doi: 10.1172/JCI7272.

[206]E. A. Heller *et al.*, "Chemokine CXCL10 Promotes Atherogenesis by Modulating the Local Balance of Effector and Regulatory T Cells," *Circulation*, vol. 113, no. 19, pp. 2301–2312, May 2006, doi: 10.1161/CIRCULATIONAHA.105.605121.

[207]R. Li *et al.*, "Interleukin-7 induces recruitment of monocytes/macrophages to endothelium," *Eur. Heart J.*, vol. 33, no. 24, pp. 3114–3123, Dec. 2012, doi: 10.1093/eurheartj/ehr245.

[208]A. Bikker, C. E. Hack, F. P. J. G. Lafeber, and J. A. G. van Roon, "Interleukin-7: a key mediator in T cell-driven autoimmunity, inflammation, and tissue destruction," *Curr. Pharm. Des.*, vol. 18, no. 16, pp. 2347–2356, 2012, doi: 10.2174/138161212800165979.

[209]P. M. Mihailovic *et al.*, "IL-7R blockade reduces post-myocardial infarction-induced atherosclerotic plaque inflammation in ApoE-/- mice," *Biochem. Biophys. Rep.*, vol. 19, p. 100647, Sep. 2019, doi: 10.1016/j.bbrep.2019.100647.

[210]D. Gau, T. Lewis, L. McDermott, P. Wipf, D. Koes, and P. Roy, "Structure-based virtual screening identifies a small-molecule inhibitor of the profilin 1-actin interaction," *J. Biol. Chem.*, vol. 293, no. 7, pp. 2606–2616, Feb. 2018, doi: 10.1074/jbc.M117.809137.

[211]E. Lu *et al.*, “Profilin 1 knockdown prevents ischemic brain damage by promoting M2 microglial polarization associated with the RhoA/ROCK pathway,” *J. Neurosci. Res.*, Apr. 2020, doi: 10.1002/jnr.24607.

[212]R. T. Böttcher *et al.*, “Profilin 1 is required for abscission during late cytokinesis of chondrocytes,” *EMBO J.*, vol. 28, no. 8, pp. 1157–1169, Apr. 2009, doi: 10.1038/emboj.2009.58.

[213]D. Miyajima *et al.*, “Profilin1 Regulates Sternum Development and Endochondral Bone Formation,” *J. Biol. Chem.*, vol. 287, no. 40, pp. 33545–33553, Sep. 2012, doi: 10.1074/jbc.M111.329938.

[214]J. A. Kullmann, A. Neumeyer, C. B. Gurniak, E. Friauf, W. Witke, and M. B. Rust, “Profilin1 is required for glial cell adhesion and radial migration of cerebellar granule neurons,” *EMBO Rep.*, vol. 13, no. 1, pp. 75–82, Dec. 2011, doi: 10.1038/embor.2011.211.

[215]M. Di Domenico, M. Jokwitz, W. Witke, and P. Pilo Boyl, “Specificity and Redundancy of Profilin 1 and 2 Function in Brain Development and Neuronal Structure,” *Cells*, vol. 10, no. 9, p. 2310, Sep. 2021, doi: 10.3390/cells10092310.

[216]M. O. Alberti *et al.*, “Derivation of a Myeloid Cell-Binding Adenovirus for Gene Therapy of Inflammation,” *PLOS ONE*, vol. 7, no. 5, p. e37812, May 2012, doi: 10.1371/journal.pone.0037812.

[217]Z. H. Lu *et al.*, “The myeloid-binding peptide adenoviral vector enables multi-organ vascular endothelial gene targeting,” *Lab. Investig. J. Tech. Methods Pathol.*, vol. 94, no. 8, pp. 881–892, Aug. 2014, doi: 10.1038/labinvest.2014.78.

[218]D. Gau, L. Vignaud, P. Francoeur, D. Koes, X. Guillonneau, and P. Roy, “Inhibition of ocular neovascularization by novel anti-angiogenic compound,” *Exp. Eye Res.*, vol. 213, p. 108861, Dec. 2021, doi: 10.1016/j.exer.2021.108861.